NOISE PERFORMANCE OF VERY LARGE ANTENNA ARRAYS

Heng-Cheng Lin

The Ohio State University

ElectroScience Laboratory

Department of Electrical Engineering
Columbus, Ohio 43212

Technical Report 3931-1

September 1975

National Aeronautics and Space Administration
Goddard Space Flight Center
Greenbelt, Maryland 20771

NOTICES

When Government drawings, specifications, or other data are used for any purpose other than in connection with a definitely related Government procurement operation, the United States Government thereby incurs no responsibility nor any obligation whatsoever, and the fact that the Government may have formulated, furnished, or in any way supplied the said drawings, specifications, or other data, is not to be regarded by implication or otherwise as in any manner licensing the holder or any other person or corporation, or conveying any rights or permission to manufacture, use, or sell any patented invention that may in any way be related thereto.

TECHNICAL REPORT STANDARD TITLE PAGE

1. Report No.	2. Government Accession No.	3. Recipient's Catalog No.

4. Title and Subtitle
NOISE PERFORMANCE OF VERY LARGE ANTENNA ARRAYS

5. Report Date

6. Performing Organization Code

7. Author(s)
Heng-Cheng Lin

8. Performing Organization Report No.
3931-1

9. Performing Organization Name and Address
The Ohio State University ElectroScience Laboratory, Department of Electrical Engineering, Columbus, Ohio 43212

10. Work Unit No.

11. Contract or Grant No.
NAS 5-20521

12. Sponsoring Agency Name and Address
National Aeronautics and Space Administration
Goddard Space Flight Center, Greenbelt MD
E. Hirschmann, Code 951, Technical Officer

13. Type of Report and Period Covered
Type II
5/16/74 to 8/31/75

14. Sponsoring Agency Code

15. Supplementary Notes
This report was submitted as a thesis in partial fulfillment of the requirements for the degree Master of Science.

16. Abstract

The maximum size, and hence resolution, of receiving antenna arrays is found to be limited by signal-to-noise ratio considerations. For square arrays containing no active elements a practical limit at 30 GHz appears to be on the order of 10 meters for communications and one to two meters for radiometry. These limitations can be overcome by use of active devices at various levels of the array organization. The nature of the resulting tradeoffs is indicated. Explicit formulas are developed for both passive and active arrays, and sample computations and the computer programs are given.

17. Key Words (Selected by Author(s))		18. Distribution Statement
Antenna	Resolution	
Array	Radiometry	
Noise		

19. Security Classif. (of this report)	20. Security Classif. (of this page)	21. No. of Pages	22. Price*
Unclassified	Unclassified	121	

*For sale by the Clearinghouse for Federal Scientific and Technical Information, Springfield, Virginia 22151.

PREFACE

The objective of this contract is to define feasible and useful experiments for employing a large millimeter-wave electronically steered array on the Space Shuttle generation of vehicles. This report treats the limitations imposed on array size by signal-to-noise considerations when no active devices are used internally to the array. It also explores the tradeoffs encountered when active devices are used at various levels of the array organization.

TABLE OF CONTENTS

TABLE OF CONTENTS (continued)

LIST OF TABLES

LIST OF FIGURES

LIST OF FIGURES (continued)

LIST OF FIGURES (continued)

CHAPTER I

INTRODUCTION

Recent advances in the technology of manned space flight make it reasonable to propose the use of very large high-gain antennas. By using large antennas on orbiting space vehicles, many desirable properties can be obtained more easily, e.g., high gain and good resolution. However, certain physical considerations limit the performance of the system as the size of the antenna is increased. One such consideration is the thermal noise coming from the system itself. When the size of an array is sufficiently large, the noise coming from the transmission elements must be taken into consideration in the evaluation of the performance of the array.

It is well known that noise phenomena greatly constrain the performance of a communication system. This thesis explores the effect of internally generated noise on communications and radiometer antenna performance. In particular, we wish to show how the array organization, i.e., the manner of interconnecting the elements in proper phase relationship, affects the signal-to-noise ratio.

Another consideration is the noise behavior of active devices which may need to be inserted into very large antenna arrays. Active devices not only amplify the input signal and noise, but also add additional noise; however, the noise contributions of circuits which follow the amplification are greatly de-emphasized. Consequently, as is

well known, the earlier in the signal path we place active devices of a given noise figure, the better the noise performance will be. We will investigate this effect quantitatively and explore the noise performance of very large antenna systems by using the principle of superposition.

In this thesis the methods of noise calculation are reviewed for 2-ports and some other multiports and then these methods are applied to specific summing networks. With these results, the noise performance of some large antenna arrays is calculated. The last part of this study deals with the noise from active elements and compares the performance of several different ways of inserting the active devices. The available tradeoffs are indicated through the curves obtained as a result of the calculations in the last two chapters.

For the sake of simplicity, all the performance curves are based on a 30 GHz operation frequency, centrally located in the frequency range to be used in remote sensing and radiometry in the Space Shuttle experiments of the 80's [1, 2].

CHAPTER II

THE THERMAL NOISE OF PASSIVE JUNCTIONS

A. Introduction

The choice of junction networks for combining the signals originating at the array elements depends on the means by which the signals are transmitted to the summing point. In the case of waveguides, usually hybrid-tee networks are used to sum the signals. In the case of transmission lines, hybrids can also be used or, as will be shown later, under some special conditions signals can be combined in parallel in order to sum the signal powers.

B. Thermal Noise

Thermal (or Johnson or Nyquist) noise is caused by the random thermal motion of charges or polarizable molecules in lossy materials. It is directly related to dissipation. Therefore, before considering the noise behavior of junctions, we shall first look at the origin and transmission of noise in the dissipative devices which are the sources of noise.

Since thermal noise is caused by random thermal motion of molecules, noise voltages arriving from different sources are statistically independent and have zero mean. Therefore, noise voltages from different sources are uncorrelated in time. As we will see later, the uncorrelated property of thermal noise causes noise powers to combine in a way which

is quite different from that of correlated-signal powers. This is the basis of the signal-to-noise improvement when signals are combined at junctions.

C. A Brief Review of Noise in a One-Port Termination

Any termination at temperature T will send out a thermal noise wave. The emitted available noise power P_N in bandwidth (f_1, f_2) is given from quantum thermodynamics by [3, 4, 5].

$$P_N = \int_{f_1}^{f_2} \left[\frac{1}{2} hf + \frac{hf}{\exp(hf/KT) - 1} \right] df \qquad (1)$$

where

h is Planck's constant (6.6257×10^{-34} joule-sec),

f is the frequency in Hz,

K is the Boltzmann constant (1.38×10^{-23} joule/^oK), and

T is the absolute temperature of the termination in ^oK.

In another form, this can be written as

$$P_N = \int_{f_1}^{f_2} s(f)\, df, \qquad (2)$$

where

$$s(f) = \frac{1}{2} hf + \frac{hf}{\exp(hf/KT) - 1} \qquad (3)$$

is called the noise power spectrum.

For a fairly "narrow" bandwidth over which s(f) is a constant, equation (2) can be expressed as

$$P_N = \left[\frac{1}{2} hf + \frac{hf}{\exp(hf/KT - 1)} \right] (f_2 - f_1) \qquad (4)$$

or

$$P_N = \left[\frac{1}{2} hf + \frac{hf}{\exp(hf/KT - 1)} \right] B \qquad (5)$$

where $B = f_2 - f_1$ is the noise bandwidth measured in Hertz.

Fig. 1 shows the normalized available noise power (P_N/KTB) as a function of hf/KT.

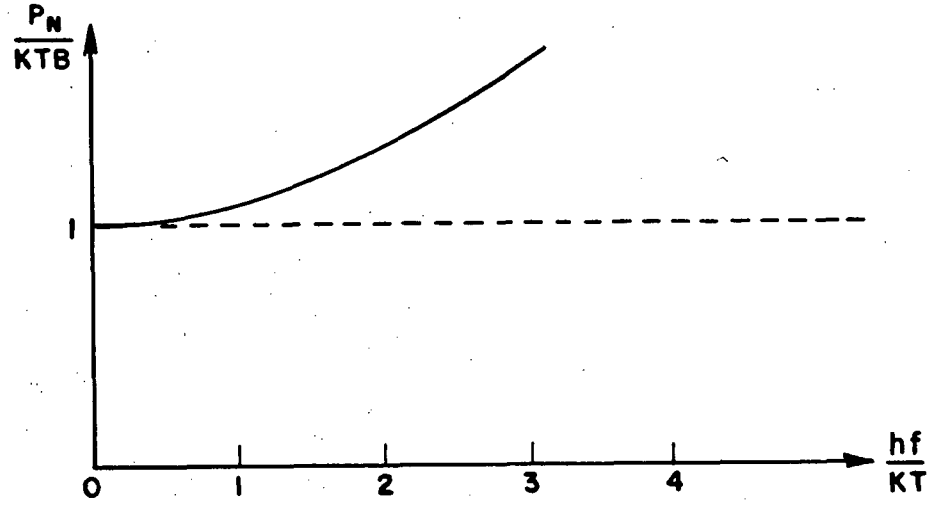

Fig. 1. The normalized thermal noise P_N/KTB as a function of hf/KT.

At room temperature, say, $T = 300^{o}K$, and in the frequency range up to 100 GHz, we find

$$\frac{hf}{KT} = 1.60 \times 10^{-2} \ll 1 \, . \qquad (6)$$

Then P_N can be approximated as (Fig. 1)

$$P_N \approx KTB \, . \qquad (7)$$

This is the form often used at microwave frequencies.

Consider a resistance R delivering noise power $P_N = KTB$ to a terminating element Z. The available noise power $P_N = KTB$ can be

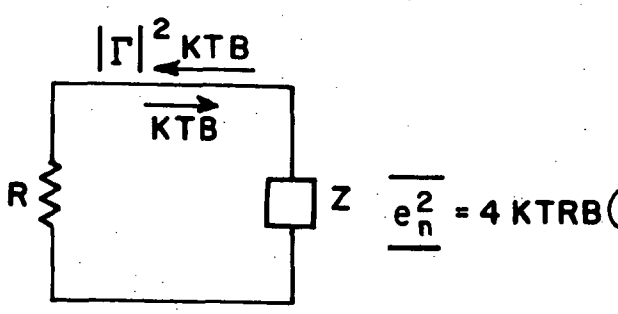

Fig. 2. A resistor delivers noise power $P_N = KTB$ to a load Z.

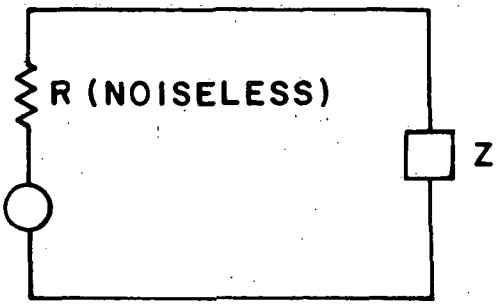

Fig. 3. The noisy resistor in Fig. 2 can be replaced by a noiseless resistor R in series with an equivalent noise voltage $\underline{e}_n$.

totally delivered to the load if and only if the load impedance is matched with the source impedance, viz., Z = R. Then no reflection occurs in the circuit and the average power absorbed by Z is given by

$$P_N = \frac{\overline{e_n^2}}{4R} = KTB, \tag{8}$$

where the bar on top denotes time-average and the underline a random variable of time.

Therefore, we can use an equivalent noise voltage $\underline{e}_n$, such that

$$\overline{\underline{e}_n^2} = 4\,KTBR, \tag{9}$$

which, in series with a noiseless resistor R, is fully equivalent to the actual noise source in the resistor.

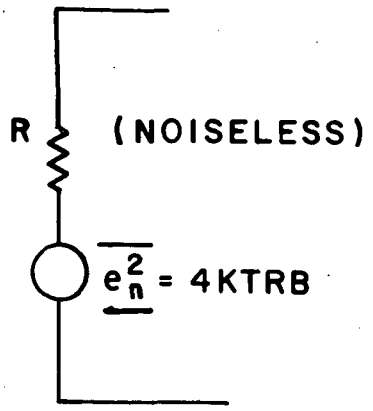

Fig. 4. Equivalent noise circuit of a resistor at temperature T.

Pure inductors and capacitors do not contribute any thermal noise since they are not dissipative elements. Lossy inductors and capacitors may be represented at any one frequency by either a series or parallel combination of a resistance and a pure reactive element; equation (9) may then be applied to the series (or parallel) resistance.

Strictly speaking, R may also be a function of frequency. The exact equivalent noise voltage e_n should be expressed as

$$\overline{e_n^2} = 4 \int_{f_1}^{f_2} R(f)s(f)df \qquad (10)$$

where s(f) is defined in equation (3).

Note that, while thermal noise is a random phenomenon, at thermal equilibrium its statistics will not vary with time. At thermal equilibrium, noise can therefore be considered a stationary process. P_N is the expected value of the noise power and $\overline{e_n^2}$ is the expected value of the square of the noise voltage, while the expected value of the noise

voltage is zero.

D. Noise Flow in Lossy Transmission Elements

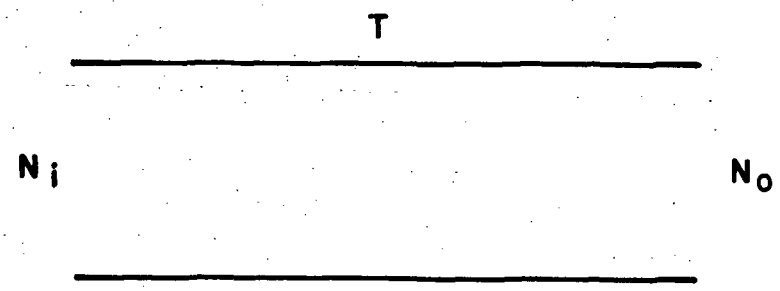

Fig. 5. A transmission element at temperature T.

Suppose we have noise power N_i (expected value) to be transmitted through a lossy element at temperature T. Then the noise coming from the lossy element should contribute part of its noise power to the output noise power N_o. Thus we expect an equation of the form

$$N_o = A_t N_i + CKTB, \tag{11}$$

where A_t is the transmission coefficient of the lossy transmission element. C is also a factor depending on the physical constants of the lossy element; it can be determined as follows.

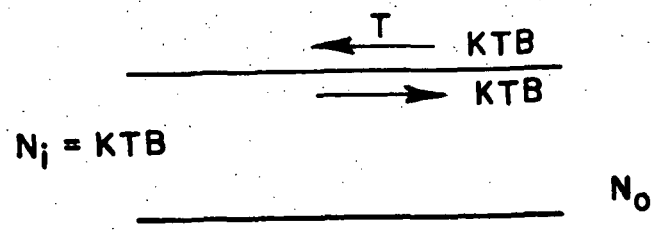

Fig. 6. Noise flow at thermal equilibrium.

Let N_i = KTB and assume the whole system is at thermal equilibrium. Then the same noise power must flow in both directions; so the noise output is also

$$N_o = KTB . \tag{12}$$

Therefore we can determine C from equation (11) as

$$C = 1 - A_t , \tag{13}$$

so that equation (11) becomes

$$N_o = A_t N_i + (1 - A_t) KTB . \tag{14}$$

For a lossy transmission line or waveguide having attenuation constant α neper/m with length ℓ,

$$A_t = e^{-2\alpha\ell} , \tag{15}$$

and we have

$$N_o = e^{-2\alpha\ell} N_i + (1 - e^{-2\alpha\ell}) KTB . \tag{16}$$

E. Noise of Directional Couplers

To determine the noise coming from a directional coupler, first consider the ways by which a signal is attenuated in it. By this means, we can find the dissipation of a signal in a directional coupler and then, in turn, get the thermal noise coming from a directional coupler since thermal noise is related to dissipation.

There are three mechanisms by which a signal may be attenuated in a directional coupler:

1) The reflection caused by mismatched terminations;

2) Energy division at the junction; and

3) Attenuation caused by waveguide walls.

The reflection of signal in each arm of a directional coupler will cause imperfect transmission of signals. However, reflection loss is not dissipative and therefore will not contribute thermal noise to the circuit.

At the junction the incident energy is divided into several parts which are propagated toward the ports. This division per se is not dissipative; therefore, this mechanism is not a source of thermal noise either.

The currents in the walls of imperfect conductors introduce dissipation by resistive (Joule) heating. Therefore, energy is dissipated in the waveguide walls. This dissipative wall loss does cause noise. We'll treat this kind of loss by considering the lossy walls as transmission or waveguiding elements and using the method described in the previous section to evaluate the noise contributed from them.

Although the loss may be distributed through the coupler, a reasonable approximation is to lump the dissipative loss at the input and output ports, and then to treat the coupler as a lossless junction.

F. 4-Port Directional Couplers

Consider a lossless directional coupler as shown in Fig. 7, and assume that port 1 is uncoupled from port 2 and port 3 from port 4. Such a coupler is called a hybrid. Fig. 8 shows the physical structure of one kind of practical hybrid.

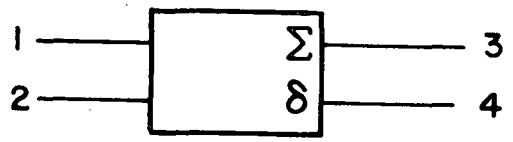

Fig. 7. A directional coupler.

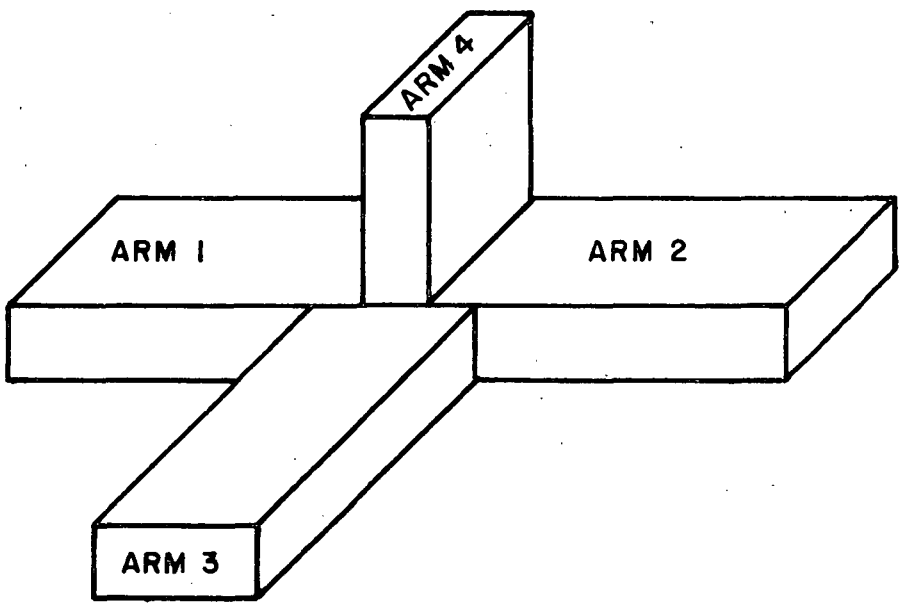

Fig. 8. Physical structure of a practical hybrid.

If there is no reflection in each input arm when the coupled arms are properly terminated in external impedances, the hybrid is often called a "magic tee".

If the characteristic impedances of all arms are identical and the network is lossless, then it has the scattering matrix [4, 5]

$$[S] = \begin{bmatrix} 0 & 0 & \sqrt{A} & \sqrt{1-A} \\ 0 & 0 & -\sqrt{1-A} & \sqrt{A} \\ \sqrt{A} & -\sqrt{1-A} & 0 & 0 \\ \sqrt{1-A} & \sqrt{A} & 0 & 0 \end{bmatrix} \tag{17}$$

where $$0 \leq |A| \leq 1 \, . \tag{18}$$

In the case of summing the input signals, A may be adjusted to be real in order to get the summation of coherent input signals. If coherent signals are applied to ports 1 and 2, the output signals can be computed by

$$S_{03} = (\sqrt{AS_1} + \sqrt{(1-A)S_2})^2 \, , \tag{19}$$

$$S_{04} = (\sqrt{(1-A)S_1} - \sqrt{AS_2})^2 \, , \tag{20}$$

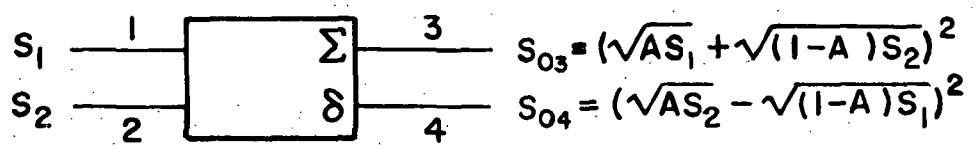

Fig. 9. Transmission of coherent input signals.

where S_{03} is the output signal power at port 3,

S_{04} is the output signal power at port 4,

S_1 is the input signal power at port 1, and

S_2 is the input signal power at port 2.

Note that

$$S_{03} + S_{04} = S_1 + S_2 , \tag{21}$$

showing that energy conservation holds at this junction, as is proper for a lossless network.

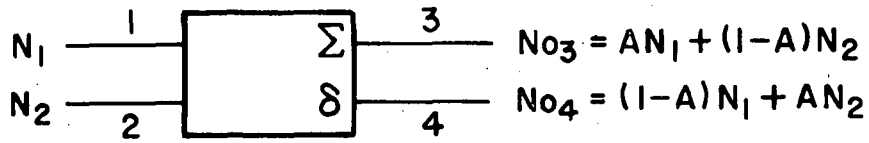

Fig. 10. Transmission of incoherent noise inputs.

The incoherent output noise powers will be (see Appendix C)

$$N_{03} = AN_1 + (1-A)N_2 \tag{22}$$

$$N_{04} = (1-A)N_1 + AN_2 \tag{23}$$

where N_1, N_2 are input noise powers at ports 1 and 2, and N_{03} and N_{04} are output noise powers at ports 3 and 4, respectively.

Similar to the coherent-signal case, we have

$$N_{03} + N_{04} = N_1 + N_2 . \tag{24}$$

If the input noises are identical, $N_1 = N_2 = N$, then we find

$$N_{03} = N_{04} = N, \tag{25}$$

i.e., the output noise at each output port will be independent of A and the same as the single-channel input noise.

The S/N ratio at port 3, which is called the summing port because of the + sign in equation (19), is

$$\frac{S_{03}}{N_{03}} = \frac{[\sqrt{AS_1} + \sqrt{(1-A)S_2}]^2}{AN_1 + (1-A)N_2} \tag{26}$$

The value of A for which the optimum noise performance is achieved is [8]

$$A = \frac{N_2^2 S_1}{N_2^2 S_1 + N_1^2 S_2} , \tag{27}$$

and the best SNR under this condition is

$$\left(\frac{S_o}{N_o}\right)_{max} = \frac{S_1}{N_1} + \frac{S_2}{N_2} . \tag{28}$$

G. 3 - db Hybrid

In many situations, the two inputs of a coupler are symmetrical. From equation (27), we choose for this case

$$A = \frac{1}{2} , \tag{28}$$

and the outputs become

$$S_{03} = \frac{1}{2}(\sqrt{S_1} + \sqrt{S_2})^2 , \tag{29}$$

$$S_{04} = \frac{1}{2}\left(\sqrt{S_1} - \sqrt{S_2}\right)^2 , \tag{30}$$

$$N_{03} = N_{04} = \frac{1}{2}\left(N_1 + N_2\right) . \tag{31}$$

This is called a "3-db hybrid tee" and its noise behavior is given by equation (31).

Notice that, for identical input signals $S_1 = S_2 = S$, the network still gives 100% power transmission to the sum port and none to the difference port,

$$S_{03} = 2S , \tag{32}$$

$$S_{04} = 0 . \tag{33}$$

With equal but incoherent noise powers applied to ports 1 and 2, $N_1 = N_2 = N$, the sum-port output is

$$N_{03} = N_{04} = N , \tag{34}$$

which is the same as the single-channel input noise.

From equations (25) and (27), one can calculate the signal-to-noise ratio

$$\frac{S_0}{N_0} = 2\,\frac{S}{N} , \tag{35}$$

or

$$\frac{(S_0/N_0)}{(S_i/N_i)} = 2 \tag{36}$$

showing a 3 - db SNR improvement over either of the inputs.

H. Combination of More Than 2 Inputs

Suppose a n-port input and n-port output network, as in Fig. 11,

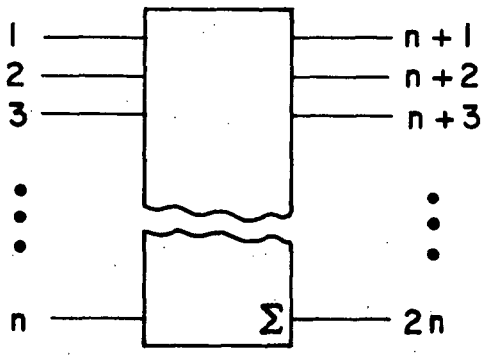

Fig. 11. A n-port input and n-port output summing network.

consists only of lossless directional couplers to sum more than 2 input signals. Figure 12(a) shows an example used in practical circuits; Fig. 12(b) shows another example, where some lossy devices, such as phase shifters, are inserted between directional couplers. We shall consider a lossless network first, in this section, and generalize to lossy cases later in this chapter.

Consider the lossless, reciprocal network in Fig. 11. By suitable

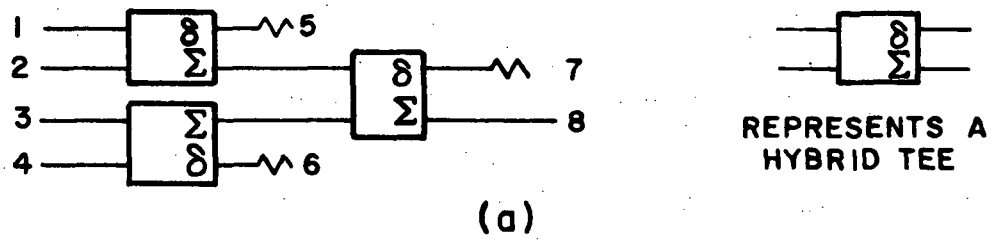

Fig. 12. Some examples of combining more than 2 inputs by using directional couplers:
(a) Combiner with terminal 8 as the output.

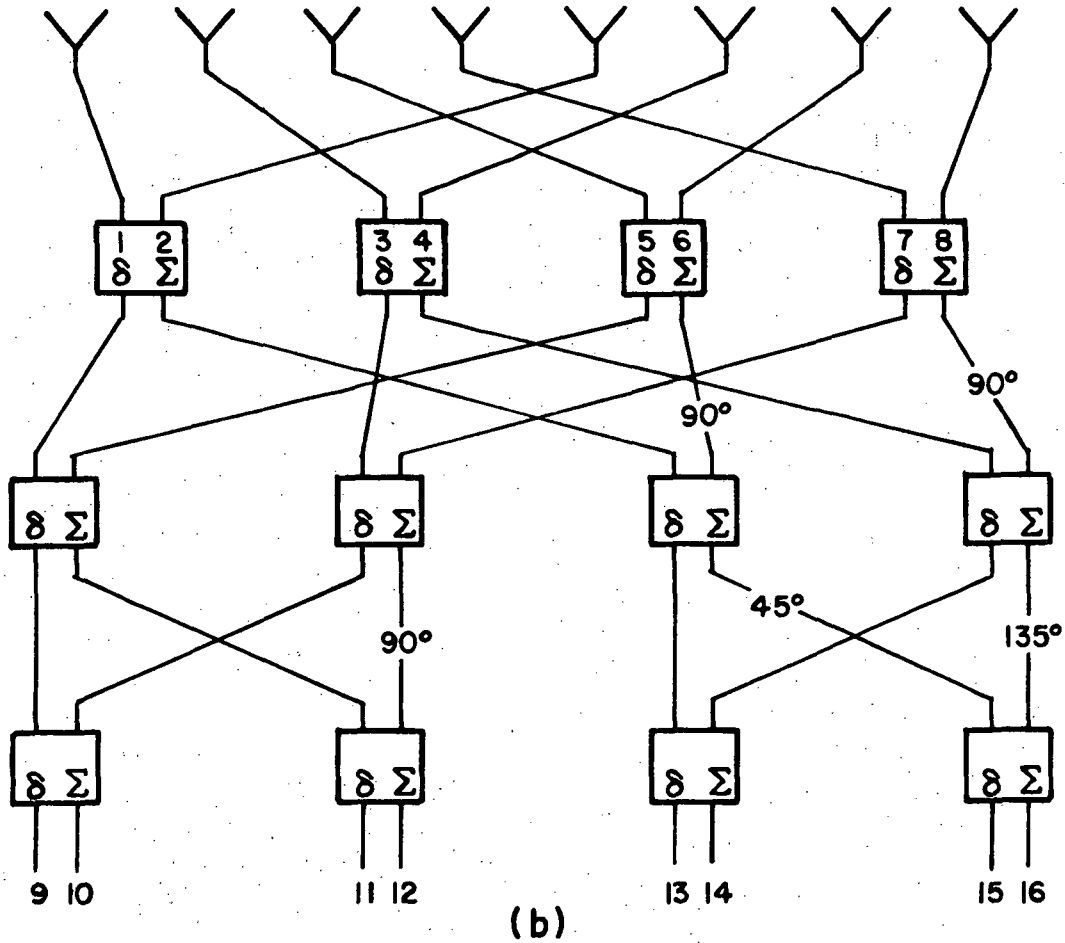

(b) Beam-forming matrix using hybrid-tee devices and phase shifters in a multiple-beam array.

design, we can have all input ports and output ports uncoupled, respectively, and all ports matched. The scattering matrix then is [9, 10]

$$S = \left[\begin{array}{ccc|ccc} 0 & \cdots & 0 & S_{1n+1} & \cdots & S_{12n} \\ \vdots & & \vdots & \vdots & & \\ 0 & \cdots & 0 & S_{nn+1} & \cdots & S_{n2n} \\ \hline S_{n+11} & \cdots & S_{n+1n} & 0 & \cdots & 0 \\ \vdots & & \vdots & \vdots & & \vdots \\ S_{2n1} & \cdots & S_{2nn} & 0 & \cdots & 0 \end{array}\right] . \tag{37}$$

The upper left quadrant indicates that the inputs are matched and isolated; the lower right quadrant indicates that the outputs are also matched and isolated.

If all the characteristic impedances are identical and the junction is lossless [11], the scattering matrix will obey

$$[S]\,[S]^{+} = [E] , \tag{38}$$

where $[S]^{+}$ is the Hermitian conjugate of [S] and [E] is the unit matrix, which has 1 for all elements on the principal diagonal and zero for all other elements.

An equivalent statement is

$$\sum_{i=1}^{2n} S_{\ell i}\, S_{ki}^{*} = \delta_{\ell k} . \tag{39}$$

With the reciprocity relationship

$$S_{ij} = S_{ji} , \tag{40}$$

the output signal of the summation at port 2n is

$$S_0 = \left| \sum_{i=1}^{n} S_{2ni} \sqrt{S_i} \right|^2 . \tag{41}$$

If all the inputs are identical and equal to S, then

$$S_0 = \left| \sum_{i=1}^{n} S_{2ni} \right|^2 S . \tag{42}$$

The corresponding noise output is

$$N_0 = \sum_{i=1}^{n} | S_{2ni} |^2 N_i , \tag{43}$$

subject to all noise outputs being incoherent. (See Appendix C).

If all noise inputs have the same average power N, then equation (43) becomes

$$N_0 = \sum_{i=1}^{n} |S_{2ni}|^2 N = N \tag{44}$$

since from equation (39), we have

$$\sum_{i=1}^{n} |S_{2ni}|^2 = 1 . \tag{45}$$

If all the inputs are equally transferred to the summing port, then it follows

$$\sum_{i=1}^{n} |S_{2ni}|^2 = n|S_{2ni}|^2 = 1,$$

or

$$|S_{2ni}| = \frac{1}{\sqrt{n}} \quad . \tag{46}$$

In case that all inputs are identical, $S_i = S$ for all i, equations (42) and (46) lead to

$$S_0 = nS \quad . \tag{47}$$

The output SNR then becomes

$$\frac{S_o}{N_o} = n \frac{S}{N} \quad . \tag{48}$$

Such a network therefore yields an n-fold improvement in SNR.

I. More General Cases

In some cases the characteristic impedances of the ports of a multiport network are not identical; instead, let them be designated $Z_1, Z_2, \ldots, Z_n$ for ports 1, 2, - - - , n, respectively.

Suppose all these characteristic impedances are real, then the scattering matrix for a n-port lossless network should be modified into (see Appendix A)

$$S = \begin{bmatrix} \sqrt{\frac{Z_1}{Z_1}}\alpha_{11} & \sqrt{\frac{Z_1}{Z_2}}\alpha_{12} & \cdots & \sqrt{\frac{Z_1}{Z_n}}\alpha_{1n} \\ \sqrt{\frac{Z_2}{Z_1}}\alpha_{21} & \sqrt{\frac{Z_2}{Z_2}}\alpha_{22} & \cdots & \sqrt{\frac{Z_2}{Z_n}}\alpha_{2n} \\ \vdots & \vdots & & \vdots \\ \sqrt{\frac{Z_n}{Z_1}}\alpha_{n1} & \sqrt{\frac{Z_n}{Z_2}}\alpha_{n2} & & \sqrt{\frac{Z_n}{Z_n}}\alpha_{nn} \end{bmatrix} \tag{49}$$

with the energy conservation relationship

$$\sum_{i=1}^{n} |\alpha_{ij}|^2 = 1 , \tag{50}$$

(see Appendix A), the reciprocity relationship

$$\frac{S_{ij}}{Z_i} = \frac{S_{ji}}{Z_j} , \tag{51}$$

and the definition of the α_{ij},

$$\alpha_{ij} = \sqrt{\frac{Z_j}{Z_i}}\, S_{ij} . \tag{52}$$

Substituting equation (52) into equation (51), we get

$$\alpha_{ij} = \alpha_{ji} . \tag{53}$$

The output signal power at port n is

$$S_o = \left(\sum_{i=1}^{n} |S_{ni}| \sqrt{S_i Z_i} \right)^2 / Z_n \tag{54}$$

provided that all the signals at the output are coherent.

Applying equation (52) to equation (54), we obtain

$$S_o = \left(\sum_{i=1}^{n} |\alpha_{ni}| \sqrt{S_i} \right)^2 . \tag{55}$$

Suppose all the input noise is incoherent, the output noise at port n will be

$$N_o = \left(\sum_{i=1}^{n} |S_{ni}|^2 N_i Z_i \right) / Z_n . \tag{56}$$

Applying equation (52) again, we obtain

$$N_o = \sum_{i=1}^{n} |\alpha_{in}|^2 N_i . \tag{57}$$

If all signal and power inputs are identical, then we have

$$S_o = \left(\sum_{i=1}^{n} |\alpha_{ni}|\right)^2 S \,, \tag{58a}$$

and

$$N_o = N \,. \tag{58b}$$

Once again, we get the same output noise as the input single-channel noise of any input provided that all these noise inputs are identical.

J. Parallel Connection of Transmission Lines

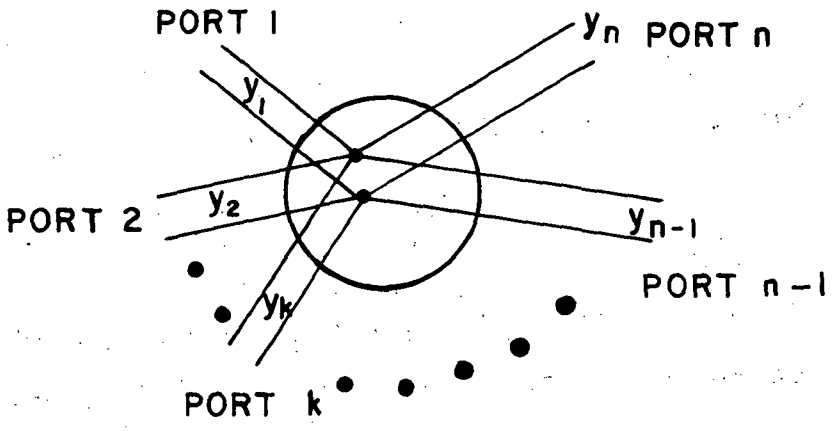

Fig. 13. Parallel connection of transmission lines.

1. General Considerations

Consider a junction of n transmission lines with characteristic admittances $Y_1, Y_2, \ldots, Y_n$ connected in parallel (Fig. 13). Suppose every transmission line is externally terminated in its own characteristic impedance, then we can have the scattering matrix as (See Appendix B)

$$S = \begin{bmatrix} \frac{2Y_1 - \Sigma Y_j}{\Sigma Y_j} & \frac{2Y_2}{\Sigma Y_j} & \cdots & \frac{2Y_n}{\Sigma Y_j} \\ \frac{2Y_1}{\Sigma Y_j} & \frac{2Y_2 - \Sigma Y_j}{\Sigma Y_j} & \cdots & \frac{2Y_n}{\Sigma Y_j} \\ \vdots & \vdots & & \vdots \\ \frac{2Y_1}{\Sigma Y_j} & \frac{2Y_2}{\Sigma Y_j} & \cdots & \frac{2Y_n - \Sigma Y_j}{\Sigma Y_j} \end{bmatrix} . \tag{59}$$

Notice that equation (59) satisfies equations (49), (50) and (51).

The output voltage at port n is

$$V_n^- = \sum_{i=1}^{n-1} \frac{2Y_i V_i^+}{\sum_{j=1}^{n} Y_j} + \frac{2Y_n - \sum_{j=1}^{n} Y_j}{\sum_{j=1}^{n} Y_j} V_n^+ , \tag{60}$$

or

$$V_n^- = \sum_{i=1}^{n} \frac{Y_i(2V_i^+ - V_n^+)}{\sum_{j=1}^{n} Y_j} . \tag{61}$$

For identical input voltages,

$$V_1^+ = V_2^+ = \cdots = V_{n-1}^+ = V , \tag{62}$$

and

$$V_n^+ = 0 , \tag{63}$$

this yields

$$V_n = \frac{\sum_{i=1}^{n-1} 2Y_i V}{\sum_{j=1}^{n} Y_j} . \tag{64}$$

Even when the input voltages are not identical, the power output, by using equations (52) and (55), is seen to be

$$S_o = \left(\sum_{i=1}^{n} \frac{2\sqrt{Y_i Y_n S_i}}{\sum_{j=1}^{n} Y_j} - \sqrt{S_n} \right)^2 \tag{65}$$

subject to all input signals adding coherently at the output. When all incident input powers are identical,

$$S_1 = S_2 = S_3 = \ldots = S_{n-1} = S , \tag{66}$$

and the output is terminated in a matched load,

$$S_n = 0 , \tag{67}$$

then the output power will become

$$S_o = 4\left(\frac{\sum_{i=1}^{n-1} \sqrt{Y_i S}}{\sum_{i=1}^{n} Y_i} \right)^2 \quad Y_n = \frac{4\left(\sum_{i=1}^{n-1} \sqrt{Y_i} \right)^2 Y_n S}{\left(\sum_{i=1}^{n} Y_i \right)^2} \tag{68}$$

And the noise output power is

$$N_o = \sum_{i=1}^{n-1} \frac{4Y_i Y_n}{\left(\sum_{j=1}^{n} Y_j \right)^2} N_i + \frac{\left(2Y_n - \sum_{j=1}^{n} Y_j \right)^2}{\left(\sum_{j=1}^{n} Y_j \right)^2} N_n$$

$$= \sum_{i=1}^{n} \frac{4Y_i Y_n}{\left(\sum Y_i \right)^2} (N_i - N_n) + N_n \quad . \tag{69}$$

If all incident noise inputs are identical

$$N_1 = N_2 = \ldots = N_n = N \tag{70}$$

then

$$N_o = N . \tag{71}$$

If $N_n = 0$, then we obtain

$$N_o = \frac{4Y_n \sum_{i=1}^{n-1} Y_i N_i}{\left| \sum_{j=1}^{n} Y_j \right|^2} . \tag{72}$$

It should be noted that, for the general case discussed so far, there may be outward directed signal waves as well as noise waves at input ports. The inputs will not present a match to their respective sources when either equal incident voltages or coherent and equal incident powers are applied. Special cases which allow such a matched condition are discussed next.

2. Some Useful Special Cases

Suppose we have a port, say port n, having the characteristic admittance equal to the sum of those of all others, i.e.,

$$Y_n = \sum_{i=1}^{n-1} Y_i , \tag{73}$$

then the scattering matrix will be reduced to (Fig. 14)

$$S = \begin{bmatrix} \frac{Y_1 - Y_n}{Y_n} & \frac{Y_2}{Y_n} & \cdots & \frac{Y_{n-1}}{Y_n} & 1 \\ \frac{Y_1}{Y_n} & \frac{Y_2 - Y_n}{Y_n} & \cdots & \frac{Y_{n-1}}{Y_n} & 1 \\ \vdots & \vdots & & \vdots & \vdots \\ \frac{Y_1}{Y_n} & \frac{Y_2}{Y_n} & \cdots & \frac{Y_{n-1}}{Y_n} & 0 \end{bmatrix} . \tag{74}$$

Then equation (49) becomes

$$V_n^- = \sum_{i=1}^{n-1} \frac{Y_i}{Y_n} V_i^+ , \tag{75}$$

and the output voltage at other ports will be

$$V_j^- = \sum_{i=1}^{n} \frac{Y_i}{Y_n} V_i^+ - V_j^+ , \; j \neq n. \tag{76}$$

Applying equal excitation voltages to the network,

$$V_1^+ = V_2^+ = \cdots = V_{n-1}^+ = V^+ , \tag{77}$$

and terminating the output in Y_n, so that

$$V_n^+ = 0 , \tag{78}$$

we will have

$$V_n^- = \sum_{i=1}^{n-1} \frac{Y_i}{Y_n} V^+ = V^+ \tag{79}$$

and all other output voltages will become

$$V_j^- = 0 \ , \quad j \neq n \ , \tag{80}$$

i.e., one obtains 100% efficiency at port n for summing the signal powers incident on all other ports whenever equation (73) holds.

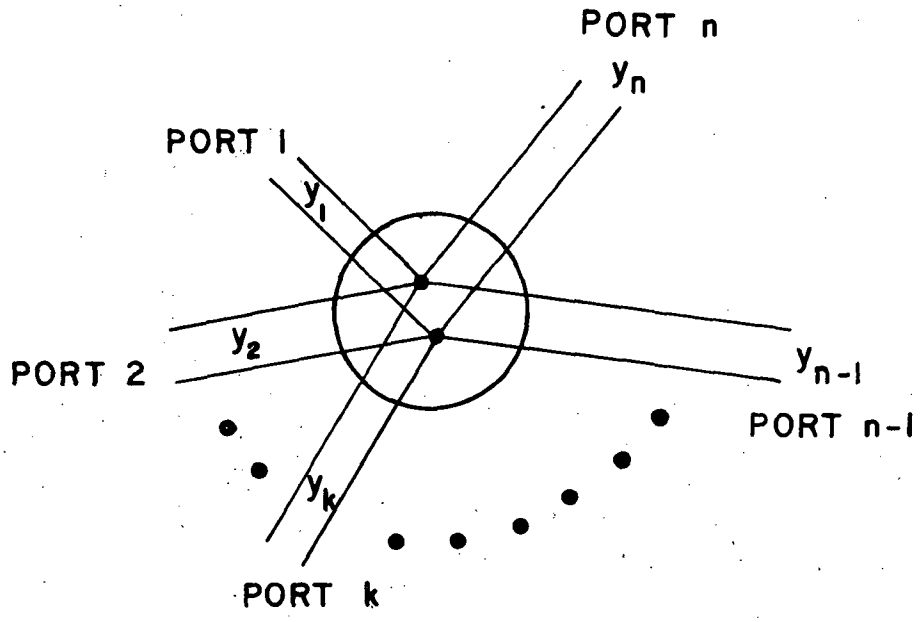

Fig. 14. Connected parallel lines with the condition $Y_n = \sum_{i=1}^{n-1} Y_i$.

The output signal power and noise power are given, for arbitrary excitation, by

$$S_o = \frac{1}{Y_n} \left(\sum_{i=1}^{n-1} \sqrt{Y_i S_i} \right)^2 \ , \tag{81}$$

$$N_o = \sum_{i=1}^{n-1} \frac{Y_i}{Y_n} N_i \ , \tag{82}$$

$$N_o = \frac{1}{Y_n} \sum_{i=1}^{n-1} Y_i N_i \ , \tag{83}$$

or

$$N_o = Z_n \sum_{i=1}^{n-1} \frac{N_i}{Z_i} \ . \tag{84}$$

A frequently used special case (Fig. 15) of this network is that of equal characteristic impedances of the input ports, so that

$$Z_1 = Z_2 = \ . \ . \ . \ = Z_m = mZ_o \ , \tag{85}$$

and

$$Z_{m+1} = Z_o \ . \tag{86}$$

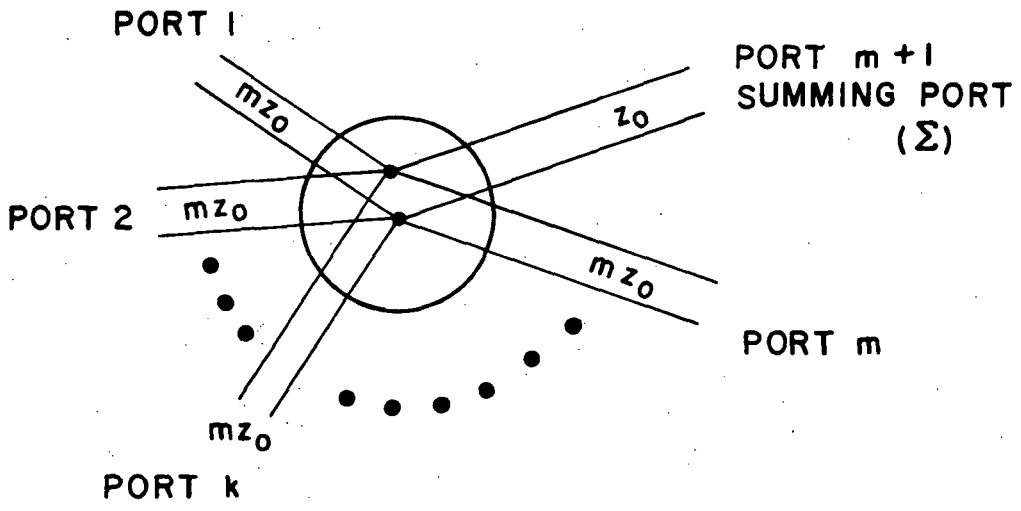

Fig. 15. A special case.

Then we have

$$V_o^- = \frac{1}{m} \sum_{i=1}^{m} V_i^+ \ , \tag{87}$$

$$S_o = \frac{1}{m} \left(\sum_{i=1}^{m} \sqrt{S_i} \right)^2 , \tag{88}$$

and

$$N_o = \frac{1}{m} \sum_{i=1}^{m} N_i , \tag{89}$$

respectively.

For identical coherent signal inputs and equal average noise power inputs, one obtains

$$S_o = mS \tag{90}$$

and

$$N_o = N . \tag{91}$$

Then the signal-to-noise ratio becomes

$$\frac{S_o}{N_o} = m \frac{S}{N} , \tag{92}$$

showing an m-fold SNR improvement over any of the single inputs.

K. Lossy Junctions

As stated in Appendix A, the more general case for a reciprocal *n-port network is that the scattering matrix is given by*

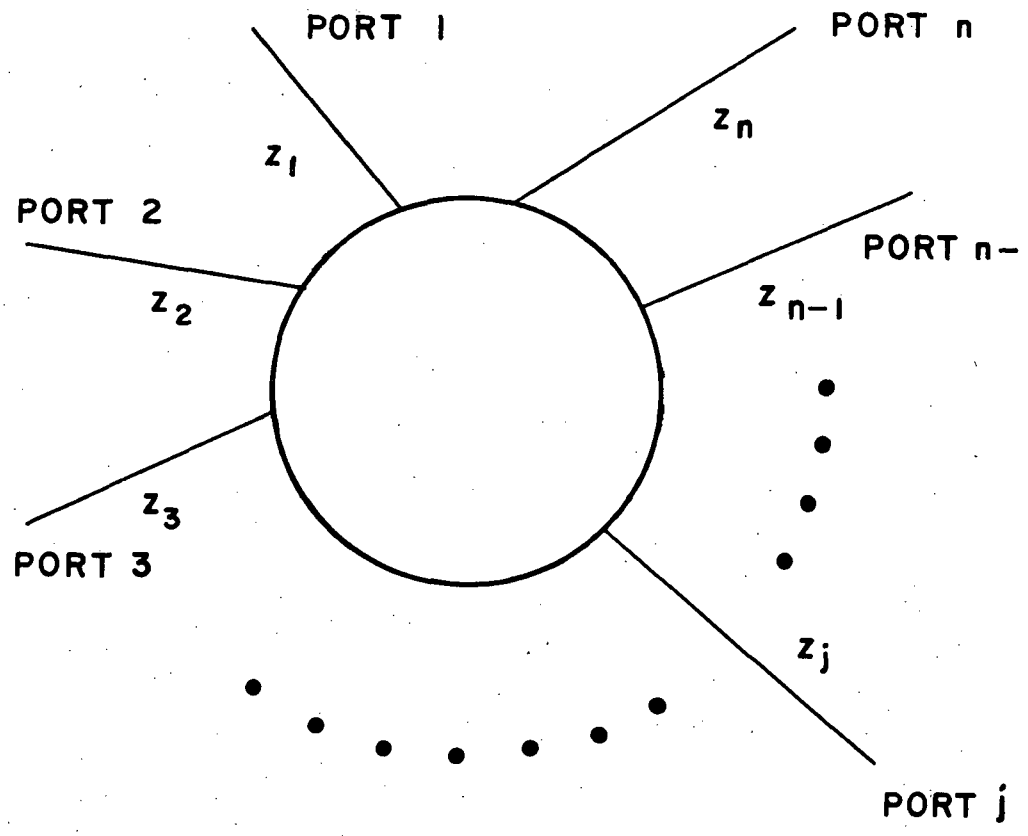

Fig. 16. A lossy network.

$$S = \begin{bmatrix} \sqrt{\frac{Z_1}{Z_1}}\,\alpha_{11} & \sqrt{\frac{Z_1}{Z_2}}\,\alpha_{12} & \cdots & \sqrt{\frac{Z_1}{Z_n}}\,\alpha_{1n} \\ \sqrt{\frac{Z_2}{Z_1}}\,\alpha_{21} & \sqrt{\frac{Z_2}{Z_2}}\,\alpha_{22} & \cdots & \sqrt{\frac{Z_2}{Z_n}}\,\alpha_{2n} \\ \vdots & \vdots & & \vdots \\ \sqrt{\frac{Z_n}{Z_1}}\,\alpha_{n1} & \sqrt{\frac{Z_n}{Z_2}}\,\alpha_{n2} & & \sqrt{\frac{Z_n}{Z_n}}\,\alpha_{nn} \end{bmatrix} , \tag{93}$$

with

$$\sum_{i=1}^{n} |\alpha_{ij}|^2 \leq 1 , \tag{94}$$

and

$$\alpha_{ij} = \alpha_{ji} . \tag{95}$$

The output signal at port k is

$$S_{ko} = \left(\sum_{i=1}^{n} \alpha_{ik} \sqrt{S_i} \right)^2 \tag{96}$$

The contribution of inward uncorrelated noise to the output is

$$N_o \text{ by input noise} = \sum_{i=1}^{n} |\alpha_{in}|^2 N_i , \tag{97}$$

and the total output noise is [12, 13, 14]

$$N_o = \sum_{i=1}^{n} |\alpha_{in}|^2 N_i + (1 - \sum_{i=1}^{n} |\alpha_{in}|^2) P_N \qquad (98)$$

where P_N is the thermal noise power defined in equation (1).

Our formulation differs from that of Wait in that equation (98) gives the outward-traveling noise power at port i when all inward-traveling noise powers (including that at terminal i) are specified, while Wait gives the available noise powers. The two formulations become identical when port i is terminated in a matched load.

CHAPTER III

NOISE PERFORMANCE IN PASSIVE ARRAYS

A. Introduction

As discussed in the previous chapters, noise behavior depends on system (or network) parameters, which are closely related to the element organization, i.e., the manner of interconnecting the elements. The theory developed in the previous chapter can be applied directly to antenna arrays. For example, the beam-forming matrix of Fig. 12b is precisely a multiport of the type shown in Fig. 11, with the antenna elements connected to the input ports 1-8 and the formed beams available at the output ports 9-16. If, as is usual, the output ports are uncoupled with respect to each other, or if there is only a single output, then the noise at the outputs will consist of that contributed from the inputs and that originating from within the network. The elements contribute noise because of two effects. First, they receive noise just as they receive signal; this noise is termed "external noise". Secondly, since they are lossy, they contribute also thermal noise. In large arrays, the thermal noise arising in the elements is usually much less than that arising in the combining networks; at any rate the elements usually can, to a good approximation, be represented as lossless elements followed by a lossy network which can then be included in the

multiport. The thermal noise arising from the multiport (including the thermal contribution from the elements) is termed "internal noise".

In this thesis, only the internal noise will be considered. One reason is that the definition of external noise depends strongly on the application for which the array is to be used. For example, if an array in space is to be used to receive communication signals from the Earth, the thermal emission of the Earth would be considered noise. If the same array were to be used for radiometry, the same thermal radiation would be considered signal. A second reason for neglecting external noise is that it does not appear incoherently at the inputs; its contribution is therefore governed not only by the array organization but also by the antenna pattern and the brightness distribution of the external noise sources. This makes it difficult to draw general conclusions when external noise is included. A third reason for neglecting the external noise is that in the frequency range under consideration it is generally not large and, in any case, the limitations and trade-offs of large arrays which are of interest in this thesis are related to the internal, not the external, noise.

The quantity of most interest in this Chapter will be the normalized, or relative, ratio of signal to internal noise. The normalization factor is employed to eliminate variables which are unrelated to the array organization. One such variable is the signal strength available from each element, which depends on the incident signal power, its direction of arrival, and the directive

gain of the elements. Similarly, the internal noise contribution depends on the system bandwidth and the ambient temperature of the combining multiport, which is restricted to be passive in this Chapter (active combiners will be considered in Chapter IV).

We can write the ratio of signal to internal noise at an output as

$$S_o/N_o = R\, S/P_N \approx RS/KTB \,, \qquad (1)$$

where S is the signal power available at the terminals of each element, R is the relative signal-to-noise ratio, and the other symbols have the same meaning as in the previous chapters. The signal will be assumed to be coherently summable at the output. A sufficiently narrow band or cw signal arriving from a specific direction meets this requirement for even large arrays. The meaning of R is simply that of a number which, when multiplied by (S/KTB), gives the ratio of signal to internally generated noise at the output. It does not imply a signal-to-noise ratio relative to some other reference array nor an improvement over some other technique of organizing the array.

It will be seen below that for small arrays, the relative signal-to-noise ratio increases as more elements are added. After a certain size is reached, however, additional elements must be quite distant from the sum port; the lossy signal path between the element and the sum port then attenuates the signal and contributes thermal noise increasingly as the array is made larger, so that R increases more slowly, becomes stationary, and finally decreases as the array size is increased. This effect is illustrated in this Chapter by a

series of parametric calculations of the relative signal-to-noise ratio, plotted with either the number of elements or the array dimension as the independent variable and such quantities as transmission line loss factor and phase shifter loss as parameters.

A variety of algorithms may be adopted for increasing the array size in the calculations. The weight or emphasis to be given the added elements is completely at the designer's disposal. One possible algorithm is to weight the elements in such a way that a given aperture distribution is preserved. This has the disadvantage that elements furthest from the output will be weighted most, since they experience the greatest attenuation. Weighting these noisiest elements heavily is very detrimental to the output signal-to-noise ratio. Another algorithm is to weight each element according to its signal-to-noise ratio; this produces an optimum output signal-to-(internal) noise ratio. It also results in a high weighting of the near elements relative to distant ones, and therefore in greatly reduced directivity. The objectives of achieving high signal-to-noise ratio and high directivity become incompatible, in general, as array size is increased, and a compromise must be made. An infinity of such compromises is possible; in the calculations the compromise is made on the basis of computational ease. It should be noted that when the array is small and has low loss, the range of compromises is small. The choice of algorithm has a substantial effect only when the array losses and internal noise are large. Under these circumstances the array is likely to have limited utility. The calculations have been carried into this region, not to provide design curves, but to show the generality of

the deterioration of the relative signal-to-noise ratio as arrays become large. An exception to the divergence of the criteria for preserving the aperture distribution and optimizing signal-to-noise ratio is the case of corporate-fed arrays. In these, equal attenuation is maintained in all signal paths as the array size is increased; thus, signal-to-noise ratio is optimized (within the class of corporate-fed structures) and the aperture distribution is maintained simultaneously if the weighting algorithm is kept constant. The details of the algorithms used to increase array size are given below for each class of arrays treated. Here we wish only to call attention to the fact that the aperture distribution is not necessarily maintained in these calculations, and give the reasons for this procedure.

In principle, it would be possible to treat each feed configuration as a multiport, evaluate the scattering matrix elements according to the theory of Chapter II, and base the calculation of relative signal-to-noise ratio on these. This approach is, however, difficult to generalize to active multiports which are treated in Chapter IV as a possible solution to the signal-to-noise deterioration of large arrays. In order to allow generalization to the active case, the procedure used also in this Chapter is to trace each signal from the element to the output, keeping track of signal attenuation and noise addition as they occur along the signal path. The theory developed for multiports is, of course, used in evaluating the effects of the multiports used to combine signal paths.

B. One-Dimensional Parallel-Fed Arrays

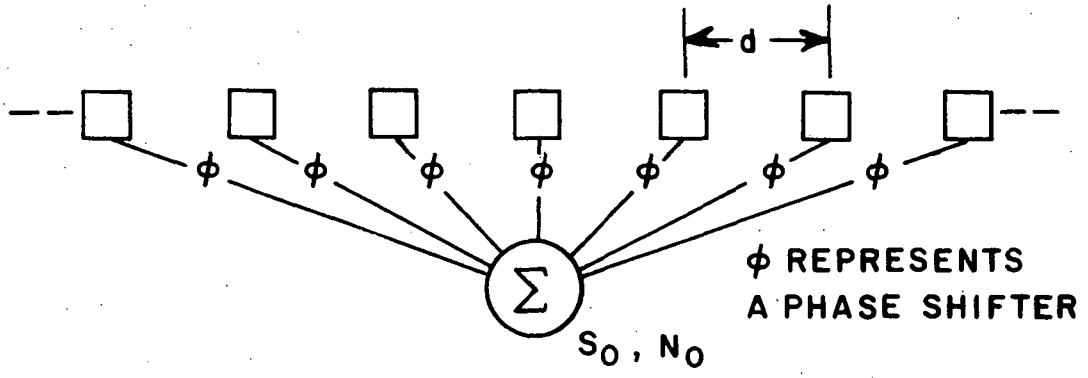

Fig. 17. A linear parallel-fed array.

A linear array with the signals from all elements passing through passive phase shifters, which are used to adjust the patterns of the array, and connected to the input ports of a summing network is shown in Fig. 17. If the number of elements is at all large, this array organization is impractical; nevertheless, it is useful to calculate the relative signal-to-noise ratio, assuming no loss in the summing network, because this configuration minimizes the length of the signal path and hence optimizes the noise behavior for a given class of transmission lines (or waveguides) and phase shifters. It can therefore be considered a case which establishes the performance limit for one-dimensional arrays.

Suppose all elements are equally spaced and designate the signal power received at the n-th element by S_n. Let the whole system be at the same temperature T, so that we have the same thermal noise powers P_N everyplace. (P_N is defined by equation (1) and an

approximation is given by equation (7) in Chapter II). The phase shift of each phase shifter is adjusted so as to have all signals arrive at the summing network coherently in order to get the maximum reception. The summing network is symmetrical with respect to all inputs. As stated in Chapter II, if all signals at the input ports are equally transferred to the output ports, we have

$$S_o(n) = \frac{1}{n} \left(\sum_{K=1}^{n} \sqrt{A_K S_K} \right)^2 , \tag{2}$$

where S_K is the signal power received at the k-th array element in watts,

$$A_K = e^{-(2\alpha d_K + \theta_K)} \tag{3}$$

is the transmission through the phase shifter and the transmission element used to connect the K-th element and the summing network, α is the attenuation constant of the transmission lines or waveguides, in nepers per meter, and d_K is the distance from K-th element to the summing network.

θ_K is the logarithmic transmission factor of the phase shifters, it can be related to the required phase shifts by [15]

$$\theta_K = F\phi_K \quad , \tag{4}$$

where ϕ_K is the maximum phase shift required of the phase shifter between K-th element and the summing network for all desired scan angles, in degrees, and F is the figure of merit of the phase shifter, nepers per degree.

$S_o(n)$ is the output power of the summing network, which is

assumed to have n inputs.

The transmission factor $e^{-\theta K}$ comes from the insertion loss of a phase shifter, such as low-loss ferrite phase shifters, for which the attenuation is proportional to the maximum required phase shift. The output internal noise power is shown by equations (14), (43), and (46) of Chapter II to be equal to

$$N_o(n) = \frac{1}{n} \sum_{K=1}^{n} P_N (1-A_K) \quad . \tag{5}$$

The S/N ratio of the n-element array is therefore

$$I_n = \frac{S_o(n)}{N_o(n)} = \frac{\left(\sum_{K=1}^{n} \sqrt{A_K S_K} \right)^2}{\sum_{K=1}^{n} (1-A_K) P_N} \quad . \tag{6}$$

With one more element, it becomes

$$I_{n+1} = \frac{S_o(n+1)}{N_o(n+1)} = \frac{\left(\sum_{K=1}^{n+1} \sqrt{A_K S_K} \right)^2}{\sum_{K=1}^{n+1} (1-A_K) P_N} \quad . \tag{7}$$

To yield an improvement for SNR of the array, we should have

$$\frac{I_{n+1}}{I_n} > 1 \tag{8}$$

or

$$A_{n+1} \frac{S_o(n+1)}{S_o(n)} + 2 \sqrt{A_{n+1} \frac{S_o(n+1)}{S_o(n)}} > (1-A_{n+1}) \frac{P_N}{N_o(n)} \quad . \tag{9}$$

By using this equation, one can estimate whether adding one more array element will yield any SNR improvement.

If all elements have identical signal reception, i.e., if

$$S_1 = S_2 = S_3 = \cdots = S_n = S \tag{10}$$

is true, equation (6) becomes

$$I_n = \frac{S_o(n)}{N_o(n)} = \frac{S}{P_N} \frac{\left(\sum_{K=1}^{n} \sqrt{AK}\right)^2}{\sum_{K=1}^{n} (1-A_K)} \tag{11}$$

and equation (7) yields

$$\frac{\left(\sum_{K=1}^{n+1} \sqrt{AK}\right)^2}{\left(\sum_{K=1}^{n} \sqrt{AK}\right)^2} > \frac{\sum_{K=1}^{n+1} (1-A_K)}{\sum_{K=1}^{n} (1-A_K)} \tag{12}$$

as the criterion for further S/N ratio improvement when elements are added. This relationship is completely independent of S and P_N, but depends on α, d_K and θ_K, i.e., the physical constants of the connecting elements.

Equation (12) can also be expressed as

$$A_{n+1} + 2\sqrt{A_{n+1}} \left(\sum_{K=1}^{n} \sqrt{A_K}\right) > (1 - A_{n+1})\, I_n \tag{13}$$

Notice that A_K is always less than unity and decreases exponentially as K increases. What is more, I_n is a monotonically increasing function as long as equation (13) holds. Therefore, the right-hand side of equation (12) gets larger but the left-hand side, while increasing initially, eventually becomes smaller as the number of array elements increases. After reaching some sufficiently large n, the inequality of equation (13) will be violated. At this value the signal-to-noise ratio will begin to decrease and the sys-

tem will gain no further benefit by adding more array elements. This type of signal-to-noise behavior is also typical of other array configurations, as shown in the plotted results of the following sections.

C. Two-Dimensional Parallel-Fed Arrays

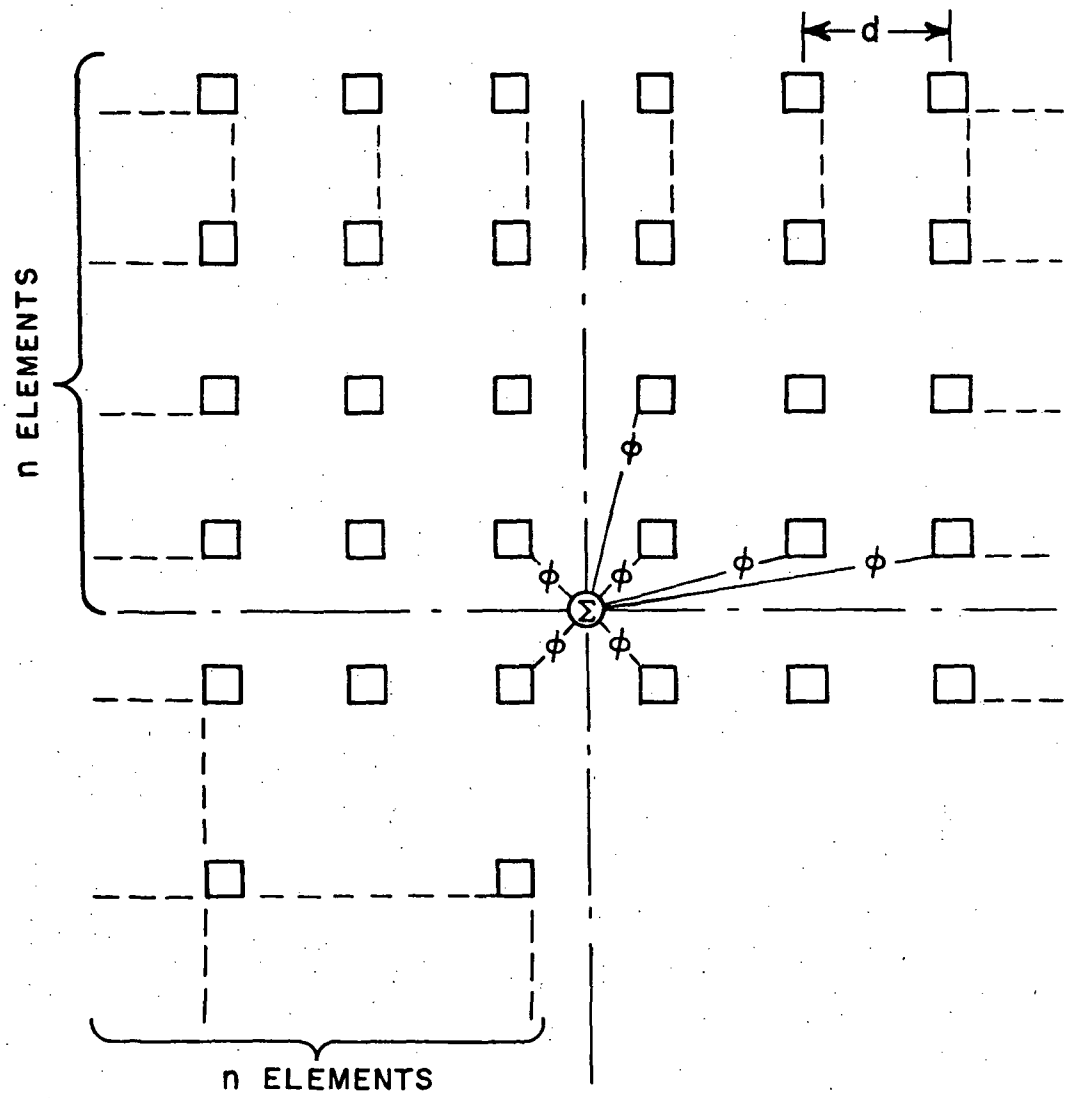

Fig. 18. A centrally parallel-fed array of $4n^2$ elements.

Two-dimensional (planar) arrays will now be discussed. Many ways of connecting the elements are available, depending on the function of the array, and it is impossible to perform a signal-to-noise analysis for all configurations. Instead, we shall examine again the parallel-fed case as an upper limit of the signal-to-noise performance, and some corporate structures as examples of more practical arrangements of an array.

Consider a square centrally parallel-fed array as shown in Fig. 18. By using similar arguments as in the previous sections, one can easily get the following:

$$S_o(n) = \left(\frac{1}{2n} \sum_{K=-n}^{n} \sum_{m=-n}^{n} \sqrt{S_{mK}\, e^{-2\alpha d_{mK} - \theta_{mK}}}\right)^2 , \tag{14}$$

$$N_o(n) = \frac{1}{4n^2} \sum_{K=-n}^{n} \sum_{m=-n}^{n} P_N\left(1 - e^{-(2\alpha d_{mK} + \theta_{mK})}\right) \tag{15}$$

with $m, K \neq 0$, where d is the spacing of elements, and

$$d_{mK} = d\sqrt{(m-1/2)^2 + (K - 1/2)^2} \tag{16}$$

is the distance from the element in row m and column K to the feed point.

Suppose we have a lossless summing network with $4n^2$ identical inputs, one for each element, and that the maximum required phase shifts are symmetrical, leading to the relations

$$\phi_{mn} = \phi_{-m-n} \cdot \tag{17}$$

Then the equations (14) and (15) can be simplified as

$$S_o(n) = \frac{1}{4n^2}\left(\sum_{K=1}^{n}\sum_{m=1}^{n}\sqrt{Se^{-2\alpha d_{mK}-\theta_{mk}}}\right)^2 , \qquad (18)$$

$$N_o(n) = \frac{1}{4n^2}\left(\sum_{K=1}^{n}\sum_{m=1}^{n} P_N\left(1 - e^{-2\alpha d_{mK}-\theta_{mK}}\right)\right) . \qquad (19)$$

Notice we have kept the same assumptions as before,

(1) the summing network is lossless and adds all the signals coherently at the summing port,

(2) all the noise adds incoherently since each term represents thermal noise from a separate group of dissipative elements.

Figures 19 to 21 show the relative signal-to-noise of centrally parallel-fed planar arrays as calculated by using equations (18) and (19).

The choice of parameters in Figs. (19) to (21) was dictated by the intended application of this work to a very large array aboard the Shuttle Spacelab. Dimensions on the order of 10 to 30 meters square were considered in the initial experiment definition. At 30 GHz, these should lead to a resolution capability of better than one milli-radian. If filled, an array of this size with spacings on the order of one wavelength would require between 10^6 and 10^7 elements. To reduce the cost, thinning is highly desirable for those applications for which it is permissible. The calculations of Figs. (19) to (21) represent thinning factors of 100-400. In practice, such thinning would be done on a random or pseudo-random basis, but the randomness has very little effect on the relative signal-to-noise ratio since only internal noise is considered here. Thus Figs. (19) to (21) should be representative

of thinned arrays of these dimensions. Another approach being considered is to use subapertures, with dimensions on the order of the spacings used in the calculations, to avoid the need for thinning. Not all problems related to this approach have been solved, but encouraging results are being obtained, both in connection with this program and by others [16].

In equations (18) and (19) the phase shifter loss for each set of phase shifters characterized by a pair of values m, k was left arbitrary and designated θ_{mk}. For the large arrays considered here and reasonable scan angles, all phase shifters must have a phase shift capability of 360°; this value was assumed in the calculations together with a figure of merit of 300° per db to obtain the phase shifter losses.

The range of attenuation constants corresponds, for the higher values, to commercially available silver-plated waveguide. Since attenuation in this frequency range depends on surface roughness and can be reduced by electropolishing and other methods of reducing roughness, the lower values represent an estimate of what might be achieved with a customized technology. No loss was assumed for the summing network since networks with so many inputs are not available and no reasonable estimate can be made. It should be remembered, however, that the parallel-fed array calculations are intended only to show limits which practical arrays cannot exceed, not for system implementation. The assumption of no loss is consistent with a very conservative limit estimate.

The significant aspect of the curves presented in Figs. (19) to

(21), is that they rise very rapidly for small arrays, but very slowly for large arrays, and that eventually for large attenuations and dimensions they even decrease. In the range where the curves rise steeply, added elements contribute as much as those already present toward an improvement in the signal-to-noise ratio. Beyond the knee of each curve, this is far from true. Moreover, as discussed in the introduction to this Chapter, the algorithm chosen for increasing the array size in these calculations is not one which preserves the array aperture distribution. For small apertures, the distribution is almost uniform; for larger arrays it becomes tapered. For the bottom curve of Fig. 20, the taper amounts to 33 decibels, so that the outer elements are not effectively contributing to directivity either. Thus the parallel-fed case shows that simply expanding array size in order to achieve better resolution runs into fundamental signal-to-noise limitations. This is shown also in the next section for the more practical configuration of a corporate-fed array.

In all these calculations all elements are considered to behave identically; edge effects are neglected. Coupling effects which pertain to an infinite array are included, but they are hidden because of the normalization with respect to S/KTB. The signal power S available from an individual element for a given field strength is a function of the spacing between the elements because of mutual coupling effects. Thus, while the relative signal-to-noise ratio in Fig. 21 is a monotonic function of spacing, this need not be true for the actual system signal-to-noise ratio.

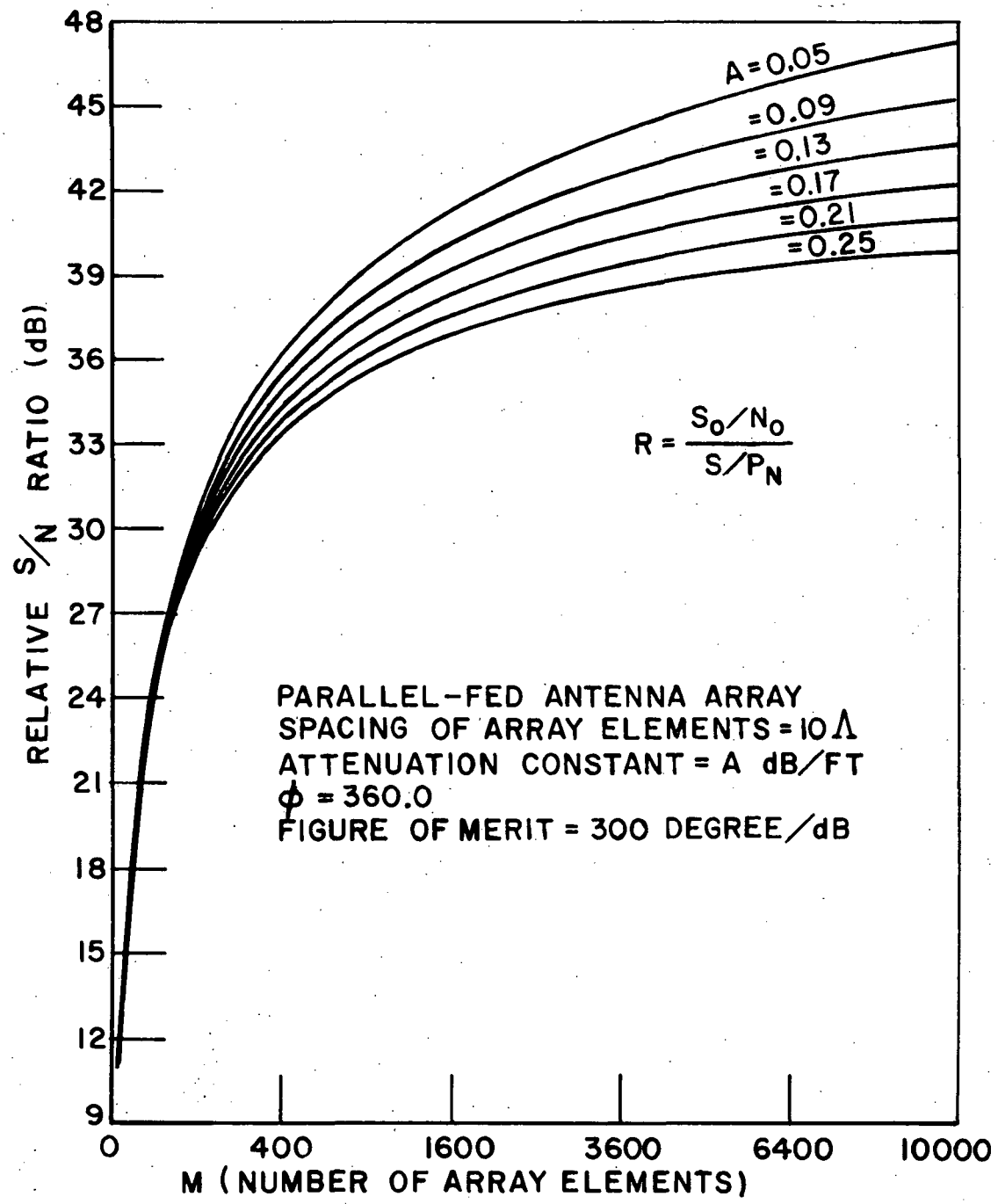

Fig. 19. SNR performance of the array in Fig. 18.

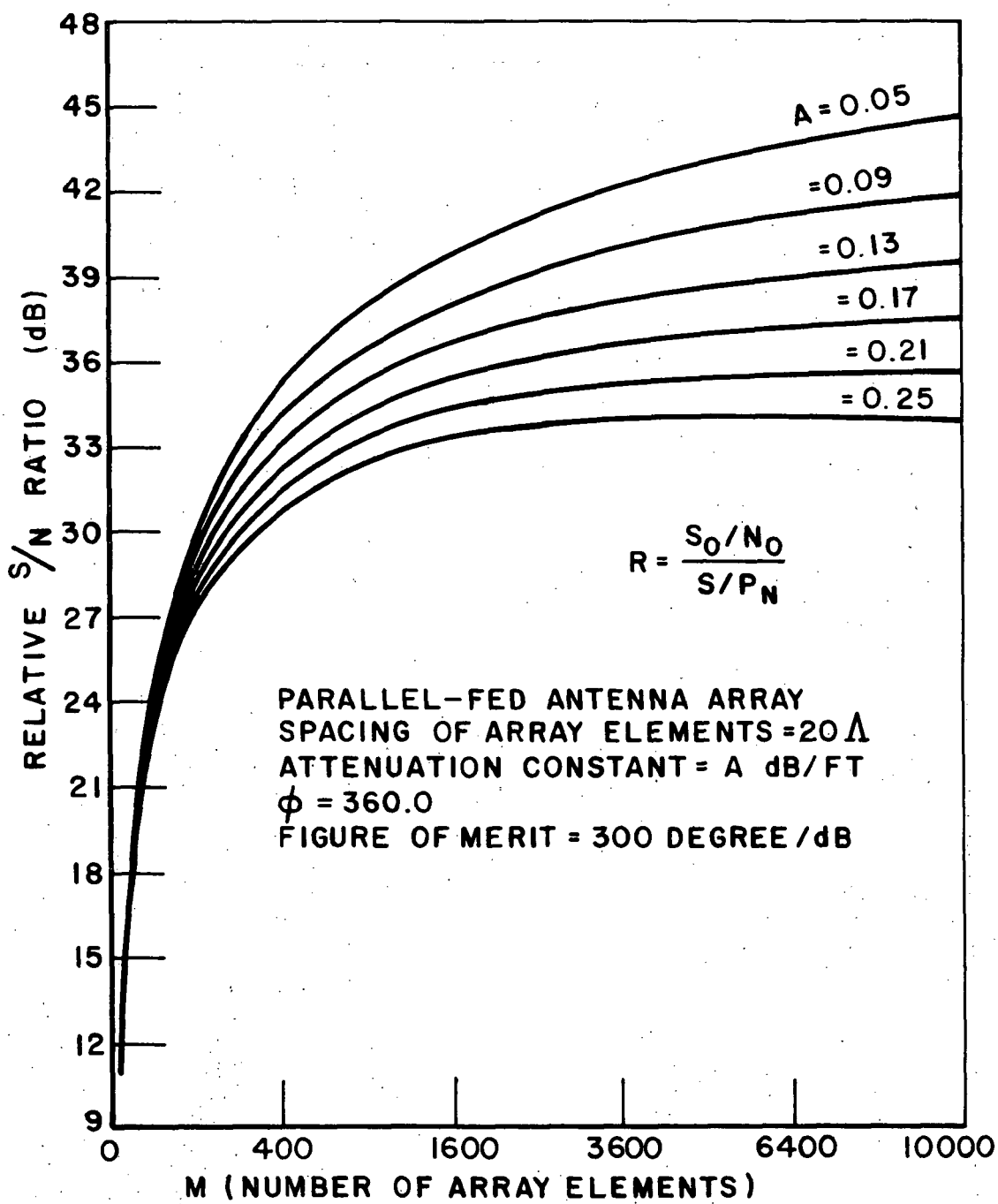

Fig. 20. SNR performance of the array in Fig. 18.

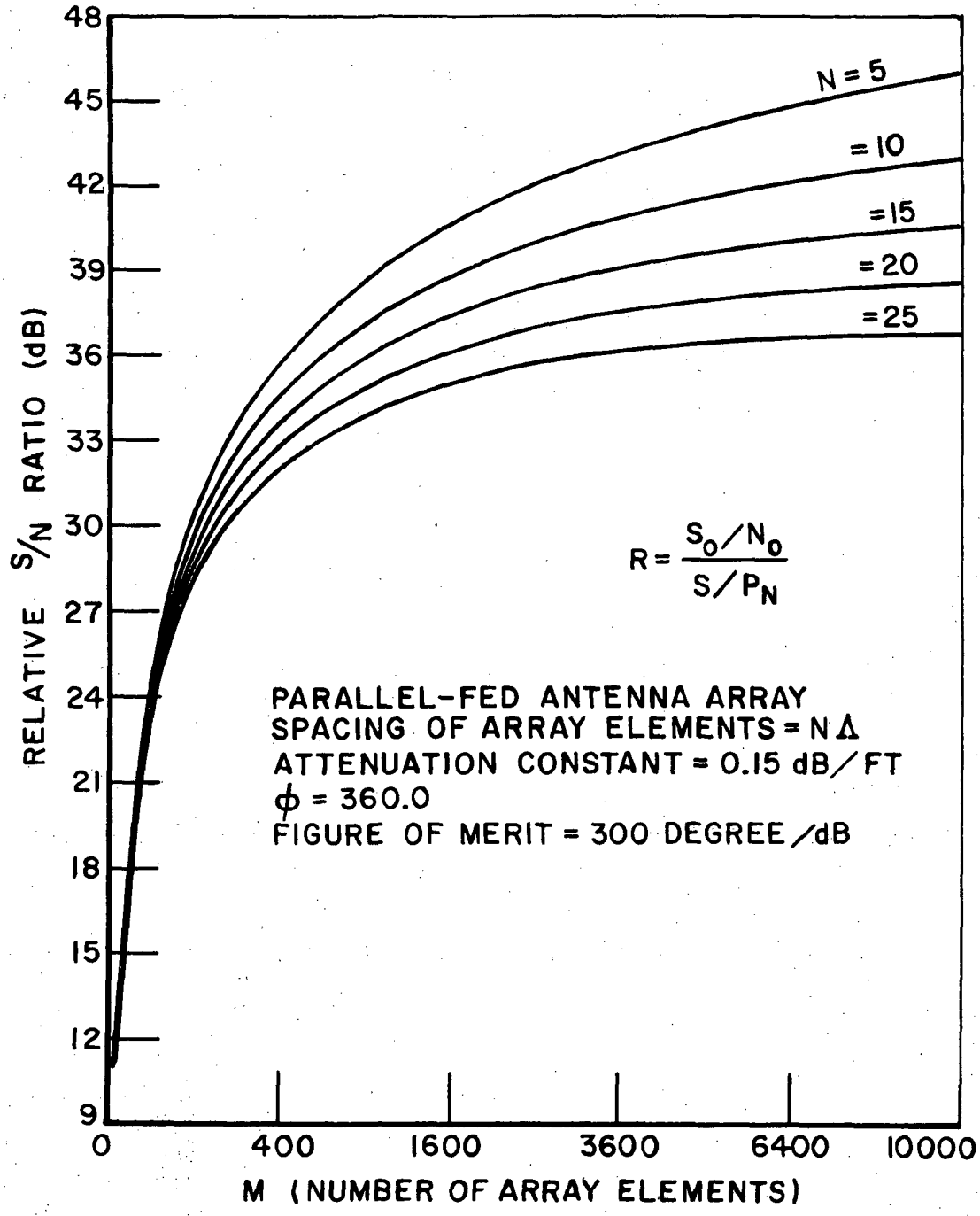

Fig. 21. SNR performance of the array in Fig. 18.

D. Two-dimensional Corporate-fed System

As the previous results show, the loss caused by phase shifters has a pronounced influence on the signal-to-noise ratio for parallel-fed arrays. Here we examine another connection, a corporate feed as shown in Fig. 22. The algorithm for increasing array size is the following.

Four adjacent elements are chosen as a primitive stage. A group of four adjacent primitive stages forms a second stage; four of these in turn form the third stage, and so on.

We have considered two different ways of locating phase shifters in this kind of feed network. One is to place phase shifters in three of the four branches of each stage, using the fourth branch as the reference for the other three (Figs. 22 and 23). The other way is to place all phase shifters in the primitive stages, one between each antenna element and the first summing network. Since the phase of the received signal of each antenna element is adjusted by the phase shifter following the element, any required phase-shifting combination can be achieved.

The algorithm equations for the relative signal-to-noise ratio of these configurations are quite easily obtained by using similar techniques as before. For the configuration of Fig. 23, the equations are

$$S_1 = \frac{1}{4} e^{-2\alpha d_1} (3e^{-\frac{\theta_1}{2}} + 1)^2 S, \tag{20}$$

$$S_2 = \frac{1}{4} e^{-2\alpha d_2} (3e^{-\frac{\theta_2}{2}} + 1)^2 S_1, \tag{21}$$

$$\vdots$$

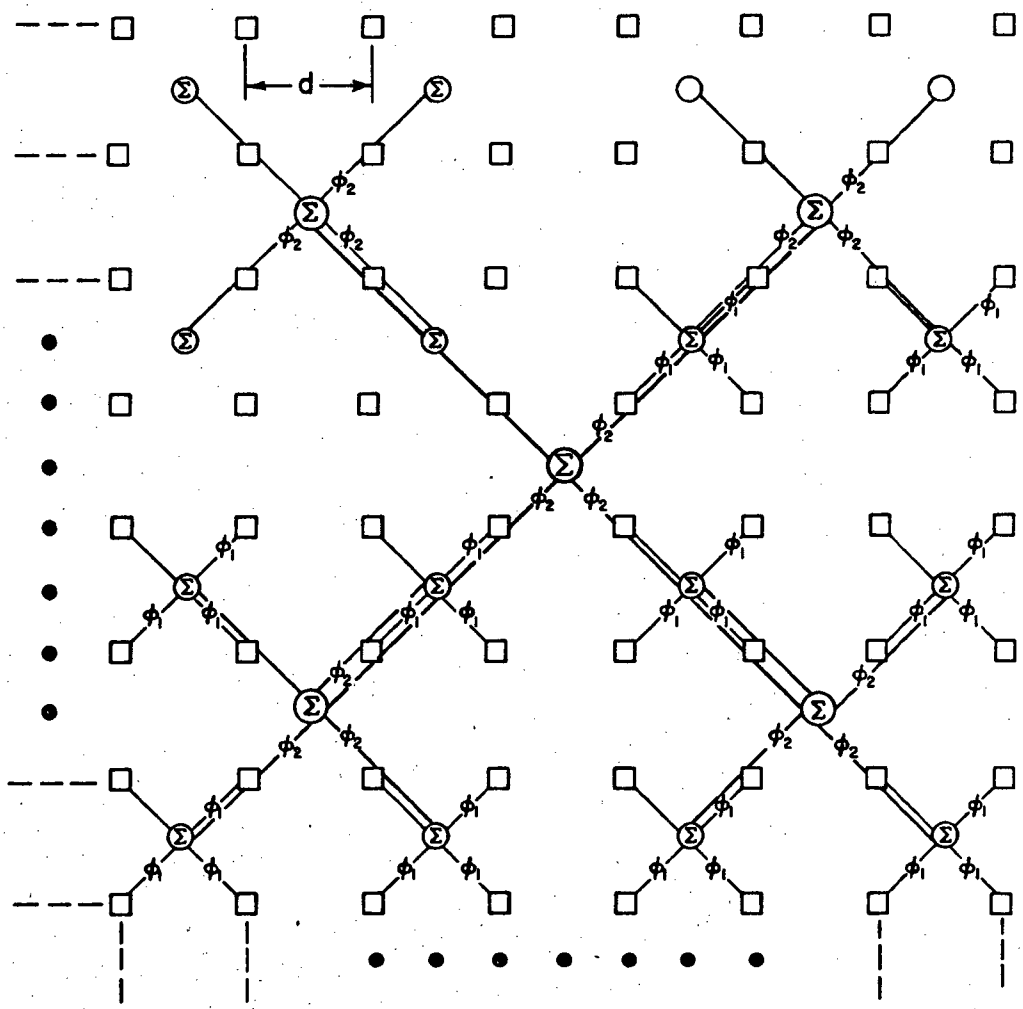

Fig. 22. A corporate-fed antenna array.

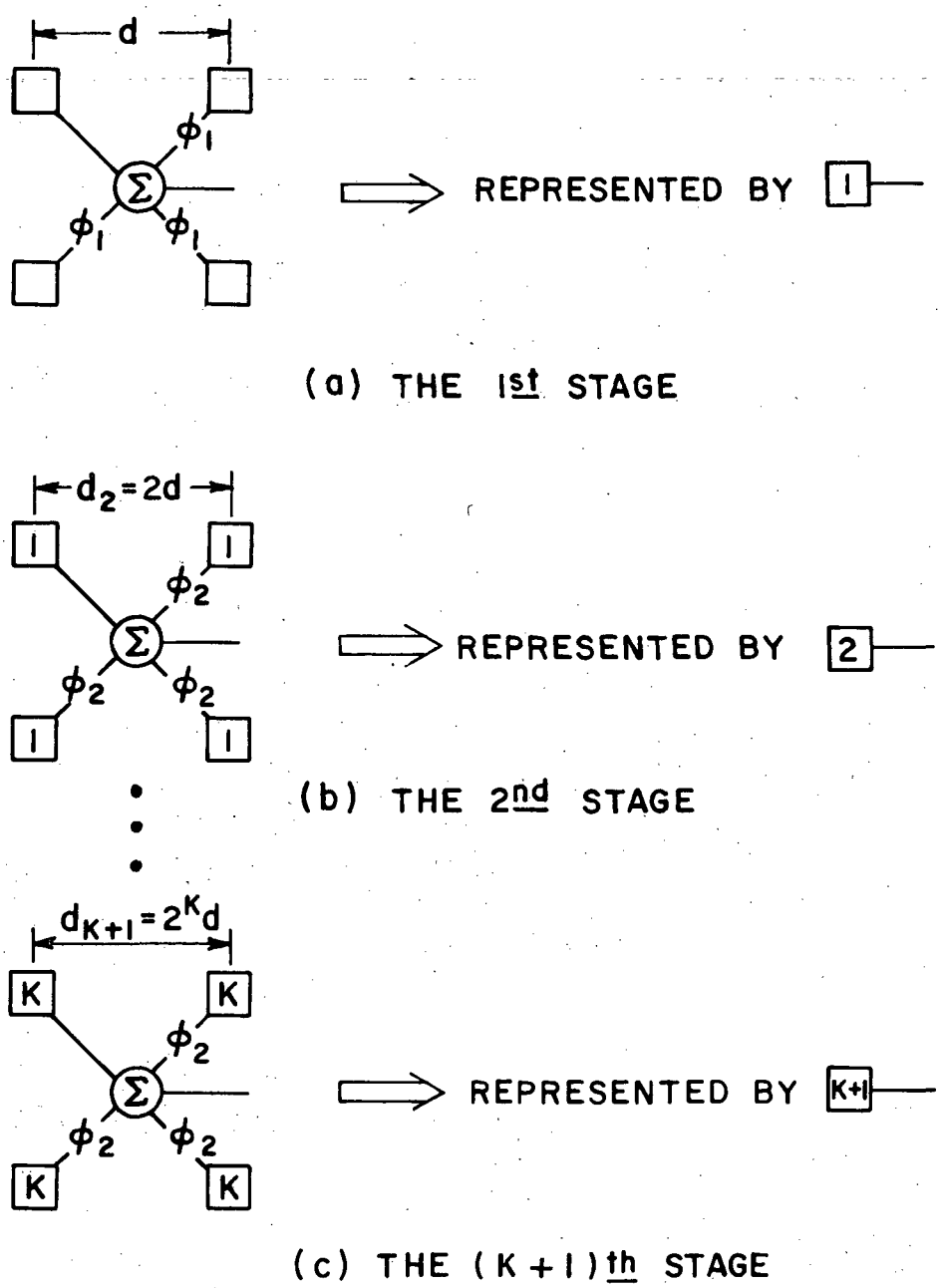

Fig. 23. Another view of the antenna array in Fig. 22.

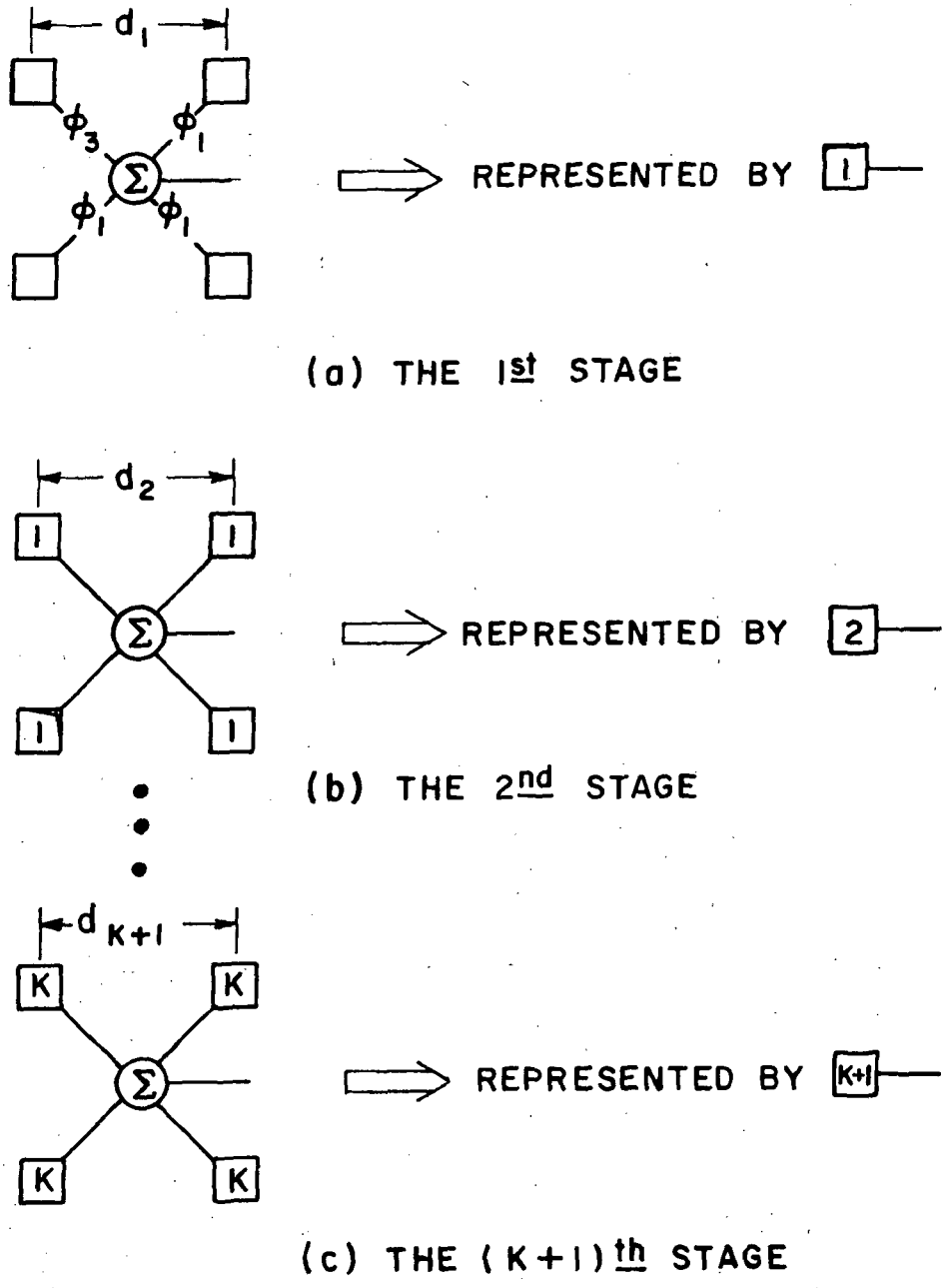

Fig. 24. The other way of arranging phase shifters in a 4-element corporate-fed antenna array.

$$S_K = e^{-2\alpha d_K}\left(3e^{-\frac{\theta_K}{2}} + 1\right)^2 S, \tag{22}$$

and

$$N_1 = \frac{1}{4} P_N\left[1 - e^{-2\alpha d_1}\left(3e^{-\theta_1} + 1\right)\right], \tag{23}$$

$$N_2 = \frac{1}{4}\left[P_N + (N_1 - P_N)e^{-2\alpha d_2}\left(3e^{-\theta_2} + 1\right)\right], \tag{24}$$

$$\vdots$$

$$N_k = \frac{1}{4}\left[P_N + (N_{k-1} - P_N)e^{-2\alpha d_k}\left(3e^{-\theta_2} + 1\right)\right] \tag{25}$$

where $$d_n = 2^{n-1}\sqrt{2}d \tag{26}$$

is the transmission line length of the n-th stage,

d is the spacing of the elements,

S is the signal power available at the terminals of any element,

S_k and N_k are the signal and noise powers, respectively, at the output of the k-th stage, and

α and θ are defined the same as in the previous sections.

In the evaluation of relative signal-to-noise ratio, we assume that all the phase shifters except those of the first (or primitive) stages are the same.

For the configuration of Fig. 24, one obtains

$$S_1 = \frac{1}{4} e^{-2\alpha d_1}\left(3e^{-\frac{\theta_1}{2}} + e^{-\frac{\theta_3}{2}}\right)^2 S, \tag{27}$$

$$S_2 = 4e^{-2\alpha d_2} S_1, \tag{28}$$

$$\vdots$$

$$S_k = 4e^{-2\alpha d_k} S_{k-1}, \tag{29}$$

and

$$N_1 = \frac{1}{4} P_N [1 - e^{-2\alpha d_1} (3e^{-\theta_1} + e^{-\theta_3})], \tag{30}$$

$$N_2 = \frac{1}{4} [P_N + 4(N_1 - P_N)e^{-2\alpha d_2}], \tag{31}$$

$$\vdots$$

$$N_k = \frac{1}{4} [P_N + 4(N_{k-1} - P_N)e^{-2\alpha d_k}], \tag{32}$$

where d_k, S_k, N_k, α and θ are defined as before. The introduction of ϕ_3 is for computational convenience. Setting ϕ_3 to zero results in the configuration of Fig. 23; setting $\phi_3=\phi_1$ and $\phi_2=0$ gives the configuration of Fig. 24; thus both can be calculated with a single computer program.

Figures 25-34 show the noise performances for some system parameters.

From the curves it is apparent that the configuration of Fig. 24 has better signal-to-noise behavior than that of Fig. 23. The physical reason is that in the former the signal encounters only one phase shifter between element and final output, while in the latter a path may include as many phase shifters as there are stages and the vast majority of paths include more than one phase shifter. For very small arrays the configuration of Fig. 23 appears to be better, but this is only a consequence of the computational algorithm. For a single stage, the configuration of Fig. 23 reduces to four elements with only three phase shifters, while that of Fig. 24 reduces to

four elements with four shifters. One of these could of course be omitted, and the two configurations would then be identical.

From the curves, we see that after the number of elements becomes sufficiently large, the array will get no more benefit as far as the SNR is concerned. One reason is that the signal from the outer elements, being attenuated by the lossy transmission elements before reaching the summing port, adds a relatively small amount of signal while the transmission elements contribute a relatively large amount of noise.

The last few figures show the SNR performance versus the array dimension. As we have been doing, the operating frequency is assumed to be 30 GHz and the aperture amplitude distribution is uniform.

From these curves, it appears that for the present state-of-the-art, i.e., assuming an attenuation constant for transmission lines (or waveguides) of about 0.15 db/ft and a figure of merit for phase shifters of about 300 degree/db, the 2-dimensional corporate-fed array may get optimum SNR performance at around 10mx10m. This, of course, will not be the optimum size in practical usage since the rate of signal-to-noise ratio increase decreases to zero at this peak value and the array gains very little benefit at high cost by increasing its size to near this value. Therefore, from the engineering point of view, this kind of array should be considerably smaller than 10mx10m.

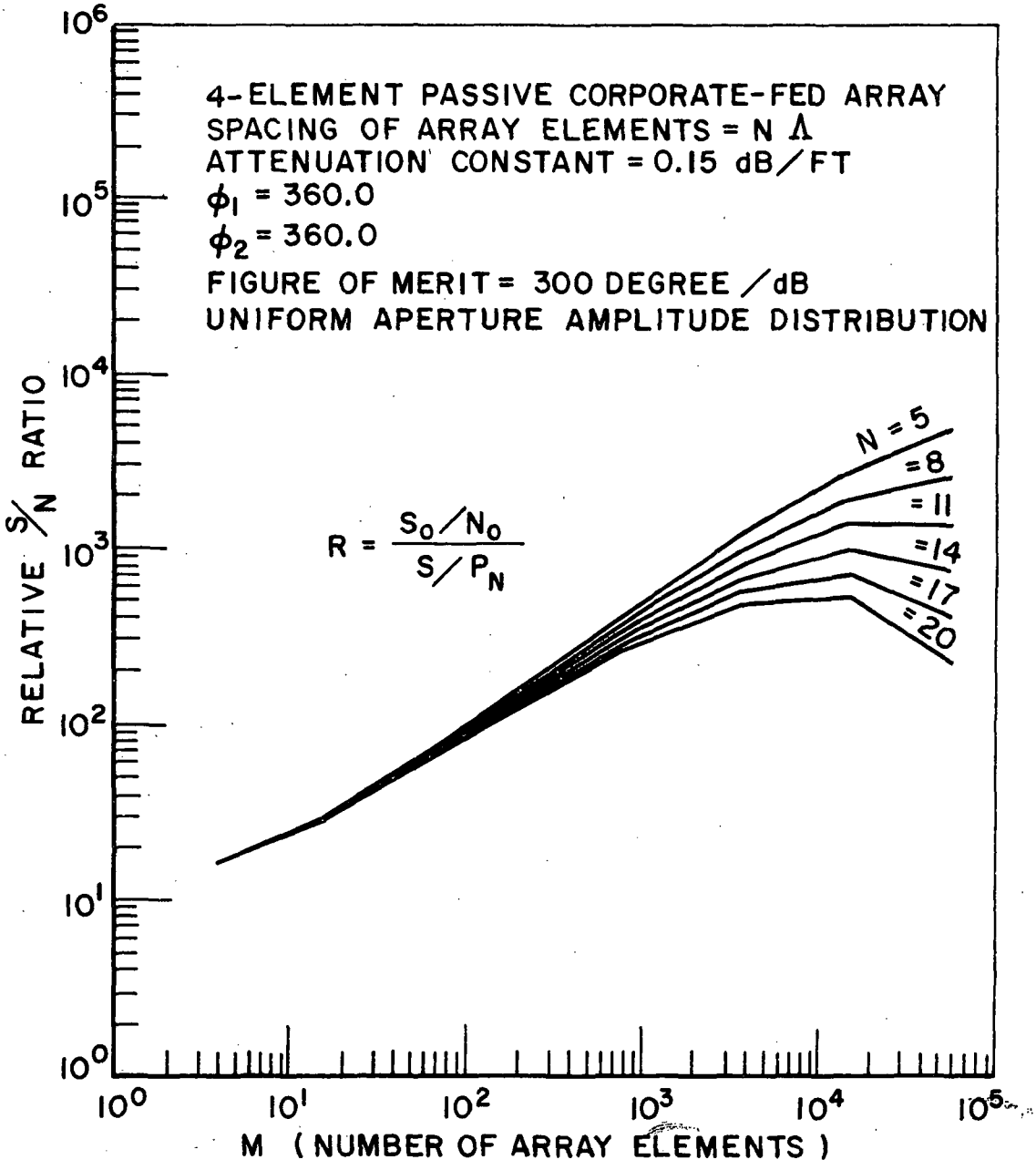

Fig. 25. SNR performance of the array in Fig. 23.

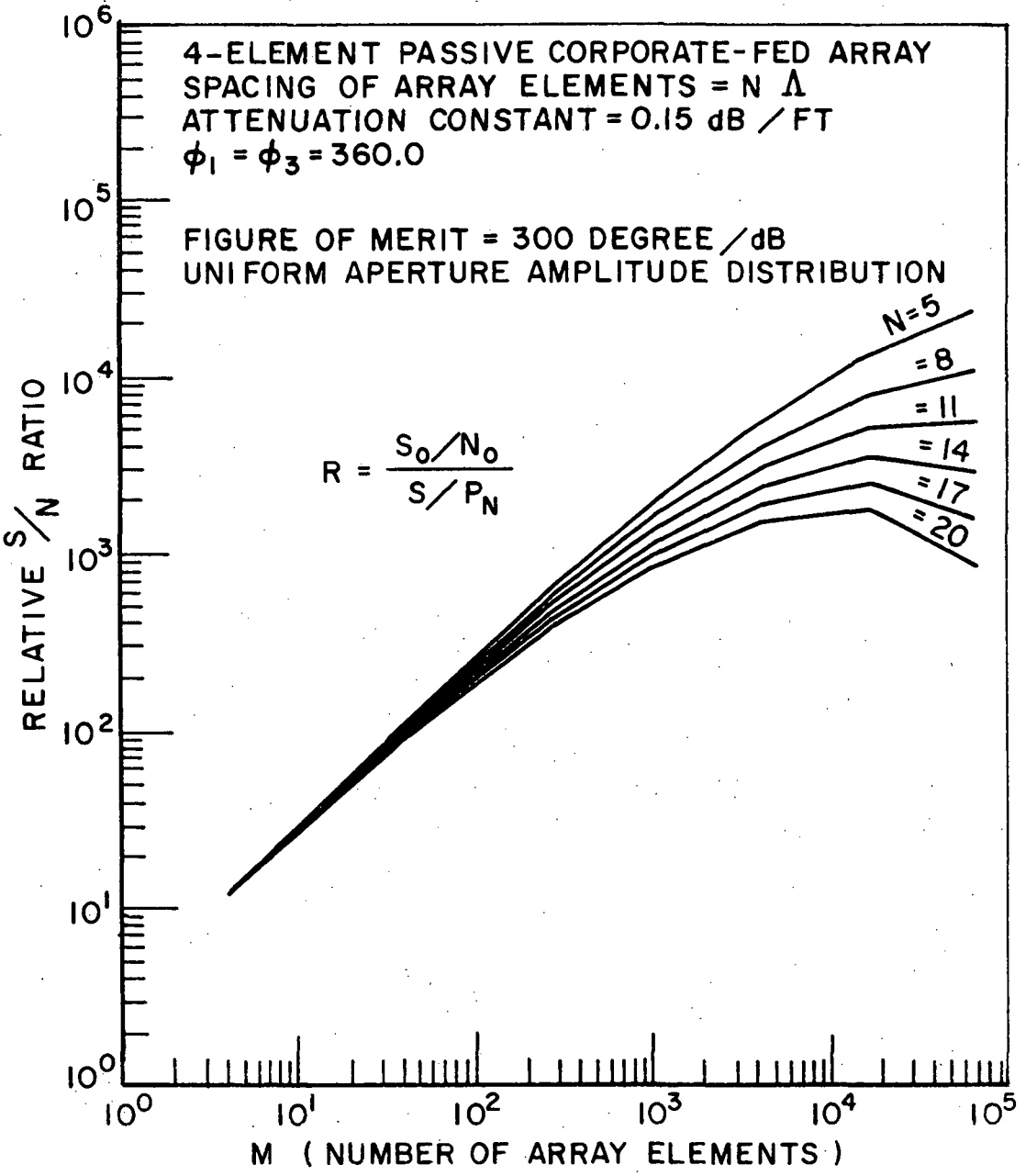

Fig. 26. SNR performance of the array in Fig. 24.

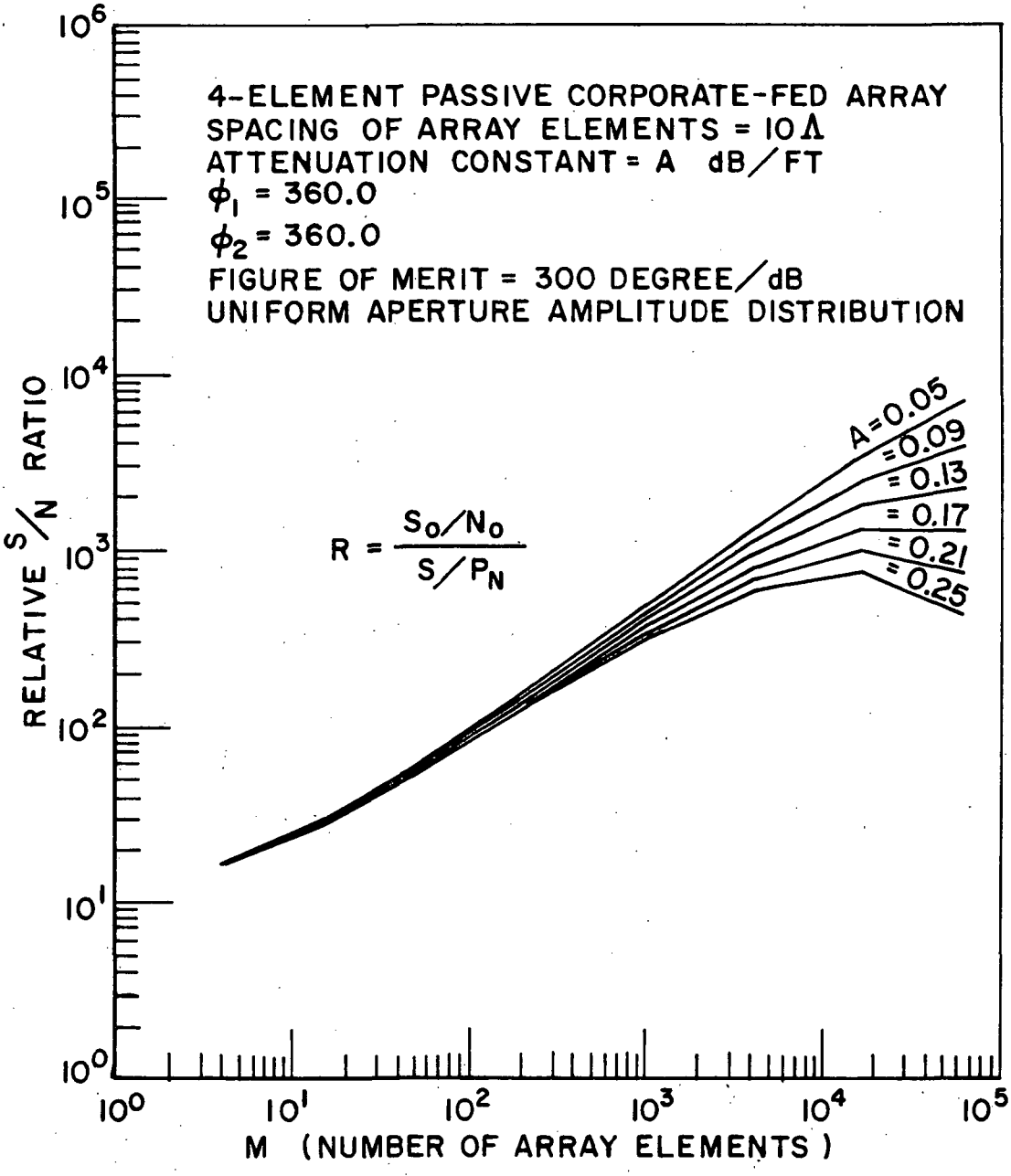

Fig. 27. SNR performance of the array in Fig. 23.

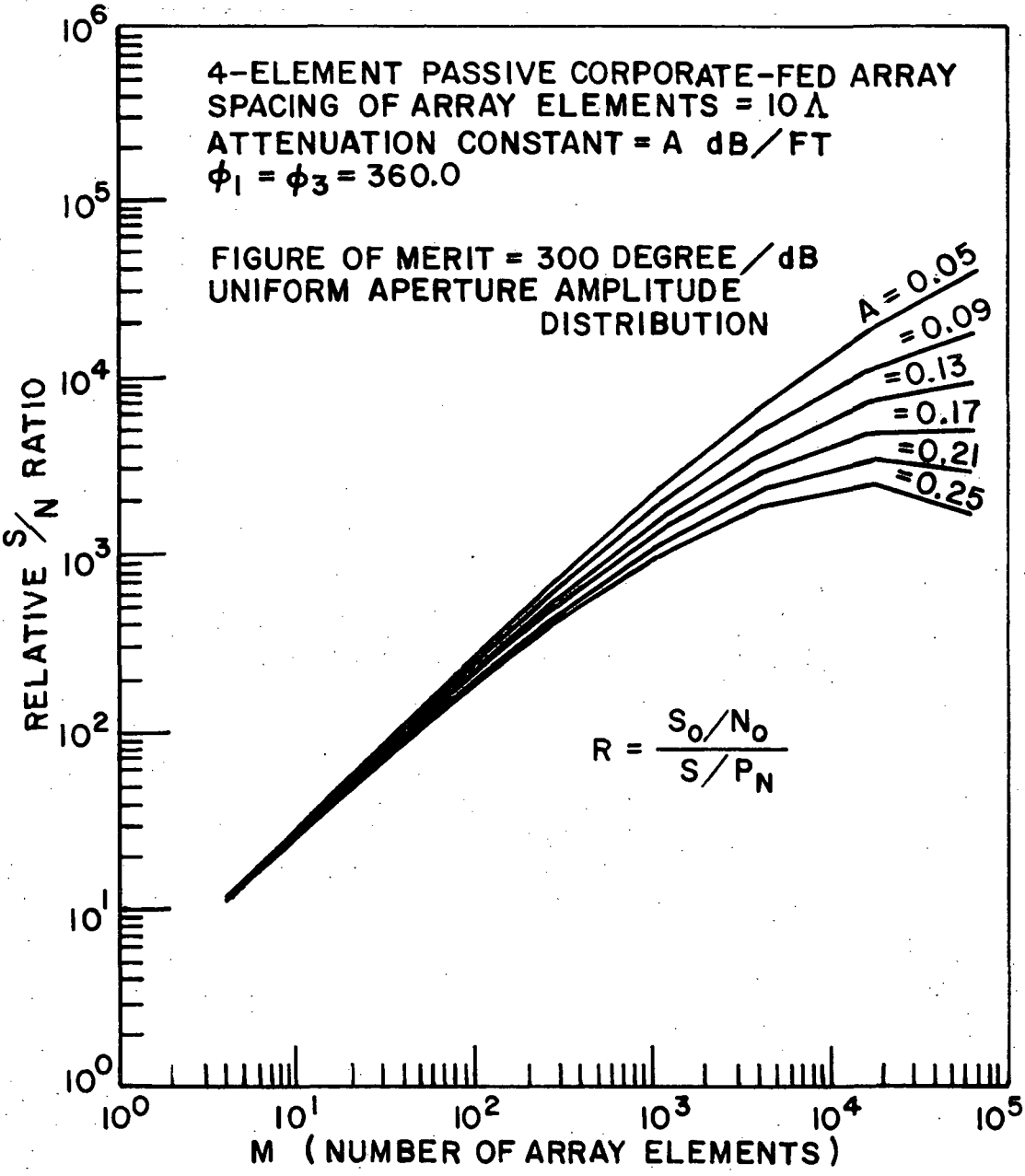

Fig. 28. SNR performance of the array in Fig. 24.

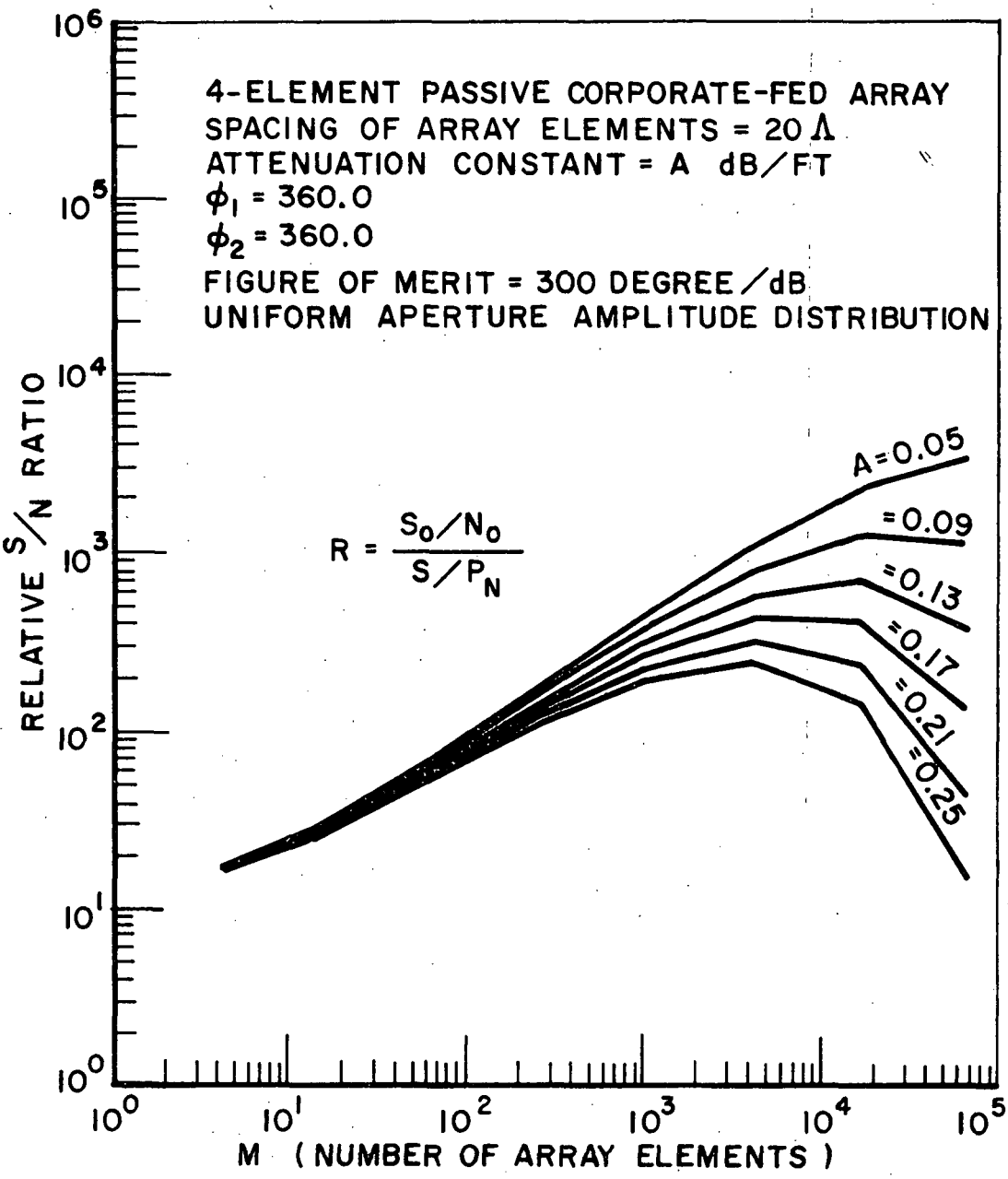

Fig. 29. SNR performance of the array in Fig. 23.

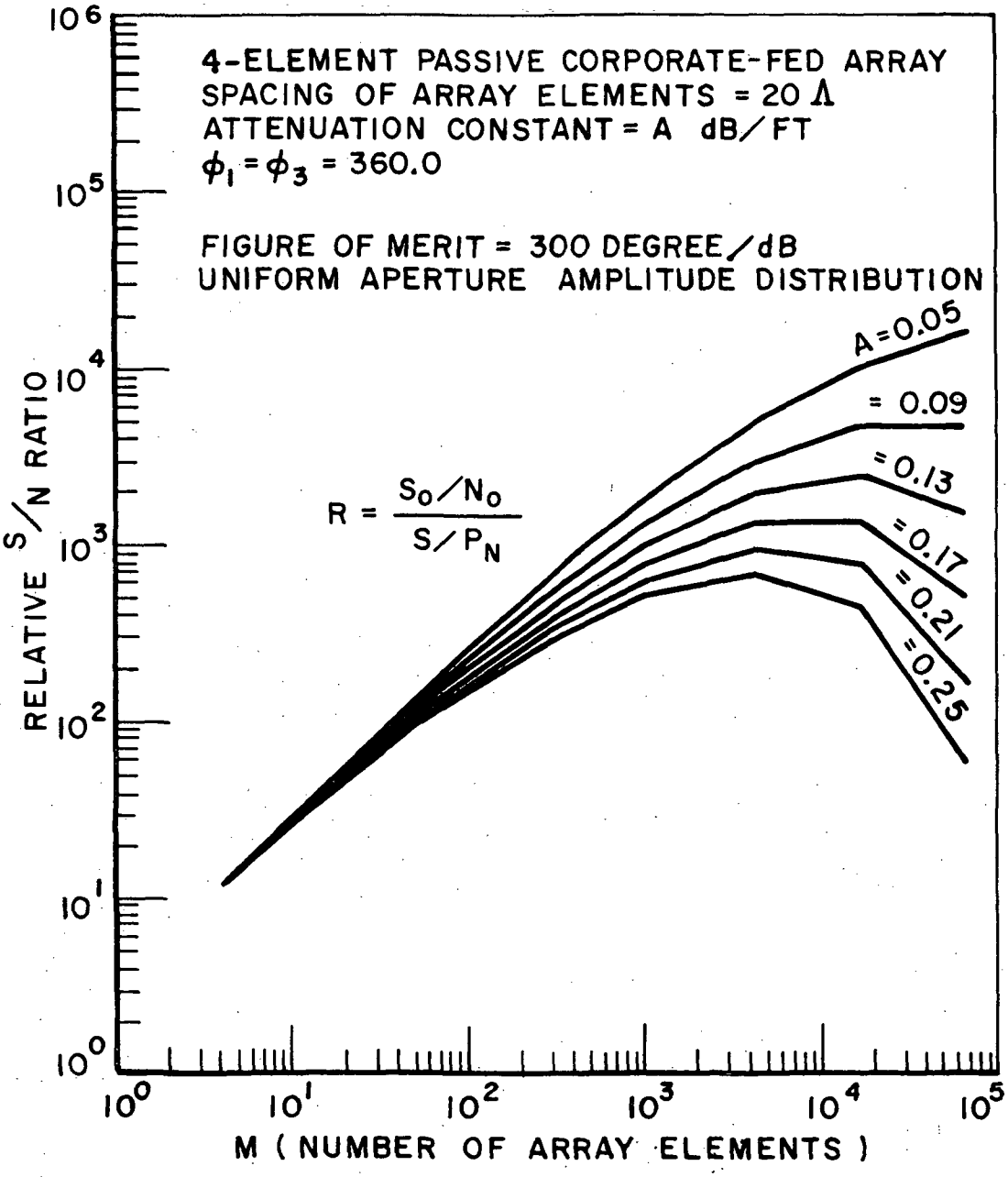

Fig. 30. SNR performance of the array in Fig. 24.

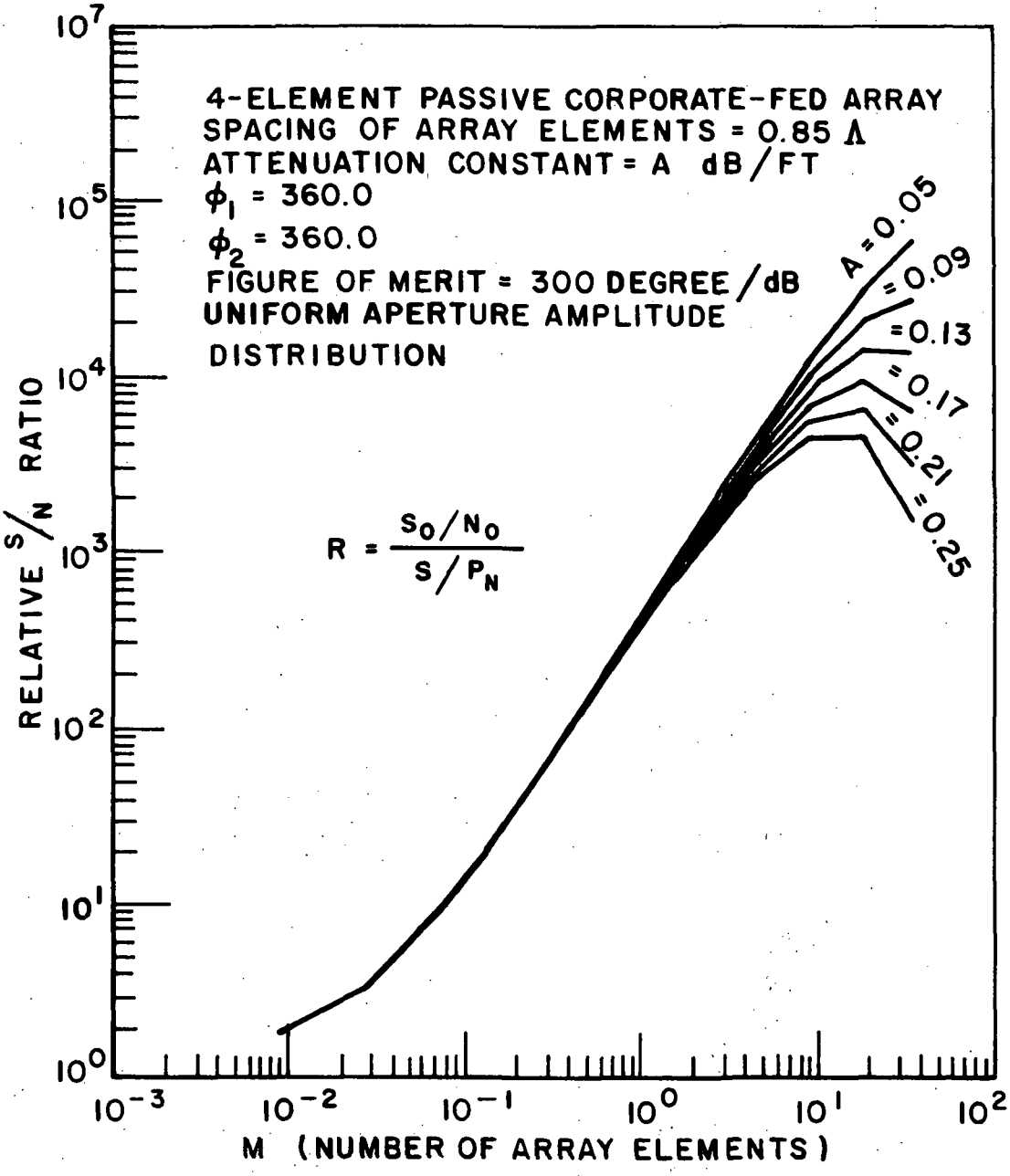

Fig. 31. SNR performance vs. dimension for the array in Fig. 23.

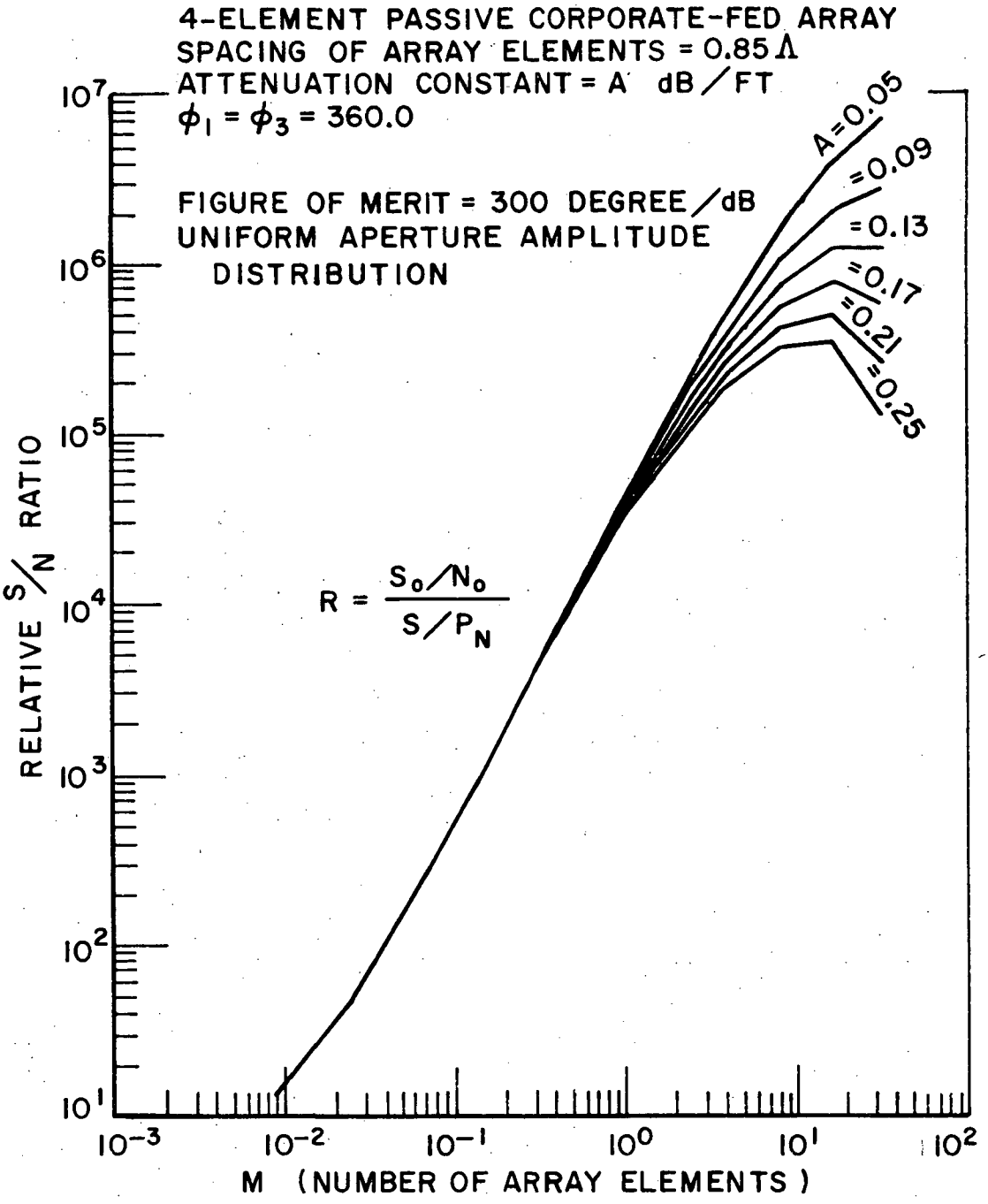

Fig. 32. SNR performance vs. dimension for the array in Fig. 24.

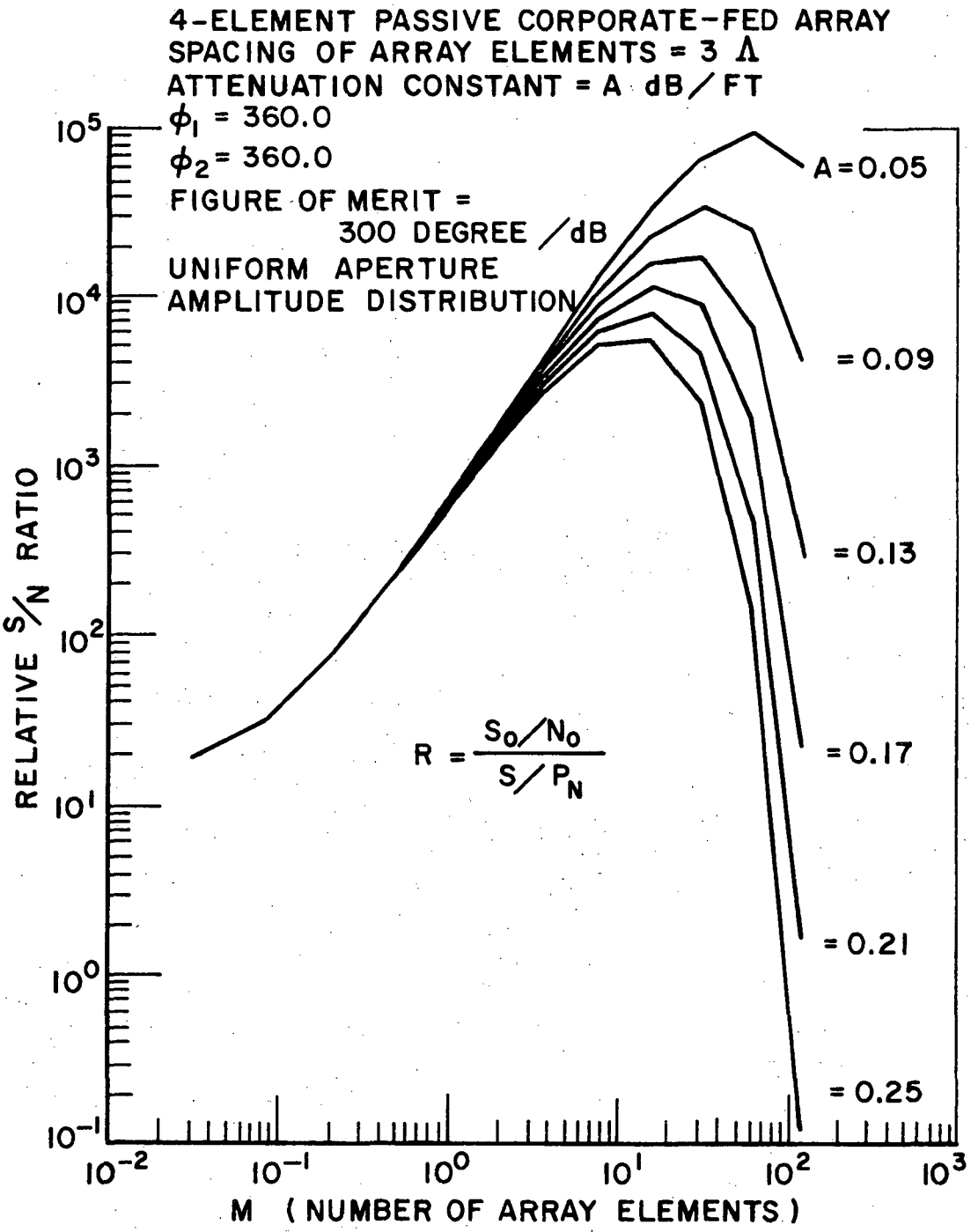

Fig. 33. SNR performance vs. dimension for the array in Fig. 24.

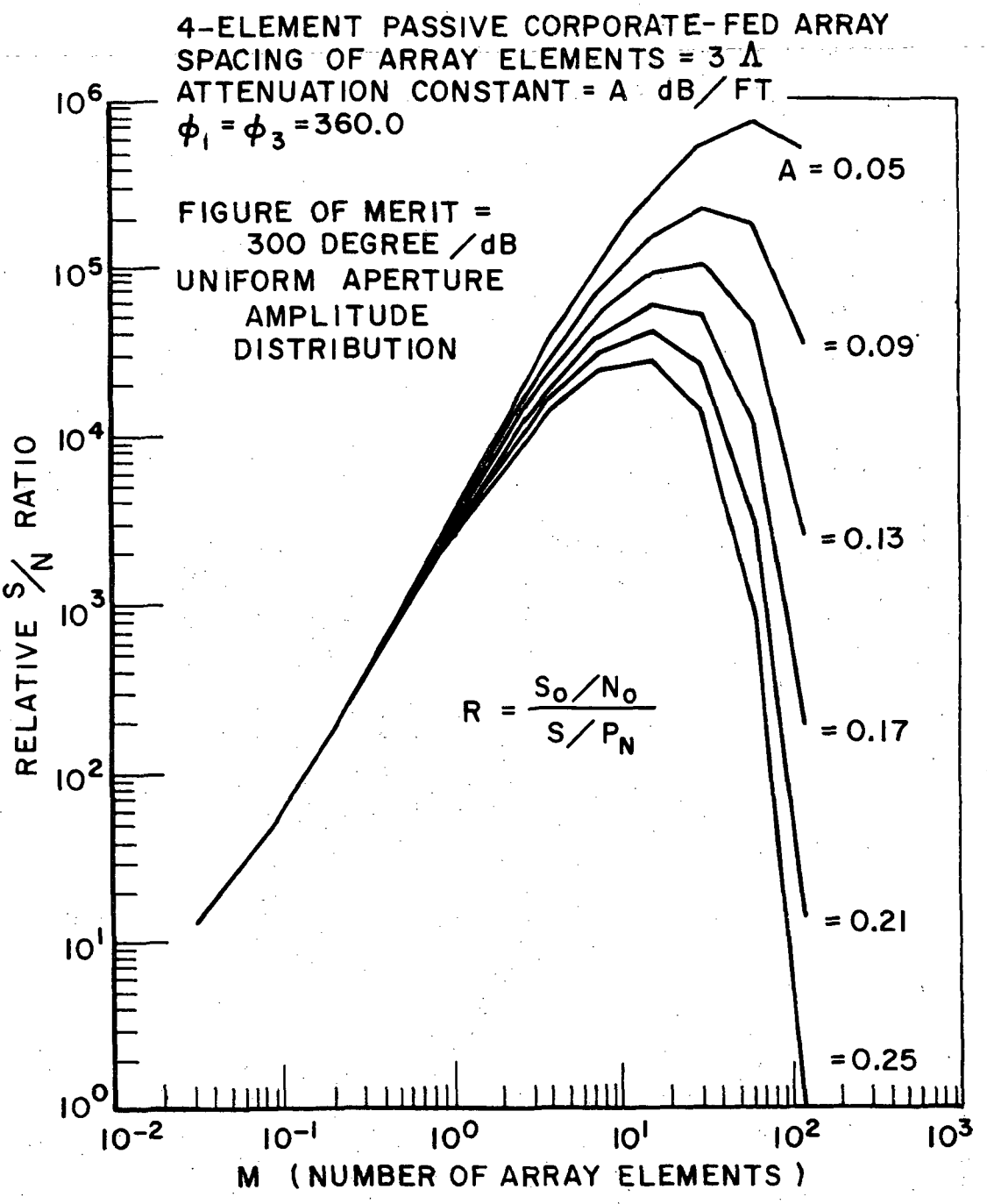

Fig. 34. SNR performance vs. dimension for the array in Fig. 23.

CHAPTER IV

NOISE PERFORMANCE OF VERY LARGE ARRAYS INVOLVING ACTIVE DEVICES

A. Introduction

Since the noise in a receiving system blurs the received signal as the latter goes through the passive elements, it is useful to increase the signal level before it gets corrupted. A commonly used approach is to place active devices early in the signal paths to amplify the signals to a sufficiently high level so that they will not be corrupted very much by the internal noise of the system.

B. Noise Figure of an Active Device

The active devices, as well as the passive ones, contribute noise to the amplified signal. This noise contribution is often expressed in terms of a noise figure. The standard noise figure [17, 18] is defined as the ratio of the available noise at the output terminals to that portion of this noise which is engendered by the input termination when the input termination is at the standard temperature (290°K).

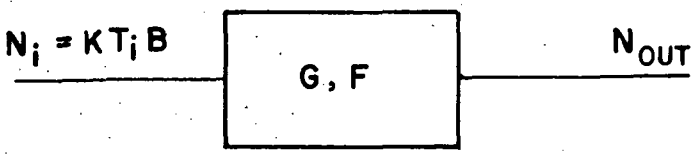

Fig. 35. Noise figure of an active device

Mathematically, this noise figure is given by

$$F = \frac{N_{out} \text{ (when } T_i = 290° \text{ at all frequencies)}}{G\ K\ T_i\ B} \tag{1}$$

where

$T_i = 290°K = T_o$, is the standard temperature of the input termination,

G is the power gain of the active device,

K is Boltzmann's Constant,

N_{out} is the available noise output power, and

B is the equivalent bandwidth.

The output noise power can be considered as the sum of the noise due to the input and that due to the internal effect of the active device; i.e.,

$$N_{out} = GN_i + GN = N_{g_i} + N_g \tag{2}$$

where

$$N_{g_i} \equiv GN_i = G\ K\ T_i\ B \tag{3}$$

is the noise contribution from the input and

$$N_g \equiv GN = G\ K\ T\ B \tag{4}$$

is the noise power contributed from the internal effect. This is often independent of the input noise power, and T is called the equivalent noise temperature of the device, referred to the input port.

Substituting equations (2), (3), and (4) back into equation (1), we have

$$F = \frac{T_o + T}{T} \tag{5}$$

or

$$F = 1 + \frac{T}{T_o} \quad , \tag{6}$$

and hence

$$T = (F - 1)\, T_o \quad . \tag{7}$$

F is called the standard noise figure since it relates the equivalent noise temperature of the device to a standard input noise temperature.

In many cases, the effective noise temperature of a source differs from the standard noise temperature (290°K). The noise figure

$$F_o = \frac{N_{out}}{G\, K\, T_i\, B} \tag{8}$$

is called the operating noise figure and the noise output can be obtained from this as

$$N_{out} = F_o\, G\, K\, T_i\, B \quad . \tag{9}$$

The internally generated noise is the total noise output minus that engendered by the input noise, i.e.,

$$N_g = N_{out} - N_{g_i} = (F_0 - 1)\, G\, K\, T_i\, B \quad . \tag{10}$$

This is usually not affected by the input noise (but depends on input impedance), therefore, the total noise output can be expressed by

$$N_{out} = G K T B + G K T_i B$$
$$= G K (F - 1) T_o B + G K T_i B \qquad (11)$$

as another way of calculating N_{out}.

Usually, F means standard noise figure when there is not any subscript o associated with it.

C. Noise Behavior of Arrays with Active Devices

The noise coming from the internal effect of an active device, N_g in equation (4), is statistically independent of that from other devices since it is caused by the random motion of charges in devices; therefore, we'll treat noise contributions as uncorrelated when they do not originate from the same devices.

For a very large array, it is well known that the earlier in the signal path active devices of a given noise figure are placed in a system, the better its signal-to-noise ratio. Nevertheless, there are many factors affecting the choice of array organization. Among them are the availability and cost of various types of active devices at very high frequency. Technical difficulties are often reduced if the signal is converted from the high original frequency to a lower one, so that the remainder of the system can be working at this lower frequency. Following this frequency conversion, there is an IF amplifier stage to amplify the signal. Unfortunately, the IF amplifier amplifies also the original noise, and it also adds some additional noise which is caused by the behavior of the active devices in the converter and IF amplifier.

Another factor to be considered is that if we place all active devices at each beginning stage, then the cost of the whole system

will increase very greatly as the number of array elements gets larger. The benefit we gain by placing active devices in the early stages must be balanced against the additional cost.

We shall now quantitatively analyze the performance of several different arrangements from the noise point of view to see what compromises between noise behavior and cost are available to a design engineer. As will be shown later, it is generally not possible to get an optimum operating condition with respect to both noise and cost. The tradeoffs will depend on the requirements of the system.

D. Noise Equations Including Active Devices

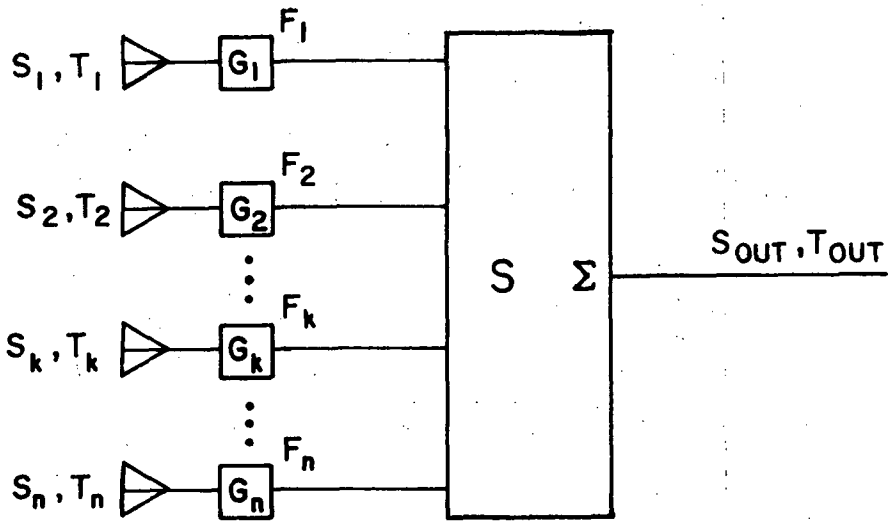

Fig. 36. A network summing all the received signals after amplification.

We want to calculate the noise of a very large array involving active devices. First, suppose all the active devices are situated right after each receiving element. If the active device following the k-th element has power gain G_k and noise figure F_k, the noise temperature and the signal power measured right after the amplifier would be

$$S_k' = G_k S_k \tag{12}$$

$$T_k' = T_k G_k + (F - 1) T_o G_k , \tag{13}$$

where S_k is the received (input) signal power at k-th element,

T_k is the received (input) equivalent noise temperature at k-th element,

S_k', T_k' are the signal power and equivalent noise temperature after the amplifier, respectively, and

T_o is the standard noise temperature (290°K).

From equation (98) of Chapter II, the summed noise and signal at terminal m under the ideal situation, i.e., with all terminals terminated in their respective characteristic inpedances and all signals coherently added, are

$$T_{out,\,m} = \sum_{k=1}^{n} T_k' \, |\alpha_{mk}|^2 + \left(1 - \sum_{k=1}^{n} |\alpha_{mk}|^2\right) T_a , \tag{14}$$

$$S_{out,\,m} = \left(\sum_{k=1}^{n} \sqrt{S_k'} \; \alpha_{mk} \right)^2 \tag{15}$$

where T_a is the ambient temperature of the system. Notice we've assumed that the noise outputs T_k' of all amplifiers are uncorrelated.

Substituting equations (10) and (11) into these two equations, one obtains

$$T_{out,\,m} = \sum_{k=1}^{n} \left[T_k + (F_k - 1) T_o \right] |\alpha_{mk}|^2 \; G_k + \left(1 - \sum_{k=1}^{n} |\alpha_{mk}|^2\right) T_a , \tag{16}$$

and

$$S_{out,\,m} = \left(\sum_{k} \sqrt{S_k\, G_k}\ \alpha_{mk} \right)^2 \quad . \tag{17}$$

If every active device has the same noise figure F and gain G, then the above equations reduce to

$$T_{out,\,m} = G\,(F - 1)\,T_o \sum_{k=1}^{n} |\alpha_{mk}|^2 + G \sum_{k=1}^{n} |\alpha_{mk}|^2\, T_k + (1 - \sum_{k=1}^{n} |\alpha_{mk}|^2\ )\, T_a \tag{18}$$

and

$$S_{out,\,m} = \left(\sum_{k=1}^{n} \sqrt{S_k}\ \alpha_{mk} \right)^2 G \quad . \tag{19}$$

Considering the system noise only, we assume all the inputs are signals and all input noise powers are zero, i.e.,

$$T_k = 0 \tag{20}$$

and obtain

$$T_{out,\,m} = G\,(F - 1)\,T_o \sum_{k=1}^{n} |\alpha_{mk}|^2 + (1 - \sum_{k=1}^{n} |\alpha_{mk}|^2)\, T_a \tag{21}$$

The last term $(1 - \sum_{k} |\alpha_{mk}|^2\ )\, T_a$ is precisely the noise calculated in the last chapter. For the same organization of antenna elements, we can get $\sum_{k=1}^{n} |\alpha_{mk}|^2$ from the procedures of that chapter and evaluate the noise performance of the corresponding antenna array systems involving active devices by equation (21), provided that F and G are given.

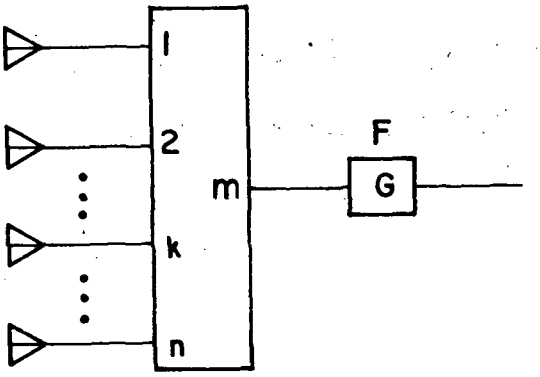

Fig. 37. The second arrangement.

Another way of placing active devices is to have a single active device situated after the summing port, which is usually preceded by a beam-forming or summing network, as shown in Fig. 37.

Employing the same techniques, one can easily get

$$T_{out,\,m} = G\left[\sum_{k=1}^{n} |\alpha_{mk}|^2\, T_k + \left(1 - \sum_{k=1}^{n} |\alpha_{mk}|^2\right) T_a\right] + G\,(F - 1)\,T_o \qquad (22)$$

and

$$S_{out,\,m} = \left(\sum_{k=1}^{n} \sqrt{S_k}\ \alpha_{mk}\right)^2 G \quad . \qquad (23)$$

Note that if G and F are the same as those in the previous case, then for the same network (or system), we would have the same signal but different noise outputs.

E. Effect of Internal Noise

We have shown that the signal output will not be changed no matter where we put active devices. However, noise behaves quite differently for the two arrangements. For the sake of convenience, let

$$\sum_{k=1}^{n} |\alpha_{mk}|^2 = A \tag{24}$$

and assume the noise outputs of all array elements are negligible, then the output noise temperature for the two different arrangements would be

$$(T_{out})_{arr\ I} = G\ (F - 1)\ T_o\ A + (1 - A\ )\ T_a\ , \tag{25}$$

$$(T_{out})\ arr\ II = G\left[(F - 1)\ T_o + (1 - A)\ T_a\right]\ . \tag{26}$$

Tables I-III show the output noise temperature for a few values of the system parameters. The antenna is very lossy if $A << 1$ and lossless if $A = 1$. As seen from the tables, if an antenna system is lossless, then the sensitivity of the array is independent of the placement of the active devices but depends only on their noise performance as specified by their noise figure F (or equivalently to T) and gain G. As the antenna array gets lossier, the thermal noise from the array contributes more and more, and it can be seen that the placement of the active devices becomes increasingly important in this case.

The other important result we can see from these results is that for the noisier active devices (Table III), lowering the ambient temperature gives very little benefit with respect to the SNR performance of the antenna system.

Table I. Comparison of Output Noise Temperatures of Putting Active Devices in Two Different Ways

Low Noise Active Devices

$G = 10^{db}$, $F = 2^{db}$ ($T = 169.6°K$)

Ambient Temperature	Arrangement \ A	0	0.25	0.5	0.75	0.9	1
T_a =	I	290	641	993	1344	1555	1696
290°K	II	4596	3871	3146	2421	1986	1696
	The system is at standard temperature						
T_a =	I	150	536	923	1309	1541	1696
150°K	II	3196	2821	2446	2071	1846	1696
	The system is at T_a = 150°K						
T_a =	I	50	461	873	1284	1531	1696
50°K	II	2196	2071	1946	1821	1746	1696
	The system is at T_a = 50°K						

Table II. Output Noise Temperature for More Noisy Active Devices

$G = 10^{db}$, $F = 3^{db}$ ($T = 290°K$)

Ambient Temperature	Arrangement \ A	0	0.25	0.5	0.75	0.9	1
T_a =	I	290	942	1595	2247	2639	2900
290°K	II	5800	5075	4350	3625	3190	2900
	The system is at standard temperature						
T_a =	I	150	837	1529	2212	2625	2900
150°K	II	4400	4025	3650	3275	3050	2900
	The system is at T_a = 150°K						
T_a =	I	50	762	1475	2187	2615	2900
50°K	II	3400	3275	3150	3025	2950	2900
	The system is at T_a = 50°K						

Table III. Noise Response with Noisy Devices

$G = 10^{db}$, $F = 6^{db}$ ($T = 864.5°K$)

Ambient Temperature	Arrangement \ A	0	0.25	0.5	0.75	0.9	1
T_a =	I	290	2378	4467	6556	7809	8645
290°K	II	11540	10820	10095	9370	8935	8645
	The system is at standard temperature						
T_a =	I	150	2273	4397	6521	7795	8645
150°K	II	10140	9770	9395	9020	8795	8645
	The system is at T_a = 150°K						
T_a =	I	50	2198	4347	6496	7785	8645
50°K	II	9145	9020	8895	8770	8695	8645
	The system is at T_a = 50°K						

F. Signal-to-noise Ratio Improvement

As pointed out in the last section, the signal-to-noise ratios for different active device placements will differ from each other only in the noise parts because the signal parts are the same, no matter where the devices are placed. Therefore, it follows that

$$\frac{(S/N)_{arr\ I}}{(S/N)_{arr\ II}} = \frac{(T_{out})_{arr\ II}}{(T_{out})_{arr\ I}} \quad , \tag{27}$$

where arrangement I is the system having the active devices at the beginning of each signal path (see Fig. 36) and arrangement II is the other one (Fig. 37).

Considering the internal noise only, i.e., $T_k \equiv 0$, we obtain by equations (23) and (24)

$$\frac{(S/N)_{arr\ I}}{(S/N)_{arr\ II}} = \frac{G\ (F - 1)\ T_o + G\ (1 - A)\ T_a}{G\ (F - 1)\ T_o\ A + (1 - A)\ T_a} \quad . \tag{28}$$

since $A \leq 1$ from Chapter II and $G > 1$ (29)

$$\frac{(S/N)_{arr\ I}}{(S/N)_{arr\ II}} \geq 1 \tag{30}$$

i.e., the first kind of arrangement will always yield better noise performance.

Equation (28) can be simplified as

$$\frac{(S/N)_{arr\ I}}{(S/N)_{arr\ II}} \approx \frac{(F - 1)\ T_o + (1 - A)\ T_a}{(F-1)\ T_o\ A + (1 - A)\ T_a/G} \quad . \tag{31}$$

Figs. 38 to 40 plot the ratio of the signal-to-noise ratio of Fig. 36 relative to that of Fig. 37 for several different cases.

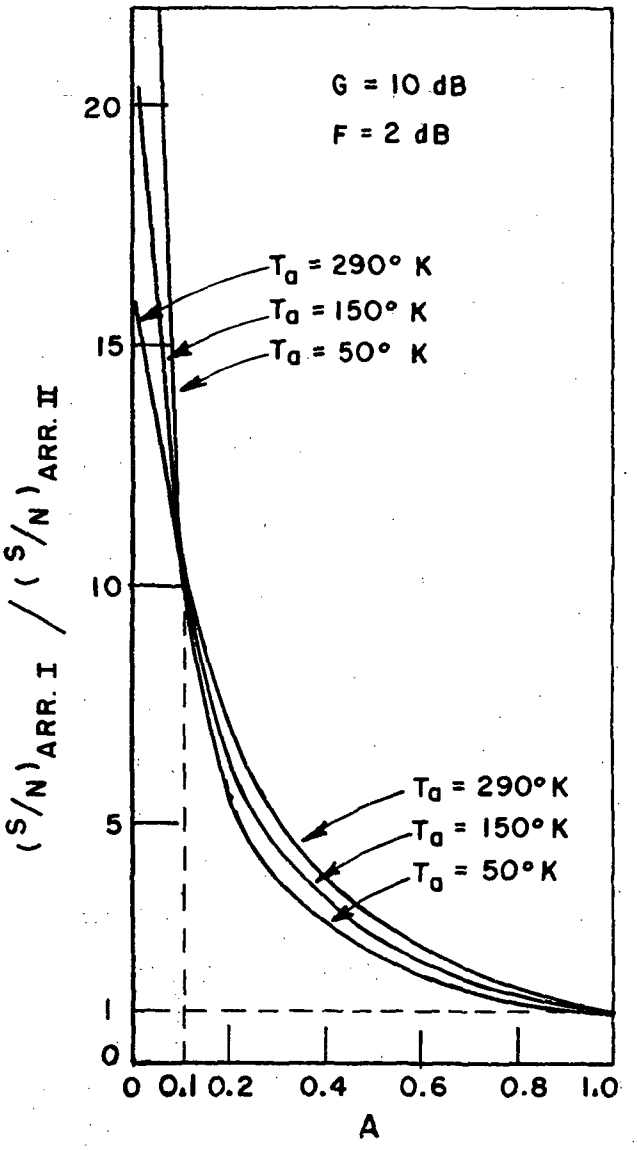

Fig. 38. SNR improvement of one antenna organization (Fig. 36) relative to another (Fig. 37).

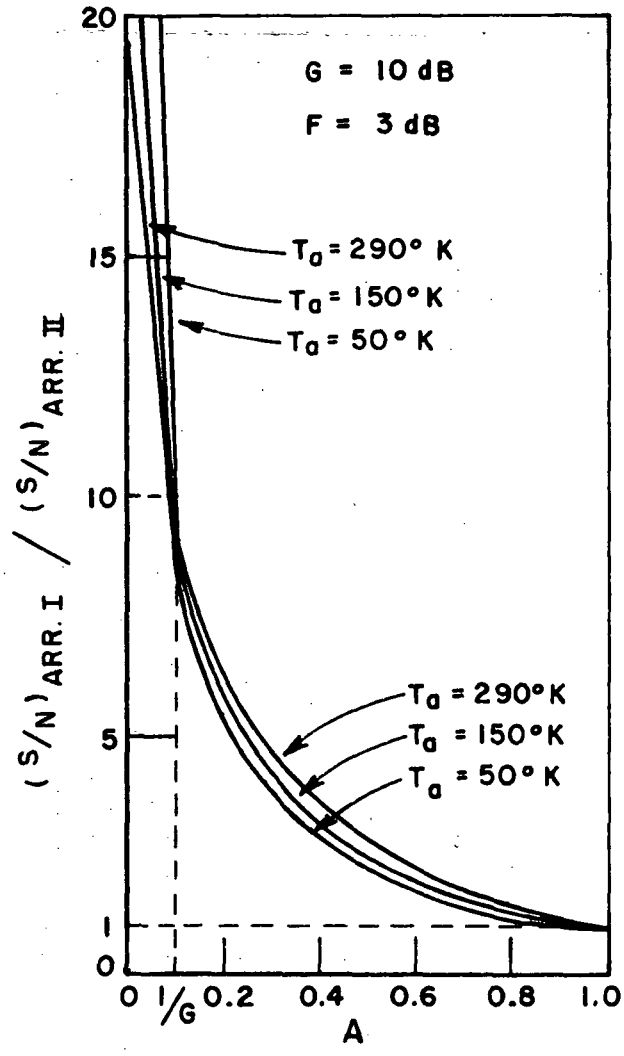

Fig. 39. SNR improvement of one antenna organization (Fig. 36) relative to another (Fig. 37).

From these curves, we see that if the system is very lossy, i.e., A << 1, the improvement depends greatly on F, G, and T_a. While these computations are for the active devices placed at the very beginning or the very end of the signal paths, intermediate placement is of course also possible. In general, the earlier in the path the devices are placed, the better the signal-to-noise

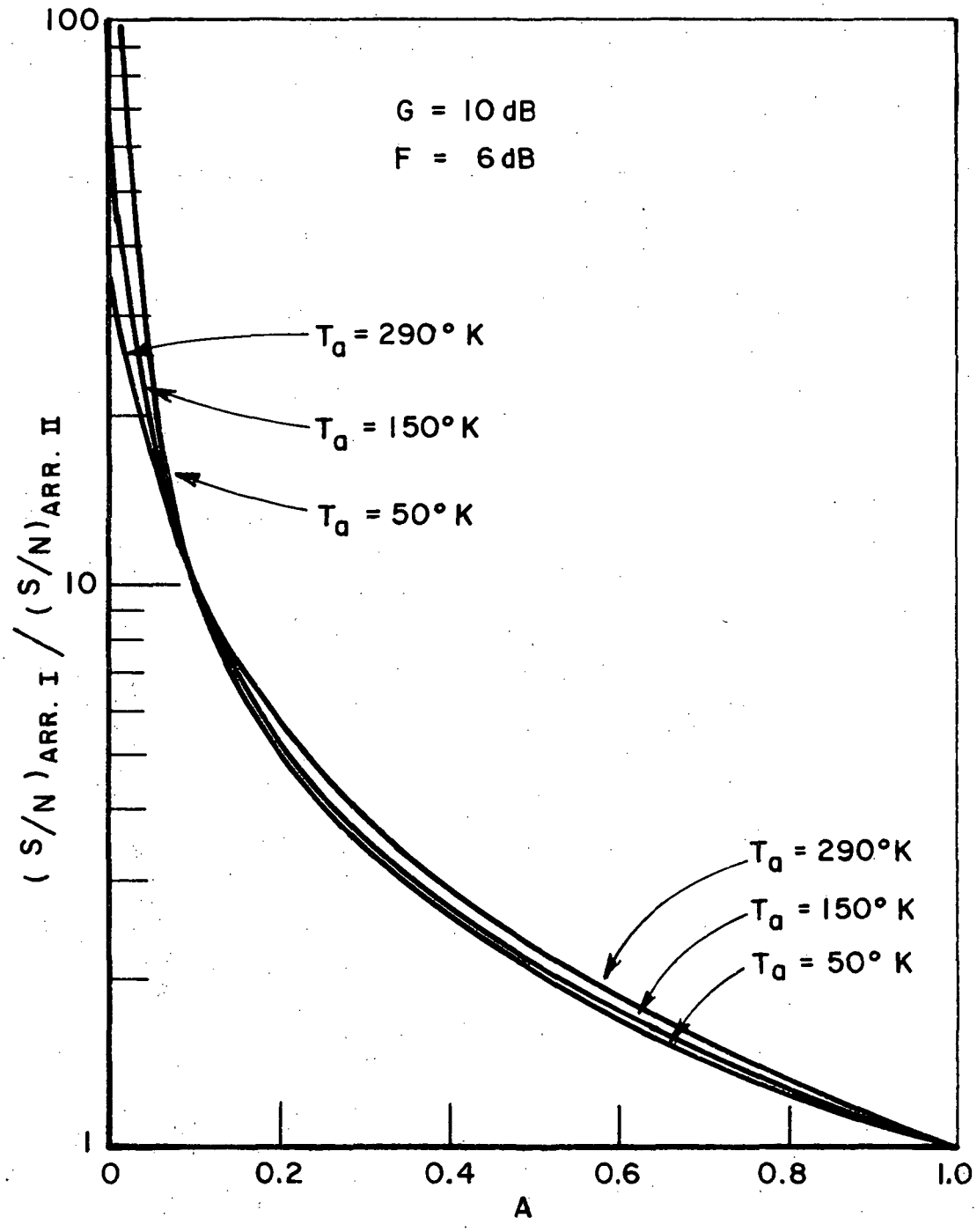

Fig. 40. SNR improvement of one antenna organization (Fig. 36) relative to another (Fig. 37).

ratio. This improvement comes at increased cost, however, since more active devices are required. The actual placement must be a compromise based on these computations.

G. Systems Using Converters

At 30 GHz and above, reliable low-noise amplifiers are difficult to obtain. Instead of RF amplifiers, usually down-converters are used in receiving systems to convert the high frequency signals into intermediate frequency ones, for which amplifiers are readily available. The noise coming from the converters and IF amplifiers can be evaluated in a way parallel to that used in RF amplifiers. Since all noise sources are thermal or shot noise, which are statistically independent [19], they are uncorrelated with one another.

The noise figure of a converter-IF amplifier system is defined in the same manner as that used for an amplifier,

$$F = \frac{N_{out}}{G_t N_i} \tag{32}$$

where N_{out} is the output noise power in the intermediate frequency band, N_i is the standard-temperature noise power available in the effective RF band at the input port, and G_t is the overall gain.

It has been shown [20, 21] that the noise figure of the overall converter (a mixer followed by an IF amplifier) is

$$F = L\,(F_{if} - 1 + N_R) \tag{33}$$

for single-sideband conversion, and

$$F = \frac{L}{2}(F_{if} - 1 + N_R) \tag{34}$$

for double-sideband conversion.

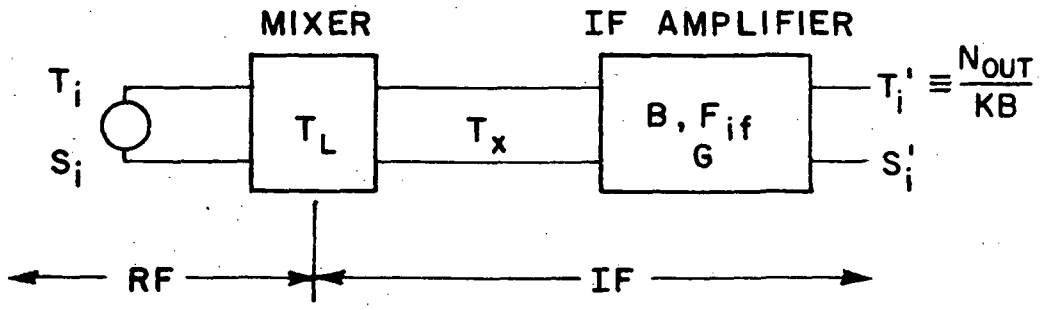

Fig. 41 The noise figure of a converter.

In the above equations, N_R is defined as

$$N_R = \frac{T_x \text{ (when } T_i = 290^\circ \text{ K)}}{T_i = 290^\circ K} \tag{35}$$

L is the insertion loss of the mixer, and F_{if} is the noise figure of the IF amplifier.

The definition of the excess noise ratio N_R is not very useful for calculations because it does not relate directly to available device parameters. It can be shown that it is also given by

$$N_R = F_m / L \tag{36}$$

where F_m is the mixer noise figure. Barber has shown that for Schottky-barrier diodes F_m and L both are functions of the pulse duty ratio, and hence of local oscillator drive [22]. If the local oscillator voltage does not contain appreciable noise components, N_R values in the range $0.5 < N_R < 1$ can be calculated from Barber's

values of F_m and L. When the IF amplifier noise figure F_{if} is high, the value $N_R \simeq 1$ is sometimes used in equations (33) and (34) to get as useful but rough estimates

$$F \approx L\ F_{if} \tag{37}$$

for single-sideband operation and

$$F \approx \frac{1}{2} L\ F_{if} \tag{38}$$

for double-sideband operation.

After passing the converter stage, a signal S_i, translated to the intermediate frequency, has amplitude

$$S_i' = \frac{G}{L} S_i \tag{39}$$

and a noise temperature

$$T_i' = \frac{G}{L} \left[T_o\ (F - 1) + T_i \right] \quad . \tag{40}$$

It is clear that we can replace equations (12), (13) by equations (39), (40) for a system employing converters, and then use the techniques and formulas for amplifiers from the preceeding sections. Of course, F in equation (4) is different from that used in equations (12), (13), and is given by equations (33) and (34). In this manner, the results of the previous sections can be applied directly to the case of a system using converters.

CHAPTER V

CONCLUSIONS

Ways of calculating the noise behavior of circuits were reviewed by using the scattering matrix and the energy conservation concepts. It was shown that by use of the voltage transmission factors of a system, it is possible to predict its thermal noise response as well as that of the signals.

The noise performance of some very large antenna arrays was calculated for passive arrays in Chapter III and the results of several different arrangements were plotted in terms of their relative signal-to-noise ratios. The results show that one cannot extend the size of an array indefinitely without running into serious signal-to noise ratio problems. The maximum size of an array depends on the manner of interconnecting the elements, their physical constants, and the application.

Chapter IV deals with the noise performance of arrays involving active devices. The noise contributions of an active device were specified by its noise figure. The effects of placing active devices at various locations in a very large array were determined in terms of the noise figure and gains of active devices as well as system parameters such as the ambient temperature and the degree of loss of the passive parts of the circuit. The tradeoffs were shown by means

of curves comparing different system arrangements and different devices. For a given class of devices, characterized by gain and noise figure, the signal-to-noise ratio improves as the active devices are moved forward in the signal path (closer to the array elements), but this requires more devices and therefore increases cost.

APPENDIX A

To get equations (49) and (50), write the scattering matrix equation explicitly as

$$\begin{bmatrix} V_1^- \\ V_2^- \\ \cdot \\ \cdot \\ \cdot \\ V_n^- \end{bmatrix} = \begin{bmatrix} S_{11} & S_{12} & & & S_{1n} \\ S_{21} & S_{22} & \cdot & \cdot & S_{2n} \\ \cdot & & & & \cdot \\ \cdot & & & & \cdot \\ \cdot & & & & \cdot \\ S_{n1} & S_{n2} & \cdot & \cdot & S_{nn} \end{bmatrix} \begin{bmatrix} V_1^+ \\ V_2^+ \\ \cdot \\ \cdot \\ \cdot \\ V_n^+ \end{bmatrix} . \qquad (A1)$$

We'll confine ourselves to the case that all the characteristic impedances are real to simplify the calculations.

Applying a voltage V = 1 volt at port i, and letting all the other input voltages equal to zero, i.e.,

$$V_i^+ = 1 , \qquad (A2)$$

$$V_j^+ = 0 \ , \quad j \neq i \ , \tag{A3}$$

we obtain from the scattering matrix the outgoing voltages at each port

$$V_j^- = S_{ji} , \qquad j = 1, 2, \ldots , n \ . \tag{A4}$$

The power flowing into the junction at port i is

$$P_i^+ = V_i^+ \, (I_i^+)^* = \frac{1}{Z_i} \ , \tag{A5}$$

subject to all characteristic impedances being real, and zero for other ports.

The power flowing out of the junction from each port j is

$$P_j^- = -V_j^- \, (I_j^-)^* = |S_{ji}|^2 \ \frac{1}{Z_j} \ . \tag{A6}$$

Applying to the input power and the output power the energy conservation relationship

$$P_i^+ \geq \sum_{j=1}^{n} P_j^- \tag{A7}$$

yields

$$\frac{1}{Z_i} \geq \sum_{j=1}^{n} |S_{ji}|^2 \ \frac{1}{Z_j} \tag{A8}$$

Define

$$\alpha_{ji} \equiv \sqrt{\frac{Z_i}{Z_j}} \ S_{ji} \ , \tag{A9}$$

then

$$\sum_{j=1}^{n} |\alpha_{ji}|^2 \leq 1 \ . \tag{A10}$$

Now, the scattering matrix becomes

$$S = \begin{bmatrix} \sqrt{\frac{Z_1}{Z_1}}\alpha_{11} & \sqrt{\frac{Z_1}{Z_2}}\alpha_{12} & \cdots & \sqrt{\frac{Z_1}{Z_n}}\alpha_{1n} \\ \sqrt{\frac{Z_2}{Z_1}}\alpha_{21} & \sqrt{\frac{Z_2}{Z_2}}\alpha_{22} & \cdots & \sqrt{\frac{Z_2}{Z_n}}\alpha_{2n} \\ \vdots & \vdots & & \vdots \\ \sqrt{\frac{Z_n}{Z_1}}\alpha_{n1} & \sqrt{\frac{Z_n}{Z_2}}\alpha_{n2} & & \sqrt{\frac{Z_n}{Z_n}}\alpha_{nn} \end{bmatrix} \quad \text{(A11)}$$

In case of the lossless junction, we have the equal sign in equation (A7). This leads to the equal sign in equation (A10), i.e.,

$$\sum_{j=1}^{n} |\alpha_{ji}|^2 = 1 \ . \quad \text{(A12)}$$

Equations (A11) and (A12) appear as equations (49) and (50) in Chapter II.

To get the reciprocity relationship (51), first apply a unity voltage at port i, and set all the other input voltages equal to zero, we then have a corresponding output current at port j

$$I_j^- = \frac{S_{ji}}{Z_j} \quad \text{(A13)}$$

Second, apply a unity input voltage at port j and let all other input voltages be zero, we then get a corresponding output current at port i

$$I_i^- = \frac{S_{ij}}{Z_i} \tag{A14}$$

Since we have $V_i^+ = V_j^+ = 1$, from the reciprocity theorem

$$I_i^- = I_j^- \tag{A15}$$

and hence

$$\frac{S_{ji}}{Z_j} = \frac{S_{ij}}{Z_i} \tag{A16}$$

This is equation (51) in Chapter II.

Notice that the theory stated in this section is quite general and is applicable to a junction of directional couplers as well as that of transmission lines. Hence equations (A9), (A10) and (A16) are true for any linear, reciprocal n-port.

For a lossless junction, all the equations are still true except equation (A10) can be simplified into equation (A12).

APPENDIX B

SCATTERING MATRIX OF N PARALLEL-CONNECTED TRANSMISSION LINES

Consider the junction of n transmission lines connected in parallel. The characteristic admittances of the transmission lines are

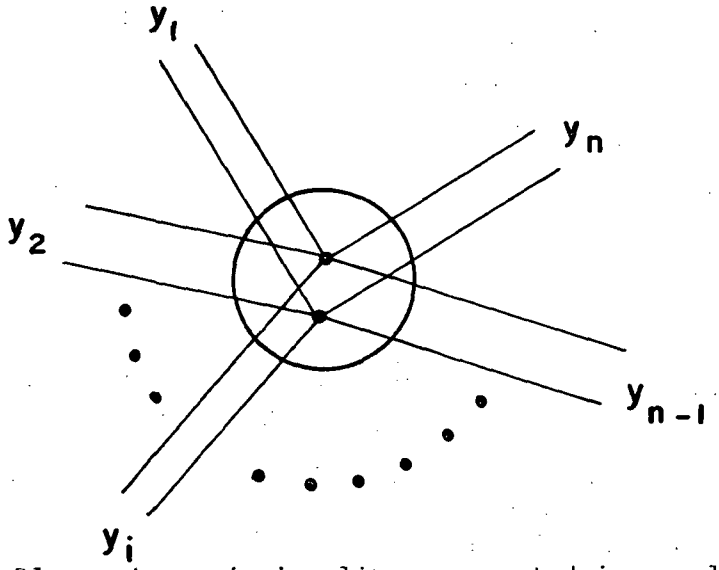

Fig. B1. n transmission lines connected in parallel.

$Y_1, Y_2, Y_3, \ldots, Y_n$. The voltage and current on each of the lines can be written as

$$V_i = V_i^+ + V_i^- , \qquad i = 1, 2, \ldots, n \tag{B1}$$

$$I_i = I_i^+ + I_i^- , \qquad i = 1, 2, \ldots, n \tag{B2}$$

where each line current and the corresponding voltage are related by

$$\frac{V_i^+}{I_i^+} = -\frac{V_i^-}{I_i^-} = Z_i = \frac{1}{Y_i} , \tag{B3}$$

with all the voltages and currents referred to the junction terminals.

To find the scattering matrix, first attach a generator at port i and adjust its voltage so that the junction voltage V is unity

$$V = 1 \tag{B4}$$

while all other ports are terminated by their own characteristic impedances.

Then we have

$$V_i^+ + V_i^- = 1 \tag{B5}$$

$$V_j^+ = 0 , \quad j \neq i , \tag{B6}$$

$$V_j^- = 1 , \quad j \neq i . \tag{B7}$$

From equation (B3), we find

$$I_i^+ = Y_i V_i^+ , \tag{B8}$$

$$I_i^- = -Y_i V_i^- , \tag{B9}$$

$$I_j^+ = 0 , \quad j \neq i , \tag{B10}$$

$$I_j^- = -Y_j V_j^- = -Y_j . \tag{B11}$$

Applying Kirchhoff's Current Law at the junction, $\sum i = 0$, gives

$$I_i^+ + I_i^- + \sum_{\substack{j=1 \\ j\neq i}}^{n} I_j^- = 0 , \tag{B12}$$

and by use of equations (B6) to (B11) in equation (B12), one obtains

$$Y_i V_i^+ + Y_i(1 - V_i^-) = \sum_{j=1}^{n} Y_j . \tag{B13}$$

Solving equations (B5) and (B13) gives

$$V_i^+ = \frac{\sum_{j=1}^{n} Y_j}{2Y_i} \tag{B14}$$

$$V_i^- = \frac{2Y_i - \sum_{j=1}^{n} Y_j}{2Y_i} . \tag{B15}$$

From these two equations we obtain

$$S_{ii} \equiv \frac{V_i^-}{V_i^+}\bigg|_{\substack{v_j^+=0 \\ \text{for } j\neq i}} = \frac{2Y_i - \sum_{j=1}^{n} Y_j}{\sum_{j=1}^{n} Y_j} . \tag{B16}$$

From equations (B7) and (B14) one gets

$$S_{ji} \equiv \frac{V_j^-}{V_i^+}\bigg|_{v_j^+=0} = \frac{2Y_i}{\sum_{j=1}^{n} Y_j} , \quad j \neq i . \tag{B17}$$

Therefore, the scattering matrix is given by

$$S = \begin{bmatrix} \frac{2Y_1 - \Sigma Y_2}{\Sigma Y_2} & \frac{\Sigma Y_2}{\Sigma Y_2} & \cdots & \frac{2Y_n}{\Sigma Y_j} \\ \frac{2Y_1}{\Sigma Y_j} & \frac{2Y_2 - \Sigma Y_j}{\Sigma Y_j} & \cdots & \frac{2Y_n}{\Sigma Y_j} \\ \vdots & \vdots & & \vdots \\ \frac{2Y_1}{\Sigma Y_j} & \frac{2Y_2}{\Sigma Y_j} & \cdots & \frac{2Y_n - \Sigma Y_j}{\Sigma Y_j} \end{bmatrix} . \tag{B18}$$

APPENDIX C

SUMMATION OF UNCORRELATED NOISE IN MICROWAVE CIRCUITS

For a linear system, we can sum up the contributions from the noise inputs, measured at the output, by adding the products obtained by multiplying each input noise power by the square of the absolute value of the corresponding voltage transmission factor to get the output noise. This will now be shown.

Consider a microwave system having the scattering matrix

$$S = \begin{bmatrix} S_{11} & S_{12} & S_{13} & \cdots & S_{1n} \\ S_{21} & S_{22} & \cdot & \cdots & S_{2n} \\ \cdot & \cdot & & & \\ \cdot & \cdot & & & \\ \cdot & \cdot & & & \\ S_{n1} & S_{n2} & \cdot & \cdots & S_{nn} \end{bmatrix} \qquad (C1)$$

where all the terms are expressed in terms of w, in the frequency domain.

The output signal at port n is

$$V_n^-(w) = \sum_{i=1}^{n} S_{ni}(w)\, V_i^+(w) \quad . \qquad (C2)$$

This is suitable for deterministic signals. Since we want to treat

uncorrelated noise, which is a random and stationary process, we introduce the impulse function $h_{ij}(f)$ such that [23]

$$h_{ij}(t) = \frac{1}{2\pi} \int_{-\infty}^{\infty} S_{ij}(w)\, e^{iwt}\, dw \,, \tag{C3}$$

i.e., $h_{ij}(t)$ is the inverse Fourier transform of $S_{ij}(w)$.

Then the output voltage, without including the internal noise of the system, would be

$$\underline{V_n}^{-}(t) = \sum_{i=1}^{n} h_{ni}(t) * \underline{V_i}^{+}(t) \tag{C4}$$

where * represents the convolution operation and the underline distinguishes random variables,

$$h_{ni}(t) * \underline{V_i}(t) = \int_{-\infty}^{\infty} h_{ni}\,(t-\alpha)\ \underline{V_i}(\alpha)\, d\alpha$$

$$= \int_{-\infty}^{\infty} h_{ni}(\alpha)\ \underline{V_i}\,(t-\alpha)\, d\alpha \,. \tag{C5}$$

Define the crosscorrelation function of V's as

$$R_{ij}\,(t_1,t_2) = E(\underline{V_i}(t_1)\underline{V_j}(t_2)) \,, \tag{C6}$$

where E denotes the expected value. If the V's are uncorrelated and stationary, then (C6) can be simplified as

$$R_{ij}\,(\tau) = 0 \qquad \text{for } i \neq j \tag{C7}$$

$$R_i\,(\tau) = R_{ii}\,(\tau) = E(\underline{V_i}(t)\ \underline{V_i}\,(t+\tau)) \,, \tag{C8}$$

which is an even function of τ.

Therefore the output autocorrelation function is, by definition,

$$R_n^-(\tau) = E(\underline{V_n^-}(t)\ \underline{V_n^-}(t+\tau))$$

$$= E \sum_{j=1}^{n} \sum_{i=1}^{n} \int\int_{-\infty}^{\infty} h_{ni}(\alpha)\ \underline{V_i}^+(t-\alpha)d\alpha h_{nj}(\beta)\underline{V_j}^+(t+\tau-\beta)d\beta$$

$$= \sum_{j=1}^{n} \sum_{i=1}^{n} \int\int_{-\infty}^{\infty} h_{ni}(\alpha)h_{nj}(\beta)E(\underline{V_i}^+(t-\alpha)\underline{V_j}^+(t+\tau-\beta))d\alpha d\beta \ . \tag{C9}$$

The spectral density $S_n(w)$ of the output is given by

$$S_n^-(w) = \int_{-\infty}^{\infty} R_n^-(\tau)\ e^{-jw\tau}d\tau \tag{C10}$$

$$S_n^-(w) = \sum_{j=1}^{n} \sum_{i=1}^{n} \int_{-\infty}^{\infty}\int_{-\infty}^{\infty}\int_{-\infty}^{\infty} h_{ni}(\alpha)h_{nj}(\beta)R_{ij}^+(\tau+\alpha-\beta)e^{-jw\tau}d\alpha d\beta d\tau \ .$$

$$= \sum_{i=1}^{n} \int_{-\infty}^{\infty}\int_{-\infty}^{\infty} h_{ni}(\alpha)d\alpha \int_{-\infty}^{\infty} h_{ni}(\beta)d\beta R_i^+(\tau')e^{-jw(\tau'-\alpha+\beta)}d\tau'$$

$$= \sum_{i=1}^{n} \int_{-\infty}^{\infty} h_{ni}(\alpha)e^{jw\alpha}d\alpha \int_{-\infty}^{\infty} h_{ni}(\beta)e^{-jw\beta}d\beta S_i^+(w)$$

$$= \sum_{i=1}^{n} S_{ni}^{\ *}(w)\ S_{ni}(w)S_i^+(w) \ , \tag{C11}$$

$$S_n^-(w) = \sum_{i=1}^{n} |S_{ni}(w)|^2\ S_i^+(w) \ . \tag{C12}$$

In this we have used the relationship

$$S_x(w) = \int_{-\infty}^{\infty} R_x(\tau) e^{-jw\tau} d\tau \quad . \tag{C15}$$

$S_x(w)$ is often called the power spectrum.

The variance of the output voltage is

$$N_n^- = E(\underline{V_n}^{-2}(t)) = R_n^-(0)$$

$$= \frac{1}{2\pi} \int_{-\infty}^{\infty} S_n^-(w)\, dw \quad , \tag{C14}$$

or

$$N_n^- = \int_{-\infty}^{\infty} S_n^-(w)\, df \quad . \tag{C16}$$

Substituting (C12) into this equation yields

$$N_n^- = \int_{\infty}^{\infty} \sum_{i=1}^{n} |S_{ni}(w)|^2 S_i^+(w) df \quad . \tag{C17}$$

For an impedance-normalized circuit, i.e., one for which the scattering matrix is written with respect to identical characteristic impedances at all ports, N_n^- is the output noise power contributed by the input noise powers.

Note that the input noise power is given by

$$N_i^+ = \int_{-\infty}^{\infty} S_i^+(w) df \quad . \tag{C18}$$

For a bandpass system having equivalent bandwidth $B = f_2 - f_1$ and over which $S_{ni}(w)$ and $S_i^+(w)$ can be considered constants, N_n is given by

$$N_n^- = \int_B \sum |S_{ni}(w)|^2 S_i^+(w)\, df$$

$$\approx \sum |S_{ni}|^2 \, S_i^+(2B)$$

$$= 2\sum |S_{ni}|^2 \, S_i^+ B \quad . \tag{C19}$$

The term $2S_i^+ B$ is just the input noise power at port i,

$$N_i^+ = \int_B S_i^+(w)df$$

$$\approx 2S_i^+(f_2 - f_1)$$

$$= 2S_i^+ B \quad , \tag{C20}$$

subject to $S_i^+(w)$ being constant over the frequency band $f_1 - f_2$.

Therefore, for an impedance-normalized circuit, we have

$$N_n^- = \sum_{i=1}^{n} |S_{ni}|^2 \, N_i^+ \, , \tag{C21}$$

which is the formula used throughout this thesis. The book by Davenport and Root [24] has a derivation parallel to what is given here.

APPENDIX D

COMPUTER PROGRAMS

The computer programs used to plot the relative SNR curves in Chapter III are listed here. Subprograms LOGAXS and ROGAXS plot the coordinate axis in log-log scale. The details are explained through the comment statements in the programs. The equations used in the calculations are explained and listed in Chapter III. The Fortran listing follows.

PROGRAM I

```
C      PARALELL FEED ANTENNA ARRAY
C      THIS PROGRAM PLOTS S/N RATIO OF A LOSSY ARRAY
C      THE PHASE SHIFT CAUSED BY A PHASE SHIFTER IS ASSUMED TO BE 2 PI
C      THE ATTENUATION CONSTANT OF THE TRANSMISSION LINES IS ALP IN DB/FT,A IN DB/M
C      THE FREQENCY F=30 GHZ
C      THE WAVELENGTH IS 0.01 METERS
C      THE FIGURE OF MERIT OF A PHASE SHIFTER IS AL IN DEGREE/DB
       COMMON AL,ED,A
       DIMENSION  IBUF(100),DIM(30,100)
       AL=300
   40  WRITE(6,20)
20     FORMAT(' ATTENUATION CONSTANT (DB/FT)=')
       READ(8,-)  ALP
       CALL DEASSN
       DO 4 II=5,25,5
       ED=II*0.01
       A=0.1*ALP*ALOG(10.0)/0.3048
       AI=EXP(-SQRT(0.5)*ED*A)/(1-EXP(-SQRT(0.5)*ED*A))
       TN=0
       SR=0
       DO 4 M=1,100
       DO 1 MM=1,M
       TN=TN+ALPHA(MM,M)+ALPHA(M,MM)
     1 SR=SR+SQRT(ALPHA(MM,M))+SQRT(ALPHA(M,MM))
       TN=TN-ALPHA(M,M)
       SR=SR-SQRT(ALPHA(M,M))
       TS=SR**2
       AIM=4*TS/TN
   4   DIM(II,M)=10*ALOG10(AIM)
       WRITE(6,300)
   300 FORMAT(' READY TO PLOT?')
       READ(8,-)XYZ
C      PLOT THE CALCULATED DATA
       CALL PLOTS(IBUF,100,3)
       CALL PLOT  (0.0,2.0,-3)
       CALL AXIS(0.0,0.0,34HM (NUMBER OF ARRAY ELEMENTS=2M*2M),-34,5.0,
```

```
PROGRAM I (continued)
      20.0,0.0,20.0,0.5,-1)
      CALL AXIS(0.0,-1.0,23HRELATIVE S/N RATIO (DB),23,9.0,90.0,-6.0
     1,6.0,0.5,-1)
      CALL AXIS(0.0,8.0,1HN,1,5.0,0.0,0.0,20.0,0.5,-1)
      CALL AXIS(5.0,8.0,2HLB,2,6.0,270.0,48.0,-6.0,0.5,-1)
      CALL SYMBOL(1.0,7.2,0.1,26HPARALLEL FED ANTENNA ARRAY,0.0,26)
      CALL SYMBOL(1.0,7.0,0.1,28HSPACING OF ARRAY ELEMENTS= N,0.0,28)
      CALL SYMBOL(1.0,6.8,0.1,31HATTENUATION CONSTANT=     DB/FT,
     20.0,31)
      CALL SYMBOL(1.0,6.6,0.2,36,0.0,-1)
      CALL SYMBOL(1.2,6.6,0.1,6H=360.0,0.0,6)
      CALL SYMBOL(4.0,7.0,0.2,18,0.0,-1)
      CALL NUMBER(3.1,6.6,0.1,ALP,0.0,2)
      DO 30 I=5,25,5
      XI=I
      CALL PLOT(1.0/20.0IM(1,1)/6.0,3)
      DO 3 N=2,100
      CI=N/20.0
      BIM=DI (I,N)/6.0
    3 CALL PLOT(CI,BIM,2)
      CALL SYMBOL(CI+0.03,BIM-0.05,0.1,2HN=,0.0,2)
   30 CALL NUMBER(CI+0.03+0.3,BIM-0.05,0.1,XI,0.0,0)
      CALL PLOT (7.0,-2.0,999)
      CALL EXIT
      END
      FUNCTION ALPHA(MM,NN)
      COMMON AL,EC,P
      D=SQRT((MM-0.5)**2+(NN-0.5)**2)*EC
      E=ALOG(10.0)*36//L
      G=-A*D-E
      ALPHA=EXP(G)
      RETURN
      END
      FUNCTION ALPHO(MM,NN)
      ALPHO=1-ALPHA(MM,NN)
      RETURN
      END
```

PROGRAM II

```
1 C      PARALELL FEED ANTENNA ARRAY
2 C      THIS PROGRAM PLOTS S/N RATIO OF A LOSSY ARRAY
3 C      THE PHASE SHIFT CAUSED BY A PHASE SHIFTER IS ASSUMED TO BE 2 PI
4 C      THE ATTENUATION CONSTANT OF THE TRANSMISSION LINES IS ALP IN DB/FT.A IN DB/M
5 C      THE FREQENCY F=30 GHZ
6 C      THE WAVELENGTH IS 0.01 METERS
7 C      THE FIGURE OF MERIT OF A PHASE SHIFTER IS AL IN DEGREE/DB
8 C      PARALELL FEED ANTENNA ARRAY
9        DIMENSION  IBUF(100),DIM(30,100)
10       AI=300
11    40 WRITE(8,20)
12 20    FORMAT('SPACING(IN WAVELENGTH)')
13       READ(8,*)  DIST
14       CALL DEASSN
15       ED=DIST*0.01
16       DO 4 II=5,25,4
17       ALP=0.01*II
18       A=0.1*ALP*ALOG(10.0)/0.3048
19       AI=EXP(-SQRT(0.5)*ED*A)/(1-EXP(-SQRT(0.5)*ED*A))
20       TN=0
21       SR=0
22       DO 4 M=1,100
23       DO 1 MM=1,M
24       TN=TN+ALPHO(MM,M)+ALPHO(M,MM)
25     1 SR=SR+SQRT(ALPHA(MM,M))+SQRT(ALPHA(M,MM))
26       TN=TN-ALPHO(M,M)
27       SR=SR-SQRT(ALPHA(M,M))
28       TS=SR**2
29       AIM=4*TS/TN
30     4 DIM(II,M)=10*ALOG10(AIM)
31       WRITE(8,300)
32   300 FORMAT(' READY TO PLOT?')
33       READ(8,*)XY7
34       CALL PLOTS(IBUF,100,3)
35       CALL PLOT  (0.0,2.0,-3)
36       CALL AXIS(0.0,0.0,34HNUMBER OF ARRAY ELEMENTS=2M*2M),-34,5.0,
```

PROGRAM II (continued)

```
      20.0,0.0,20.0,0.5,-1)
       CALL AXIS(0.0,-1.0,23HRELATIVE S/N RATIO (DB),23,9.0,90.0,-6.0
      1,6.0,0.5,-1)
       CALL AXIS(0.0,8.0,1HN,1,5.0,0.0,0.0,20.0,0.5,-1)
       CALL AXIS(5.0,8.0,2HDB,2,8.0,270.0,48.0,-6.0,0.5,-1)
       CALL SYMBOL(1.0,7.2,0.1,26HPARALLEL FED ANTENNA ARRAY,0.0,26)
       CALL SYMBOL(1.0,7.0,0.1,26HSPACING OF ARRAY ELEMENTS=,0.0,26)
       CALL SYMBOL(1.0,6.8,0.1,29HATTENUATION CONSTANT= A DB/FT,
      20.0,29)
       CALL SYMBOL(4.0,7.0,0.2,18,0.0,-1)
       CALL NUMBER(3.6,7.0,0.1,DIST,0.0,0)
       CALL SYMBOL(1.0,6.6,0.2,36,0.0,-1)
       CALL SYMBOL(1.2,6.6,0.1,6H=360.0,0.0,6)
       DO 30 I=5,25,4
       CALL PLOT(1.0/20,DIM(I,1)/6.0,3)
       DO 3 N=2,100
       CI=N/20.0
       RIM=DIM(I,N)/6
  3    CALL PLOT(CI,RIM,2)
       CALL SYMBOL(CI+0.03,RIM-0.05,0.1,2HA=,0.0,2)
 30    CALL NUMBER(CI+0.03+0.3,RIM-0.05,0.1,0.01*I,0.0,2)
       CALL PLOT (7.0,-2.0,999)
       CALL EXIT
       END
       FUNCTION ALPHA(MM,NN)
       COMMON AL,ED,A
       D=SQRT((MM-0.5)**2+(NN-0.5)**2)*ED
       E=ALOG(10.0)*36/AL
       G=-A*D-E
       ALPHA=EXP(G)
       RETURN
       END
       FUNCTION ALPHO(MM,NN)
       ALPHO=1-ALPHA(MM,NN)
       RETURN
       END
```

PROGRAM III

```
      C     8-ELEMENT PASSIVE CORPORATE FEED ARRAY
      C     THIS PROGRAM PLOTS S/N RATIO OF A LOSSY ARRAY
      C     PHI1 IS THE PHASE SHIFT OF 3 OF 4 ELEMENTS OF EACH PRIMITIVE STAGE
      C     PHI2 IS THE PHASE SHIFT OF 3 O 4 ELEMENTS OF STAGES OTHER THAN PRIMITIVE
      C     ONES
      C     PHI3 IS THE PHASE SHIFT OF THE OTHER ELEMENT IN A PRIMITIVE STAGE
            DIMENSION IBUF(100),AI(30,100)
      C     THE ATTENUATION CONSTANT OF THE TRANSMISSION LINE IS ALP IN DB/FT,A IN DB/M
      C     THE FREQENCY F=30 GHZ
      C     THE WAVELENGTH IS L METERS;THE SPAACING OF ELEMENTS IS M WAVELENGTHS
            REAL L
            F=30
            L=0.3/F
      C     THE FIGURE OF MERIT OF A PHASE SHIFTER IS AL IN DEGREE/DB
            AL=300
       40   WRITE(8,10)
       10   FORMAT('PHI1,PHI2,PHI3,ALP=')
            READ(8,*)PHI1,PHI2,PHI3,ALP
            A=ALP/0.3048
      C
      C     AL1,AL2,AL3,ARE PHASE SHIFTER POWER LOSS FACTORS
            AL1=0.1**(PHI1*0.1/AL)
            AL2=0.1**(PHI2*0.1/AL)
            AL3=0.1**(PHI3*0.1/AL)
            AL11=SQRT(AL1)
            AL22=SQRT(AL2)
            AL33=SQRT(AL3)
      C     CALCALATION OF S/N RATIO IN TERMS OF WAVELENGTH
            DO 100 M=5,20,3
            DIS=L*M
            D=DIS/SQRT(2.0)
```

PROGRAM III (continued)

```
      AD=0.1**(D*A*0.1)
      S1=0.25*AD*(3*AL11+AL33)**2
      AN1=1-0.25*(3*AL1+AL3)*AD
      AI(1,M)=S1/AN1
      AN=AN1
      DO 100 K=2,5
      S=0.25**(K-1)*AD**(2**K-2)*(3*AL22+1)**(2*K-2)*S1
      AN=1+0.25*(AN-1)*(1+3*AL2)*AD**(2**(K-1))
  100 AI(K,M)=S/AN
      WRITE(3,300)
  300 FORMAT(' READY TO PLOT?')
C      PLOT THE CALCULATED DATA
      READ(8,-)XYZ
      CALL PLOTS(IBUF,100,3)
      CALL PLOT  (0.0,2.0,-3)
      CALL LOGAXS(6.0,6.0,0.0,0.0,28HM (NUMBER OF ARRAY ELEMENTS),28)
      CALL LOGAXS(8.0,8.0,0.0,0.0,18HRELATIVE S/N RATIO,-18)
      CALL ROGAXS(6.0,6.0,0.0,8.0,1HM,1)
      CALL ROGAXS(8.0,8.0,6.0,0.0,18HRELATIVE S/N RATIO,-18)
      CALL SYMBOL(1.0,7.5,0.1,37H4-ELEMENT PASSIVE CORPORATE-FED ARRAY
     4,0.0,37)
      CALL SYMBOL(1.0,7.3,0.1,26HSPACING OF ARRAY ELEMENTS= N,0.0,28)
      CALL SYMBOL(1.0,7.1,0.1,31HATTENUATION CONSTANT=     DB/FT,
     20.0,31)
      CALL SYMBOL(1.0,6.9,0.2,36,0.0,-1)
      CALL SYMBOL(1.2,6.9,0.1,2H1=,0.0,2)
      IF (PHI3.NE.0) GO TO 123
      CALL NUMBER(1.5,6.9,0.1,PHI1,0.0,1)
      GO TO 124
  123 CALL NUMBER(1.8,6.9,0.1,PHI1,0.0,1)
      CALL SYMBOL(1.6,6.9,0.1,2H3=,0.0,2)
      CALL SYMBOL(1.4,6.9,0.2,36,0.0,-1)
```

PROGRAM III (continued)

```
 124  CONTINUE
      CALL SYMBOL(1.0,6.7,0.2,36,0.0,-1)
      CALL SYMBOL(1.2,6.7,0.1,2H2=,0.0,2)
      CALL NUMBER(1.5,6.7,0.1,PHI2,0.0,1)
      CALL SYMBOL(4.0,7.3,0.2,18,0.0,-1)
      CALL NUMBER(3.1,7.1,0.1,ALP,0.0,2)
      DO 122 M=5,20,3
      A=ALOG10(4.0)
      KN=3
      DO 111 K=1,8
      C=A*K
      D=ALOG10(AI(K,M))
      CALL PLOT(C,D,KN)
 111  KN=2
      CALL SYMBOL(C+0.2,D-0.05,0.1,2HN=,0.0,2)
      W=M
 122  CALL NUMBER(C+0.5,D-0.05,0.1,W,0.0,0)
      CALL PLOT (8.0,-2.0,999)
      WRITE(3,909)
 909  FORMAT('N=?')
      READ(8,-)NN
      GO TO(40,70),NN
  70  CALL EXIT
      END
```

PROGRAM IV

```
C      4-ELEMENT PASSIVE CORPORATE FEED ARRAY
C      THIS PROGRAM PLOTS S/N RATIO OF A LOSSY ARRAY
C      PHI1 IS THE PHASE SHIFT OF 3 OF 4 ELEMENTS OF EACH PRIMITIVE STAGE
C      PHI2 IS THE PHASE SHIFT OF 3 O 4 ELEMENTS OF STAGES OTHER THAN PRIMITIVE
C      ONES
C      PHI3 IS THE PHASE SHIFT OF THE OTHER ELEMENT IN A PRIMITIVE STAGE
       DIMENSION IBUF(100),AI(30,100)
C      THE ATTENUATION CONSTANT OF THE TRANSMISSION LINE IS ALP IN DB/FT,A IN DB/M
C      THE FREQENCY F=30 GHZ
C      THE WAVELENGTH IS L METERS;THE SPAACING OF ELEMENTS IS M WAVELENGTHS
       REAL L
       F=30
       L=0.3/F
C      THE FIGURE OF MERIT OF A PHASE SHIFTER IS AL IN DEGREE/DB
       AL=300
   40  WRITE(8,10)
   10  FORMAT('PHI1,PHI2,PHI3,SPACING(IN WAVELENGTH)=')
       READ(8,*)PHI1,PHI2,PHI3,DIS
       D=DIS*L/SQRT(2.0)
C
C      AL1,AL2,AL3,ARE PHASE SHIFTER POWER LOSS FACTORS
       AL1=0.1**(PHI1*0.1/AL)
       AL2=0.1**(PHI2*0.1/AL)
       AL3=0.1**(PHI3*0.1/AL)
       AL11=SQRT(AL1)
       AL22=SQRT(AL2)
       AL33=SQRT(AL3)
C      CALCALATION OF S/N RATIO IN TERMS OF WAVELENGTH
       DO 100 M=5,25,4
       A=0.01*M/0.3048
       AD=0.1**(D*A*0.1)
       S1=0.25*AD*(3*AL11+AL33)**2
```

PROGRAM IV (continued)

```
      AN1=1-0.25*(3*AL1+AL3)*AD
      AI(1,M)=S1/AN1
      AN=AN1
      DO 100 K=2,8
      S=0.25**(K-1)*AD**(2**K-2)*(3*AL22+1)**(2*K-2)*S1
      AN=1+0.25*(AN-1)*(1+3*AL2)*AD**(2**(K-1))
  100 AI(K,M)=S/AN
      WRITE(8,300)
  300 FORMAT(' READY TO PLOT?')
      READ(8,-)XYZ
C     PLOT THE CALCULATED DATA
      CALL PLOTS(IBUF,100,3)
      CALL PLOT  (0.0,2.0,-3)
      CALL LOGAXS(6,0,6.0,0.0,0.0,28HM (NUMBER OF ARRAY ELEMENTS),28)
      CALL LOGAXS(8,0,8.0,0.0,0.0,18HRELATIVE S/N RATIO,-18)
      CALL ROGAXS(6,0,6.0,0.0,8.0,1HA,1)
      CALL ROGAXS(8,0,8.0,6.0,0.0,18HRELATIVE S/N RATIO,-18)
      CALL SYMBOL(1.0,7.5,0.1,37H4-ELEMENT PASSIVE CORPORATE-FED ARRAY
     4,0.0,37)
      CALL SYMBOL(1.0,7.3,0.1,26HSPACING OF ARRAY ELEMENTS=,0.0,26)
      CALL SYMBOL(1.0,7.1,0.1,31HATTENUATION CONSTANT=  A  DB/FT,
     20.0,31)
      CALL SYMBOL(1.0,6.9,0.2,36,0.0,-1)
      CALL SYMBOL(1.2,6.9,0.1,2H1=,0.0,2)
      IF (PHI3.NE.0) GO TO 123
      CALL NUMBER(1.5,6.9,0.1,PHI1,0.0,1)
      GO TO 124
  123 CALL NUMBER(1.8,6.9,0.1,PHI1,0.0,1)
      CALL SYMBOL(1.6,6.9,0.1,2H3=,0.0,2)
      CALL SYMBOL(1.4,6.9,0.2,36,0.0,-1)
  124 CONTINUE
      CALL SYMBOL(1.0,6.7,0.2,36,0.0,-1)
      CALL SYMBOL(1.2,6.7,0.1,2H2=,0.0,2)
      CALL NUMBER(1.5,6.7,0.1,PHI2,0.0,1)
```

PROGRAM IV (continued)

```
      CALL SYMBOL(4.0,7.3,0.2,16,0.0,-1)
      CALL NUMBER(3.7,7.3,0.1,015,0.0,0)
      DO 90 M=5,25,4
      A=ALOG10(4.0)
      KN=3
      DO 111 K=1,8
      C=A*K
      D=ALOG10(AI(K,M))
      CALL PLOT(C,D,KN)
111   KN=2
      CALL SYMBOL(C+0.2,D-0.05,0.1,2HA=,0.0,2)
      W=0.01*M
 90   CALL NUMBER(C+0.5,D-0.05,0.1,W,0.0,2)
      CALL PLOT (3.0,-3.0,999)
      WRITE(6,909)
909   FORMAT('N=?')
      READ(8,-)NN
      GO TO(60,70),NN
 70   CALL EXIT
      END
```

PROGRAM V

```
C      4-ELEMENT PASSIVE CORPORATE FED ARRAY
C      THIS PROGRAM PLOTS S/N RATIO OF A LOSSY ARRAY
C      PHI1 IS THE PHASE SHIFT OF 3 OF 4 ELEMENTS OF EACH PPRIMITIVE STAGE
C      PHI2 IS THE PHASE SHIFT OF 3 O 4 ELEMENTS OF STAGES OTHER THAN PRIMITIVE
C      ONES
C      PHI3 IS THE PHASE SHIFT OF THE OTHER ELEMENT IN A PRIMITIVE STAGE
       DIMENSION IQUE(100),AI(30,100)
C      THE ATTENUATION CONSTANT OF THE TRANSMISSION LINE IS ALP IN DB/FT,A IN DB/M
C      THE FREQENCY F=30 GHZ
C      THE WAVELENGTH IS L METERS;THE SPAACING OF ELEMENTS IS M WAVELENGTHS
       REAL L
       F=30
       L=0.3/F
C      THE FIGURE OF MERIT OF A PHASE SHIFTER IS AL IN DEGREE/DB
       AL=300
   40  WRITE(*,10)
   10  FORMAT('PHI1,PHI2,PHI3,SPACING(IN WAVELENGTH)=')
       READ(8,*)PHI1,PHI2,PHI3,DIS
       D=DIS*L/SQRT(2.0)
C
C      AL1,AL2,AL3,ARE PHASE SHIFTER POWER LOSS FACTORS
       AL1=0.1**(PHI1*0.1/AL)
       AL2=0.1**(PHI2*0.1/AL)
       AL3=0.1**(PHI3*0.1/AL)
       AL11=SQRT(AL1)
       AL22=SQRT(AL2)
       AL33=SQRT(AL3)
C      CALCALATION OF S/N RATIO IN TERMS OF WAVELENGTH
       DO 100 M=5,25,4
       A=0.01*M/0.304
       AD=0.1**(D*A*0.1)
```

PROGRAM V (continued)

```
      S1=0.25*A0*(3*AL11+AL33)**2
      AN1=1-0.25*(3*AL1+AL3)*A0
      AI(1,M)=S1/AN1
      AN=AN1
      DO 100 K=2,12
      S=0.25**(K-1)*A0**(2**K-2)*(3*AL22+1)**(2*K-2)*S1
      AN=1+0.25*(AN-1)*(1+3*AL2)*A0**(2**(K-1))
100   AI(K,M)=S/AN
      WRITE(*,300)
300   FORMAT(' READY TO PLOT?')
      READ(5,*)YZ
C     PLOT THE CALCULATED DATA
      CALL PLOTS(IBUF,100,3)
      CALL PLOT  (0.0,2.0,-3)
      CALL LOGAXS(6,-3.0,0.0,0.0,6.0,22HDIMENSION OF ARRAY (M),22)
      CALL LOGAXS(8,9.0,6.0,90.0,0.0,18HRELATIVE S/N RATIO,-18)
      CALL ROGAXS(6,-3.0,0.0,0.0,6.0,1HM,1)
      CALL ROGAXS(8,0.0,6.0,6.0,0.0,18HRELATIVE S/N RATIO,-18)
      CALL SYMBOL(1.0,7.5,0.1,38H4-ELEMENT PASSIVE CORPORATE-FED ARRAY
     4,0.0,38)
      CALL SYMBOL(1.0,7.3,0.1,26HSPACING OF ARRAY ELEMENTS=,0.0,26)
      CALL SYMBOL(1.0,7.1,0.1,31HATTENUATION CONSTANT=  A  DB/FT,
     20.0,31)
      CALL SYMBOL(1.0,6.9,0.2,36,0.0,-1)
      CALL SYMBOL(1.2,6.9,0.1,2H1=,0.0,2)
      IF (PHI3.NE.0) GO TO 123
      CALL NUMBER(1.5,6.9,0.1,PHI1,0.0,1)
      GO TO 124
123   CALL NUMBER(1.5,6.9,0.1,PHI1,0.0,1)
      CALL SYMBOL(1.4,6.9,0.1,2H3=,0.0,2)
      CALL SYMBOL(1.4,6.9,0.2,36,0.0,-1)
```

PROGRAM V (continued)

```
      124  CONTINUE
           CALL SYMBOL(1.0,6.7,0.2,36,0.0,-1)
           CALL SYMBOL(1.2,6.7,0.1,2H2=,0.0,2)
           CALL NUMBER(1.5,6.7,0.1,PHI2,0.0,1)
           CALL SYMBOL(4.2,7.3,0.2,18,0.0,-1)
           CALL NUMBER(3.7,7.3,0.1,DIS,0.0,2)
           DO 90 M=5,25,4
           KN=3
           DO 111 K=1,12
           A=(2**K-1)*L*DIS
           C=ALOG10(A)+3
           D=ALOG10(AI(K,M))
           CALL PLOT(C,D,KN)
      111  KN=2
           CALL SYMBOL(C+0.2,D-0.05,0.1,2HA=,0.0,2)
           W=0.01*M
       90  CALL NUMBER(C+0.5,D-0.05,0.1,W,0.0,2)
           CALL PLOT (8.0,-2.0,999)
           WRITE(8,909)
      909  FORMAT('N=?')
           READ(8,-)NN
           GO TO(40,70),NN
       70  CALL EXIT
           END
```

SUBPROGRAM LOGAXS

```
      SUBROUTINELOGAXS(NCY,NO,AL,X0,Y0,LABEL,NC)
C     NCY=NUMBER OF CYCLES
C     NO=ORIGON LABEL  (POWER OF TEN)
C     AL=AXIS LENGTH IN INCHES
C     X0, Y0=COORDINATES OF ORIGON IN INCHES
C     LABEL=AXIS LABEL
C     ABS(NC)=NUMBER OF CHARACTERS IN LABEL
C        > 0 IMPLIES X AXIS
C        < 0 IMPLIES Y AXIS
      DIMENSIONIBUF(100)
      CALLWHERE(XX,YY,F)
      CALLPLOT(X0,Y0,-3)
      T1=-.05
      T2=-.1
      CL=AL/NCY
      IF(NC.LT.0)GOTO500
C
C     DRAW THE X AXI
C
      X=0.0
      Y=0.0
      DO100N=1,NCY
      DO110M=2,9
      X=ALOG10(M/1.0)*CL+(N-1)*CL
      CALLPLOT(X,0.0,2)
      CALLPLOT(X,T1,2)
      CALLPLOT(X,0.0,2)
  110 CONTINUE
      X=N*CL
      CALLPLOT(X,0.0,2)
```

SUBPROGRAM LOGAXS (continued)

```
      CALLPLOT(X,T2,2)
      CALLPLOT(X,0.0,2)
  100 CONTINUE
C
C     LABEL THE X AXIS
C
      X=0.0
      NL=NCY+1
      DO200N=1,NL
      Y=-.35
      X=(N-1)*CL-.14
      Z=NO+N-1
      CALLSYMBOL(X,Y,.14,2H10,0.0,2)
      X=X+.28
      Y=-.15
      CALLNUMBER(X,Y,.10,Z,0.0,-1)
  200 CONTINUE
      Y=-.60
      X=(AL/2.0)-(NC/2.0)*.14
      CALLSYMBOL(X,Y,.14,LABEL,0.0,NC)
      GOTO600
  500 CONTINUE
C
C     DRAW THE Y AXIS
C
      X=0.0
      Y=0.0
      CALLPLOT(0.0,0.0,3)
      DO120N=1,NCY
      DO130NN=2,9
      Y=ALOG10(NN/1.0)*CL+(N-1)*CL
      CALLPLOT(0.0,Y,2)
      CALLPLOT(T1,Y,2)
      CALLPLOT(0.0,Y,2)
  130 CONTINUE
```

SUBPROGRAM LOGAXS (continued)

```
      Y=N*CL
      CALLPLOT(0.0,Y,2)
      CALLPLOT(T2,Y,2)
      CALLPLOT(0.0,Y,2)
  120 CONTINUE
C
C     LABEL THE Y AXIS
C
      Y=0.0
      NL=NCY+1
      DO210N=1,NL
      X=-.55
      Y=(N-1)*CL-.07
      Z=NO+N-1
      CALLSYMBOL(X,Y,.14,2H10,0.0,2)
      Y=Y+.2
      X=-.30
      CALLNUMBER(X,Y,.10,Z,0.0,-1)
  210 CONTINUE
      X=-.80
      Y=(AL/2.0)+(NC/2.0)*.14
      NK=-NC
      CALLSYMBOL(X,Y,.14,LABEL,90.0,NK)
  600 CONTINUE
      X=-X0
      Y=-Y0
      CALLPLOT(X,Y,-3)
      CALLPLOT(X3,Y3,3)
      RETURN
      END
      SUBROUTINELOGAXS(NCY,NO,AL,X0,Y0,LABEL,NC)
C     NCY=NUMBER OF CYCLES
C     NO=ORIGON LABEL  (POWER OF TEN)
C     AL=AXIS LENGTH IN INCHES
C     X0, Y0=COORDINATES OF ORIGON IN INCHES
```

SUBPROGRAM LOGAXS (continued)

```
C      LABEL=AXIS LABEL
C      ABS(NC)=NUMBER OF CHARACTERS IN LABEL
C         > 0 IMPLIES X AXIS
C         < 0 IMPLIES Y AXIS
       DIMENSION IBUF(100)
       CALL WHERE(X3,Y3,F)
       CALL PLOT(X0,Y0,-3)
       T1=.05
       T2=.10
       CL=AL/NCY
       IF(NC.LT.0)GOTO500
C
C      DRAW THE X AXI
C
       X=0.0
       Y=0.0
       DO100N=1,NCY
       DO110NN=2,9
       Y=ALOG10(NN/1.0)*CL+(N-1)*CL
       CALL PLOT(X,0.0,2)
       CALL PLOT(X,T1,2)
       CALL PLOT(X,0.0,2)
110    CONTINUE
       Y=N*CL
       CALL PLOT(X,0.0,2)
       CALL PLOT(X,T2,2)
       CALL PLOT(X,0.0,2)
100    CONTINUE
C
C      LABEL THE X AXIS
C
       Y=0.0
       NL=NCY+1
       DO200N=1,NL
       Y=+.15
```

SUBPROGRAM LOGAXS (continued)

```
      X=(N-1)*CL-.14
      Z=NO+N-1
      CALLSYMBOL(X,Y,.14,2H10,0.0,2)
      X=X+.2
      Y=+.35
      CALLNUMBER(X,Y,.10,Z,0.0,-1)
200   CONTINUE
      Y=+.6
      X=(AL/2.0)-(NC/2.0)*.14
      CALLSYMBOL(X,Y,.14,LABEL,0.0,NC)
      GOTO600
500   CONTINUE
C
C     DRAW THE Y AXIS
C
      X=0.0
      Y=0.0
      CALLPLOT(0.0,0.0,3)
      DO120N=1,NCY
      DO130M=2,9
      Y=ALOG10(M/1.0)*CL+(N-1)*CL
      CALLPLOT(0.0,Y,2)
      CALLPLOT(T1,Y,2)
      CALLPLOT(0.0,Y,2)
130   CONTINUE
      Y=N*CL
      CALLPLOT(0.0,Y,2)
      CALLPLOT(T2,Y,2)
      CALLPLOT(0.0,Y,2)
120   CONTINUE
```

SUBPROGRAM LOGAXS (continued)

```
C
C       LABEL THE Y AXIS
C
        Y=0.0
        ML=NCY+1
        DO210N=1,ML
        X=.15
        Y=(N-1)*CL-.07
        Z=NO+N-1
        CALLSYMBOL(X,Y,.14,2H10,0.0,2)
        Y=Y+.28
        X=.40
        CALLNUMBER(X,Y,.10,Z,0.0,-1)
210     CONTINUE
        X=.65
        Y=(AL/2.0)+(NC/2.0)*.14
        NK=-NC
        CALLSYMBOL(X,Y,.14,LABEL,90.0,NK)
600     CONTINUE
        X=-X0
        Y=-Y0
        CALLPLOT(X,Y,-3)
        CALLPLOT(X3,Y3,3)
        RETURN
        END
```

LIST OF REFERENCES

1. L. J. Ippolito, W. H. Kummer and C. A. Levis, "Space Shuttle Millimeter Wave Experiment," IEEE 1975 Intercon Session E. (Available from Institute of Electrial and Electronics Engineers, New York, N.Y.)

2. C. A. Levis, H. C. Lin and T. K. Lai, "The Organization of Radiometric Arrays," June 1975 Meeting of International Scientific Radio Union, Urbana, Illinois.

3. R. P. Feynman, R. B. Leighton and M. Sands, Lectures on Physics, Vol. I, Chap. 41, Addison-Wesley Publishing Company, Inc., 1963.

4. W. W. Mumford and E. H. Scheibe, Noise Performance Factors in Communication Systems, Horizon House-Microwave, Inc., Dedham, Ma., 1968.

5. A. E. Siegman, "Thermal Noise in Microwave Systems," the Microwave Journal, pp. 93-104, May, 1961.

6. R. E. Collin, Foundations for Microwave Engineering, Chaps. 4 and 6, McGraw-Hill Book Company, New York, 1966.

7. H. H. Grimm, "Noise Computation in Array Antenna Receiving Systems," the Microwave Journal, pp. 86-99, June 1963.

8. R. Caldecott, J.W. Eberle and T. G. Hame, "Optimizing the Performance of Very High Gain Low Noise Antenna Systems," IRE Natl. Conv. Record, Pt. 1, pp. 87-94, 1961.

9. J. A. Allen, "A Theoretical Limitation on the Formation of Lossless Multiple Beams in Linear Arrays," IRE Trans. AP-9, pp. 350-352, July 1961.

10. J. P. Shelton and K. S. Kelleher, "Multiple Beams from Linear Arrays," IRE Trans. AP-9, pp. 154-161, March 1961.

11. R. E. Collin, op. cit.

12. W. W. Mumford and E. H. Scheibe, op. cit., Chap. 3.

13. D. F. Wait, "Thermal Noise from a Passive Linear Multiport," IEEE Trans. MTT-16, pp. 687-691, Sept. 1968.

14. Toshio Nemoto and D. F. Wait, "Microwave Circuit Analysis Using the Equivalent Generator Concept," IEEE Trans. MTT-16, pp. 866-873, Oct. 1968.

15. L. H. Yorinks, "Feasibility Study for a 60 GHz Radiometric Array," Jan. 1969, NASA-CR8614; prepared under Contract No. NAS-12-149 for NASA.

16. E. Stern and G. N. Tsandoulas, "Ferroscan: Toward Continuous-Aperture Scanning," IEEE Trans. AP-23, pp. 15-20, Jan. 1975.

17. N. B. Davenport, Jr. and W. L. Root, Random Signals and Noise, McGraw-Hill Book Company, New York, 1958.

18. H. A. Hans and R. B. Adler, Circuit Theory of Linear Noisy Networks, John Wiley & Sons, Inc., New York, 1959.

19. C. J. Summers and S. Zwerdling, "Material Characterization and Ultimate Performance Calculations of Compensated n-Type Silicon Bolometer Detectors at Liquid-Helium Temperatures," IEEE Trans. MTT-22, pp. 1009-1013, Dec. 1974.

20. J. W. Gewartowski, "Noise Figure for a Mixer Diode," IEEE Trans. MTT-19, p. 481, May 1971.

21. W. W. Mumford and E. H. Scheibe, op. cit., Chap. 7.

22. M. R. Barber, "Noise Figure and Conversion Loss of the Schottky Barrier Mixer Diode," IEEE Trans. MTT-15, pp. 629-635, Nov. 1967.

23. A. Papoulis, The Fourier Integral and Its Applications, McGraw-Hill Book Company, New York, 1962.

24. N. B. Davenport, Jr. and W. L. Root, op. cit., Chap. 9.